DESIGN AND DEVELOPMENT OF POWERED-CASTER HOLONOMIC MOBILE ROBOTS

A DISSERTATION
SUBMITTED TO THE DEPARTMENT OF MECHANICAL ENGINEERING
AND THE COMMITTEE ON GRADUATE STUDIES
OF STANFORD UNIVERSITY
IN PARTIAL FULFILLMENT OF THE REQUIREMENTS
FOR THE DEGREE OF
DOCTOR OF PHILOSOPHY

By
Robert Holmberg
August 2000

I certify that I have read this dissertation and that in my opinion it is fully adequate, in scope and quality, as a dissertation for the degree of Doctor of Philosophy.

Oussama Khatib
(Principal Adviser)

I certify that I have read this dissertation and that in my opinion it is fully adequate, in scope and quality, as a dissertation for the degree of Doctor of Philosophy.

Mark Cutkosky

I certify that I have read this dissertation and that in my opinion it is fully adequate, in scope and quality, as a dissertation for the degree of Doctor of Philosophy.

Bernard Roth

Approved for the University Committee on Graduate Studies:

Abstract

Holonomic vehicles, having three degrees of freedom, are well suited for use in congested environments and tight spaces, and can execute complex motions with ease. Use of robots in indoor environments is facilitated by the use of holonomic vehicles as the basic building block for wheeled office-type robots. Many holonomic robot designs that use compound wheels and other complex mechanisms have been proposed. These designs suffer from vibrations and poor odometry due to shifting ground contact points. Beacase of the small roller elements and complex mechanisms, these designs lack adequate clearance to roll over common indoor obstacles such as power cords and door thresholds.

This thesis presents the design and control of a holonomic robotic vehicle that uses ordinary wheels: the *Powered Caster Vehicle*, or PCV. A powered caster vehicle provides smooth accurate motion with the ability to traverse the hazards of typical indoor environments. The design can be used with two or more wheels, and is shown in this work in a four-wheeled incarnation: the Nomad XR4000 mobile robot

A PCV is a type of parallel mechanism for which there is no unique Jacobian relating the known joint velocities to the Cartesian velocities. To simplify the develpoment of the kinematic and dynamic equations, however, the PCV can be viewed as a collection of cooperating serial manipulators. This dissertation presents a new approach for a modular, efficient dynamic modeling of powered caster vehicles based on the augmented object model originally developed for the study of cooperative manipulation.

The proposed controller enables direct operational space position control and force control. Using the vehicle dynamic model, and actuation and measurement redundancy resolution, A control structure has been developed that allows vehicle dynamic decoupling and slip minimization. The effectiveness of this approach is experimentally demonstrated for

motions involving large dynamic effects.

Mobile manipulator systems hold promise in many industrial and service applications including assembly, inspection, and work in hazardous environments. The integration of a manipulator and a mobile robot base places special demands on the vehicle's drive system. For smooth accurate motion and coordination with an on-board manipulator, a holonomic vibration-free wheel system that can be dynamically controlled is needed. The PCV is shown to possess the desired mechanical properties. The PCV dynamic model and control structure have been integrated into a new mobile manipulation platform integrating the XR4000 mobile robot and a PUMA 560 arm. The experimental results illustrate the performance of this platform, and demonstrate full dynamic decoupling and its significance in mobile manipulation tasks.

Acknowledgements

Many people have helped me along the way. Their guidance, good humor, advice, and inspiration sustained me through the years of work. First of all, I'd like to thank my advisor, Oussama Khatib, for believing in me and for encouraging me when I needed it most. For helping make my orals more enjoyable than anticipated, thanks to Mark Cutkosky. Special thanks to Bernie Roth for the mind-warping kinematics lectures, the stalwart encouragement, and the gracious edits. Thanks also to Herman Bruyninckx, the final member of my defense committee, who quickly came to understand and test my knowledge of the core concepts.

For my interest in things robotic, thanks to Joel E. Peterson of the University of Pittsburgh, my alma mater. His electives on microprocessor control stretched the mechanical world into the electrical for me. Thanks to Mike Lovell for encouraging me to apply to Stanford. Your story of an afternoon in the sunshine made the difference. Thanks to Dave Williams and Sean Quinlan for the many home-built controllers, dangerous experiments, and the years we spent in the trailers. Thanks to John Meadows and Vic Scheinman for their generous design mentoring, and to Bernard Berlinger for his shared knowledge of gear design. Thanks to Craig Battles who always had the best stories of robots in the "real" world.

Thanks to Jeff Kerr for introducing me to the possibilities of a powered-caster vehicle, and to Illah Nourbakhsh for the "Aha!" that I could write this much about it. Thanks to everyone at Nomadic Technologies, Inc. for the financial and moral support which made the Nomad XR4000 possible: Anthony del Balso, Rich LeGrand, John Slater, and Jake Sprouse; and especially, Jim Slater, who both supported and counseled me. Thanks to my recent "manips" labmates, Alan Bowling, Oliver Brock, K.C. Chang, Diego Ruspini, and Oscar Madrigal. We had some killer demos!

Thanks for the unending support of everyone in my family—I'm looking forward to seeing you more. Fittingly, right before I end, thank you to Leslie Townsend who supported my writing and made this volume possible. And to my wife, Carrie, for her love, patience, and fortitude.

Contents

List of Tables

List of Figures

Chapter 1

Introduction

Wheeled, holonomic robots provide many benefits because they are maneuverable, agile, and reactive. As opposed to legged robots, wheels are efficient, easy to manufacture, and have a high payload.

Nonholonomic, wheeled robots are most prevalent because of their simple design and ease of (joint space) control. By their nature, nonholonomic mobile robots have fewer degrees of freedom than holonomic mobile robots. These few actuated degrees of freedom in nonholonomic mobile robots are often either independently controllable or mechanically decoupled, further simplifying the low-level control of the robot. Since they have fewer degrees of freedom, there are certain motions they cannot perform. This creates difficult problems for motion planning and implementation of reactive behaviors. Mobile manipulation is difficult to implement in a coordinated manner due to the large forces which can be generated by the constraints of the base.

Holonomic, wheeled robots, however, offer full mobility with the same number of degrees of freedom as the environment. This makes path planning easier because there aren't constraints that need to be integrated. Implementing reactive behaviors is easy because there are no constraints which limit the directions in which the robot can accelerate. A position controlled holonomic mobile robot with a manipulator can be coordinated, although not perfectly because of the dynamic coupling forces. The ability to force control a holonomic mobile robot allows dynamic compensation of the interaction forces for perfectly coordinated control.

Even with all the benefits, few holonomic robots have been used by researchers because of the problems introduced by the complexity of the mechanical designs used. Previous designs have used various compound wheels which consist of set of wheels mounted on, or driving, another (typically larger) wheel. Elements of a compound wheel are usually spherical or elliptical, which presents manufacturing challenges since odd-shaped wheels aren't as easily bought or made.

1.1 Mobility

Mobile robots are generally those robots which can move from place to place across the ground. Although robots that fly, swim, or float are *mobile* in the common sense of the word, they have come to be known by more specific descriptors (flying, underwater, space, etc.) [56, 97, 89, 3, 73].

Current manufacturing robots are fixed in place and typically have either an assembly line which passes by them, or are the "operators" of workcells which are arrayed around them. Wheels give a robot a much greater flexibility to perform new, complex, exciting tasks. The world does not have to be modified to bring all needed items within reach of the robot. The robots can move where needed. Fewer robots can be used. Robots with mobility can perform more natural tasks in which the environment is not designed specially for them. They can work in a human-centered space. They can cooperate by sharing a workspace together.

There are many forms of mobile robot locomotion which are adapted to different environments and purposes. Many biologically-inspired robots walk, crawl, slither, and hop. These robots have met with varying degrees of success and utility [88, 9, 99, 69]. By far, the most common form of robot locomotion is based on rolling motion provided by wheels.[1]

[1]Tracks may be thought of as very large or infinite diameter wheels with a finite local contact area with the ground.

1.2 The Wheel and Rolling

The wheel is one of the oldest human inventions and is a wonderfully efficient machine. Used as a supporting element in a vehicle, it provides a low-effort, smooth form of locomotion. It has evolved into a vast array of manufactured forms of which the pneumatic tire dominates.

A wheel (as used here) is rotationally symmetric about its principal or *roll* axis and rests on the ground on its *contact patch*. The contact patch is a small area which is in frictional contact with the ground such that the forces required to cause relative sliding between the wheel and ground are large for linear displacements and small for rotational motions. Thus, we assume that a wheel undergoing pure rolling has a contact point with no slip laterally or longitudinally, yet is free to twist about the contact point.

The kinematic constraint of rolling is called a higher-pair joint. The kinematic pair has two constraints so that two degrees of freedom are lost by virtue of the rolling constraint.

1.3 Notation

The algebra used in this dissertation will employ *spatial notation* which has been widely used in kinematic and dynamic modeling of complex mechanisms [24, 72, 54]. In spatial notation each quantity incorporates the appropriate linear and angular components. This results in a compact, unified form.

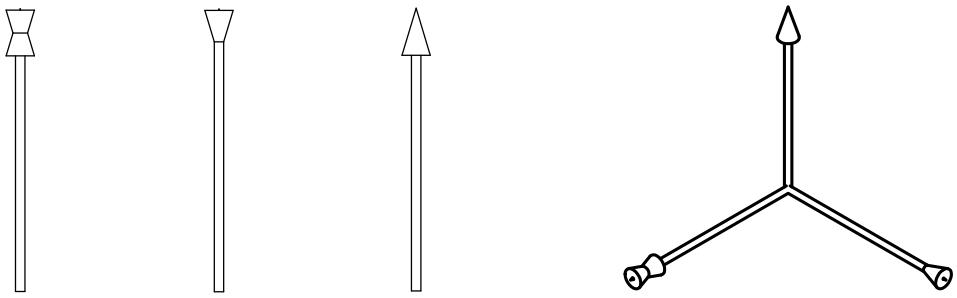

Figure 1.1: Graphical representation of x, y, and z-axes; and a coordinate system

In figures, the axes will be shown with arrowheads which evoke the letters 'X' and 'Y' for the x-axis and y-axis, and with a traditional arrowhead for the z-axis (see Figure 1.1).

The variables throughout this dissertation will follow the notation given in Table 1.1.

Table 1.1: Notation

Variable Type	Representation	Examples
Scalar	Lowercase plain	a, b
Vector	Bold	$\dot{\mathbf{x}}$, $\mathbf{F}$
Matrix	Uppercase plain	A, Λ
Frame	Uppercase sans serif bold	O, V
Frame unit vector	Lowercase sans serif bold	$\hat{\mathbf{o}}_z$, $\hat{\mathbf{f}}_x$
Point	Uppercase script	$\mathcal{O}$, $\mathcal{C}_i$
Unit vector	Bold with hat	$\hat{\boldsymbol{\varepsilon}}$

1.4 Holonomic and Nonholonomic

This thesis will use the words *holonomic* and *nonholonomic* throughout, so a quick discussion of their use should prove helpful. An unconstrained rigid body has a six-dimensional configuration space, *i.e.*, it takes six coordinates to specify its location and orientation. An unconstrained rigid body also has six degrees of freedom (DOF), *i.e.*,there are six independent motion directions in which the body could move in translation and rotation. Joints connect rigid bodies to each other or the ground to form a system of bodies with constrained motion; or more simply, a mechanism or machine with constrained motion. The joints impose constraints on the possible configurations and relative directions of motion of the "joined" rigid bodies.

1.4.1 Constraints

A *holonomic constraint* is a relationship between the configuration coordinates that reduces the dimension of the configuration space of the mechanism. By extension, a holonomic

constraint also reduces the DOF of the mechanism. The equation which contains the coordinate variables can always be differentiated to produce a relationship which constrains the speeds of the system. In contrast, a *nonholonomic constraint* is a relationship between the speeds of the system that cannot be integrated to yield an equation which contains system coordinates without speed variables. A nonholonomic constraint reduces the DOF of the mechanism without reducing the dimension of the configuration space.

A joint creates motion constraints. A holonomic joint provides only holonomic constraints. A nonholonomic joint causes one or more nonholonomic constraints in addition to any holonomic constraints.

A revolute joint, common in robotic manipulators, is a holonomic joint. Consider the first joint (waist) of a PUMA 560: If we look at the location of the origin of link 1, $\mathcal{O}_1$, a point on the vertical revolute axis then:

$$\begin{aligned} x_{\mathcal{O}_1} &= 0 \\ y_{\mathcal{O}_1} &= 0 \\ z_{\mathcal{O}_1} &= 0 \end{aligned} \tag{1.1}$$

are three constraints on the positions which the point $\mathcal{O}_1$ on link 1 can achieve. If we choose to express the orientation of link 1 using x-angles about the x, y, z axes, then the remaining holonomic constraints can be expressed:

$$\begin{aligned} \theta_x &= 0 \\ \theta_y &= 0 \end{aligned} \tag{1.2}$$

Thus, the six-dimensional configuration space of link 1 has been reduced to a one-dimensional configuration space, namely $\theta_z = \Theta$ where Θ is an arbitrary scalar. Likewise, the six DOF of link 1 have been reduced to a single DOF, namely $\dot{\theta}_z = \dot{\Theta}$ where $\dot{\Theta}$ is the time derivative of the position scalar.

A relevant example of a nonholonomic joint is the rolling contact joint of a vertical disk rolling on a plane as shown in Figure 1.2. This type of joint is common in wheeled mechanisms. For example, it is found at a rear wheel of a child's tricycle. Start with the fixed x and y axes in the plane of the ground and the z axis oriented upward. (Remember

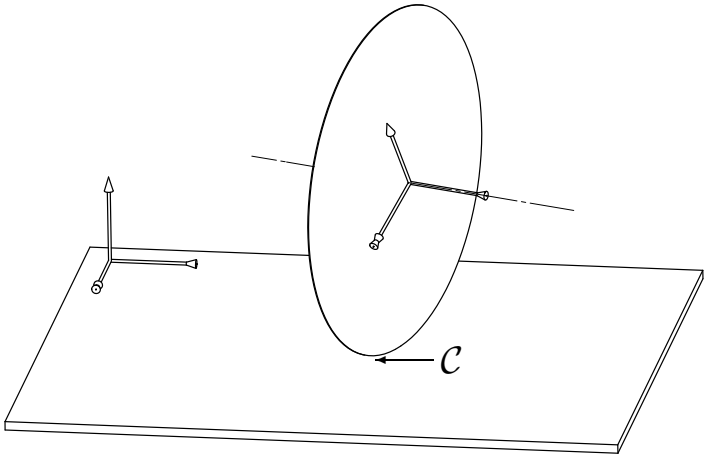

Figure 1.2: Vertical disk rolling on a plane

Section 1.3, the axes can be distinguished by the shape of their arrowheads.) If we look at the location of the contact point of the disk and ground, $\mathcal{C}$, then:

$$z_{\mathcal{C}} = 0 \tag{1.3}$$

Using x-angles, this time about the $z,\ y,\ x$ axes, to describe the orientation of the moving body, the vertical-ness of the disk is given by:

$$\theta_x = 0; \tag{1.4}$$

For a disk with radius, r, there are also two nonholonomic constraints which ensure there is no slip at the contact point:

$$\begin{aligned} \dot{x}_C &= r\dot{\theta}_y \cos(\theta_z) \\ \dot{y}_C &= r\dot{\theta}_y \sin(\theta_z) \end{aligned} \tag{1.5}$$

Thus, the six-dimensional configuration space of the disk has been reduced to a four-dimensional configuration space by the two holonomic constraints (the two coordinates $x,\ y$ of the contact point, and the two orientations, $\theta_z,\ \theta_y$ of the disk). The DOF have been reduced to two; in addition to the two holonomic constraints, there are two nonholonomic constraints which describe rolling without slip and the inability to slip perpendicularly to

the plane of the disk.

1.4.2 Mobile Robots

In the classical literature, a system which contains only holonomic constraints, *i.e.* a mechanism which contains only holonomic joints, is called a *holonomic system*. A system containing one or more nonholonomic constraints is known as a *nonholonomic system*. [30]

In the field of mobile robotics it has become common to classify a robot as a *holonomic mobile robot* or a *nonholonomic mobile robot*. These specific terms are a description of the abstract mobile robot—a description of the *robot body* without regard to the physical details of the particular drive system implementation. These terms can mask the true kinematic nature of the mobile robot mechanism. As noted by West and Asada [93]:

> In the literature, non-singular, omnidirectional vehicles have often been referred to as holonomic omnidirectional vehicles. If we neglect to describe the configuration of internal vehicle components, such as actuator displacements, then there are no non-integrable constraints involved in such vehicles and hence they are holonomic. Strictly speaking, however, the definition of holonomic systems cannot apply to those vehicles when the configuration of internal components is considered.

As an aside: as seen in the above quote, the terms holonomic and omnidirectional are sometimes used redundantly, often to the confusion of both. *Omnidirectional* is a poorly defined term which simply means the ability to move in any direction. It is not generally agreed upon whether this is a two-dimensional direction, $x,\ y$; or a three-dimensional direction, $x,\ y,\ \theta$. A synchro-drive mobile robot is often referred to as omnidirectional because it can steer in-place and thus, after waiting some amount of time for the steering direction to change, it can move in any direction. A synchro-drive robot is not, however, holonomic.

I will use the terms *nonholonomic mobile robot* and *holonomic mobile robot* consistent with their acquired usage to describe the existence or lack of nonholonomic constraints in the kinematic equations describing the abstract mobile robot. Because of the planar nature of mobile robots, the operational space they occupy contains only three dimensions which are most commonly thought of as the $x,\ y$ global position of a point on the robot and the global orientation, θ, of the robot.

In this context a *nonholonomic mobile robot* has the following properties:

- The robot configuration is described by more than three coordinates. Three values are needed to describe the location and orientation of the robot, while others are needed to describe the internal geometry that affects the nonholonomic constraints.
- The robot has two DOF, or three DOF with singularities. (One DOF is kinematically possible but is it a robot then?)

In this context a *holonomic mobile robot* has the following properties:

- The robot configuration is described by three coordinates. The internal geometry does not appear in the kinematic equations of the abstract mobile robot, so it can be ignored.
- The robot has three DOF without singularities.
- The robot can *instantly* develop a wrench in an arbitrary combination of directions x, y, θ.
- The robot can *instantly* accelerate in an arbitrary combination of directions x, y, θ.

1.5 Overview

This dissertation presents work detailing the design, modeling, and control of a Powered-Caster Vehicle or PCV, primarily to be used in the context of a holonomic mobile robot. The sections are as follows:

Chapter 2 discusses the rich background and history of holonomic mobile robots. The wide variety of earlier mechanisms are presented with a short analysis of each. The chapter culminates with the introduction of the Powered-Caster Vehicle, or PCV, a holonomic mobile robot without special wheels.

Chapter 3 begins with the geometric description of a Powered-Caster Vehicle. The development of the nonholonomic kinematics of the rolling wheels are shown as the basis for the PCV motions. The powered-caster "manipulator" concept is introduced, developed,

and extended to encompass PCV motion analogous to cooperative manipulation. The inverse kinematics of the PCV are developed using the results from the single powered-caster module in the context of the augmented object model.

Chapter 4 defines a set of design and performance goals for a prototype PCV. The design choices and tradeoffs for the geometry, layout, and component selection of the PCV are reviewed. The powered-caster module internal structure is presented. Finally, the overall performance-affecting parameters are analyzed and experimental results are given.

Chapter 5 discusses the need for accurate dynamic modeling of the PCV mechanism. The concept of a powered-caster "manipulator" is used to build an efficient, modular system of equations. These equations are combined using the augmented object model to give a method for the real-time computation of the PCV dynamic parameters.

Chapter 6 introduces a method for direct operational space control of a PCV. Equations to use the inherent redundant sensing and actuation of the PCV are developed. The dynamic parameters found in Chapter 5 are used to produce a dynamically decoupled controller and results showing improvements due to the proposed controller are given.

Chapter 7 presents a framework for integration of a PCV and robot manipulator arm in a mobile manipulation system. Using existing fast dynamic algorithms for serial mechanisms in conjunction with the presented PCV dynamic algorithm, dynamically decoupled control is achieved. Experimental results showing excellent base / arm decoupling are presented.

Chapter 8 gives suggestions for future work and concluding remarks.

Chapter 2

Background

In the last twenty years there has been increased interest in the development and control of holonomic mobile robots. Computers have become available which are capable of controlling the more complex motions of the holonomic mobile robot. Sensors are returning more better-quality data, which allows planners and controllers to plan and react more quickly; driving the desire for more capable robots.

Mobile robots are readily broken into two distinct groups: wheeled and legged. Although many legged robots with three or more DOF per leg could be classified as holonomic mobile robots, the challenges involved with legged locomotion have been great enough to keep legged robots in their own domain [88, 74]. Thus, in the study of holonomic mobile robots there is a historical focus on holonomic *wheeled* mobile robots. This chapter will discuss the historical classification, kinematic and mechanical development, and dynamic modeling of holonomic wheeled mobile robots.

2.1 Motivation

Planning paths for nonholonomic mobile robots is difficult largely because of the kinematics of the robots. The nonholonomic constraints need to be integrated forward in time to determine the state of the robot and which motions are available at each moment.

A holonomic mobile robot has simple constraints for a path planner to incorporate. The

holonomic mobile robot will have acceleration limits and velocity limits. Serial manipulator arms are also holonomic systems and many of the techniques used there can be used for holonomic mobile robots. As Mascaro, Spano, and Asada noted [55]:

> To drive a traditional, nonholonomic vehicle to a desired position and orientation, a complex nonlinear control entailing the generation of trajectories and switching between forward and backward motions is necessary. In other words, the vehicle cannot be positioned at a desired position and orientation by simply feeding back the error between the vehicle and the target positions [Walsh, *et. al.* 1992]. The holonomic omnidirectional vehicle, however, does not incur such a complex problem: direct feedback of position errors drives the vehicle to the target location.

It is difficult to implement reactive behaviors in a nonholonomic system because you do not know if you will be in a configuration which will allow motion in the direction specified as the desired motion. A holonomic mobile robot can reorient itself (and its payload) to negotiate in a tight environment. A nonholonomic mobile robot often must proceed on a geometrically longer path than that used by a holonomic robot because of the constraints.

A holonomic mobile robot is ideal for mobile manipulation. The holonomicity is necessary for many advanced control schemes which treat the mobile base and manipulator as a single system. There is a natural dichotomy between local manipulation and wide-ranging locomotion for many tasks. As early as 1988, a mobile manipulation system with a holonomic mobile base was introduced [20].

2.2 Classification of Wheeled Mobile Robots

A Wheeled Mobile Robot (WMR) is a vehicle which uses rolling elements, broadly categorized as *wheels,* in contact with the ground for locomotion. A number of researchers have looked at the general problem of classifying WMR's. A WMR can be described by detailing what type each of its wheels is, how they are configured, and how they are powered. The multitude of resulting mechanisms can be grouped in various ways.

Muir and Neuman introduce three types of wheels [63, 64]. The first, the *conventional wheel* is what most people think of when asked to picture a wheel (see Figure 2.1). It has a roll axis parallel to the plane of the floor and can change orientation by rotating about

the twist axis, an axis normal to the ground through the contact point. Depending on the mounting, the conventional wheel can be subdivided into several classifications. Conventional wheels which are mounted directly to the robot body are called *fixed conventional wheels*. A wheel which is mounted on a rotational link with the axis of rotation passing through the contact point is called a *steered conventional wheel*. A slight variation, which is used to reduce rotational slip during steering, is the *lateral offset wheel* in which the steer axis still intersects the roll axis but not at the contact point. The last type of conventional wheel is the *caster offset wheel* which has a rotational link with a vertical steer axis skew to the roll axis.

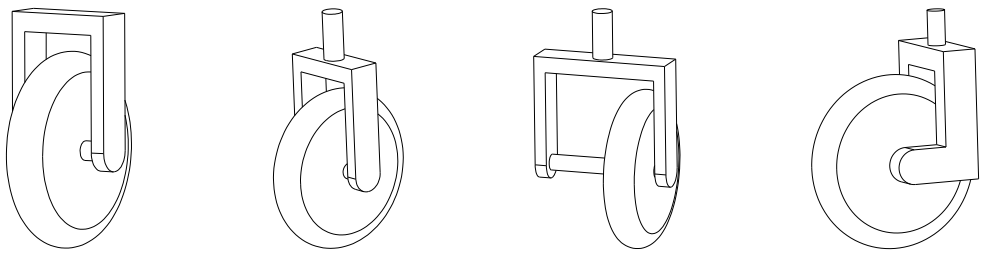

Fixed Steered Lateral Offset Caster Offset

Figure 2.1: Conventional wheels

The second type of wheel: an *omnidirectional wheel*, is a disk with a multitude of conventional wheels mounted on its periphery (see Figure 2.2). It possesses three DOF. The angle of the peripheral wheels may be changed to yield slightly different properties as will be described later.

The third type of wheel is the *ball wheel* which has three DOF. Since Muir and Neuman were not aware of any implementation for driving a ball wheel, they did not give it much attention in their examples. They stated that ball wheel kinematics may be implemented via use of a steered omnidirectional wheel. We will see practical examples of ball wheels later in this chapter.

Muir and Neuman classify the mobility of WMR's based on the solvability of the kinematic equations. Of the four types of solutions, two are useful, two are not. Of the two

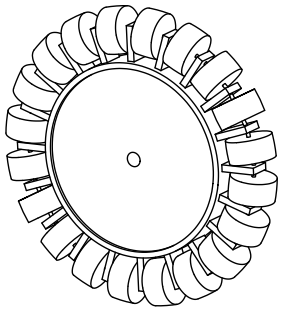

Figure 2.2: Simple omnidirectional wheel

rejected kinematic solutions, one is underdetermined with extra internal degrees of freedom, *i.e.* it cannot be fully controlled. The other is overdetermined, like a tricycle with a bent rear axle, and cannot move. The two useful solutions yield a class with a "consistent" unique solution and a class with a "determined" unique solution. The robots with a consistent unique solution must be actively controlled to remain consistent or risk falling into the overdetermined classification. Because of this, they avoid theoretical development of robots in this class. Those robots with a determined unique solution have a minimal set of freedoms and can always move. Muir and Neuman devote their attention to this last class of robots, with special attention given to the properties of minimal actuation and minimal sensing.

Alexander and Maddocks build on the conventional wheel work of Muir and Neuman with attention given to characterizing slippage with a physically intuitive Coulomb based model [1].

Campion, Bastin, and d'Andréa-Novel introduce the concepts of *degree of mobility* and *degree of steerability* for wheeled mobile robots. Using these concepts they divide all nontrivial WMR's into five classes [12, 11]. Four of the classes have degree of mobility equal to two, with various degrees of steerability. All of these robots are nonholonomic mobile robots. The remaining class, which has three degrees of mobility and no degrees of steerability, is the class of holonomic robots. They give examples with three omnidirectional wheels and three *off-centered orientable wheels*. It is shown that this type of robot is controllable in the classical sense, but the details of control focus on using only the minimum

number of actuators.

Rajagopalan uses the notation of Muir and Neuman and extends their work to include steered wheels with an angled steering axis [70]. This type of steering is often found on bicycles and cars to provide some restoring force to return the steering to its neutral position.

2.3 Holonomic Vehicles with Compound Wheels

The history of wheeled holonomic vehicles is interesting in its wide variety of mechanisms. All holonomic WMR's rely on the use of passive rolling elements or slip between the wheels and the ground.

2.3.1 Universal Wheel

One of the first mechanisms used to achieve holonomic motion is the omniwheel in one of its several forms. The *universal wheel* is the kinematically simplest example which has passive rollers on the periphery of a larger wheel (see Figure 2.3). The universal wheel has several deficiencies which limit its performance and capabilities. The diameter of the peripheral rollers must be significantly smaller than the diameter of the main wheel, which makes object traversal problematic. The gap between rollers, which must be present in order to mechanically support the rollers, introduces undesirable vibrations. Most designs

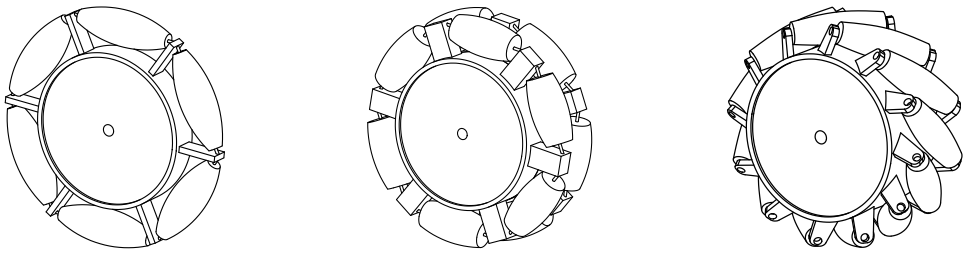

Universal Double Universal Swedish

Figure 2.3: Omniwheels

used three universal wheels mounted on the sides of an equilateral triangle, and had poor stability overall due to the proximity of the line of support to the center of gravity of the vehicle [87, 26, 13].

La, *et. al.*, early proponents of a holonomic vehicle with three universal wheels (see Figure 2.4), wrote in 1981 [53]:

> Only two existing methods aside from our own, offer true omnidirectionality in an electric wheelchair defined for our purpose as simultaneously and independently controllable rotation and two translations.

The two methods they were referring to were Swedish wheels and ball wheels, which will be introduced shortly.

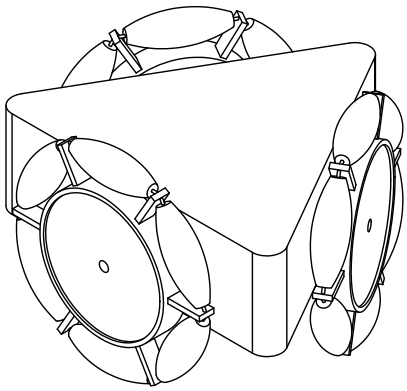

Figure 2.4: Vehicle with three universal wheels

2.3.2 Double Universal Wheel

Developed primarily to address the problem of vibration produced by roller gap, the double universal wheel (see Figure 2.3) has two rows of rollers which overlap slightly near the ends of the rollers [8]. One recent, complex example uses a system of mechanical transmissions and differentials to power four wheels using three motors. This design also incorporates a vehicle suspension to assure four-wheel ground contact at all times, which is important for the proper operation of the system kinematically [2].

The double universal wheel introduces another type of vibration—wheel speed variation. As the vehicle executes its commanded trajectory, the contact point at each wheel jumps from one set of rollers to the other many times during a wheel revolution. The jump in contact point location introduces a discrete jump in the distance to the instantaneous center of rotation. This would require that the wheel speed also have a discrete jump in speed to maintain the rolling constraint with the ground.

For example, consider the double universal wheel with wheel radius, R, in Figure 2.5 which is executing a motion with an angular speed, $\dot{\theta}$, about an axis which intersects the ground at the point which is an instantaneous center ($I.C.$). When the contact point jumps from C_1 to C_2, the distance from $I.C.$ to the contact point changes from r_1 to r_2, and consequently the wheel speed, ω, must jump from ω_1 to ω_2, where

$$\omega_1 = \dot{\theta} r_1 / R \tag{2.1}$$

$$\omega_2 = \dot{\theta} r_2 / R \tag{2.2}$$

Vibration results from the large accelerations of the wheel as it is forced, by the constraints, to approximate the step changes in speed [19]. This vibration could be minimized by sensing the contact point location and actively controlling the change in wheel speed during the transition; but this is difficult in practice. As evidenced by the historic lack of sensing of absolute wheel position, this effect has been almost universally ignored in the development of holonomic mobile robots, with the rare exception of some orthogonal wheel vehicles which will be discussed later.

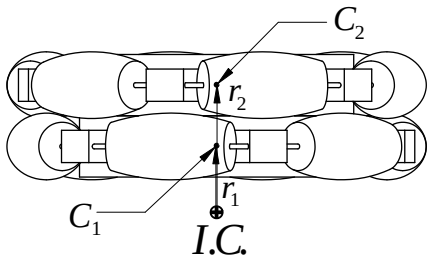

Figure 2.5: Double universal wheel contact point jumps

2.3.3 Swedish Wheel

A third form of omniwheel introduced in 1971 by Ilon working for Mecanum AB. in Sweden, has become known variously as the Swedish wheel, Mecanum wheel, and Ilonator [39, 40]. It is an omniwheel with the peripheral rollers at an angle other than 90 degrees to the main wheel (see Figure 2.3).

An Ilonator-based mobile platform was discussed by Daniel, Krogh, and Friedman in 1985, with emphasis on simple basic motions [19]. Swedish wheels were chosen by Muir, *et. al.* for the fabrication of a holonomic robot, Uranus, in 1987 [65]. This work was followed in 1989 by Feng, Friedman, and Krogh [25]. Dickerson and Lapin in 1991 explored among other things the fundamental geometry of a Mecanum wheel and the possibility of powering the peripheral rollers [21]. The Tesselator was presented in 1992 by Dowling, *et. al.* as a Swedish wheeled robot which moved beneath a parked Space Shuttle, inspecting and repairing the heat shield tiles [23]. In 1993, Saha, Angeles, and Darcovitch pro-

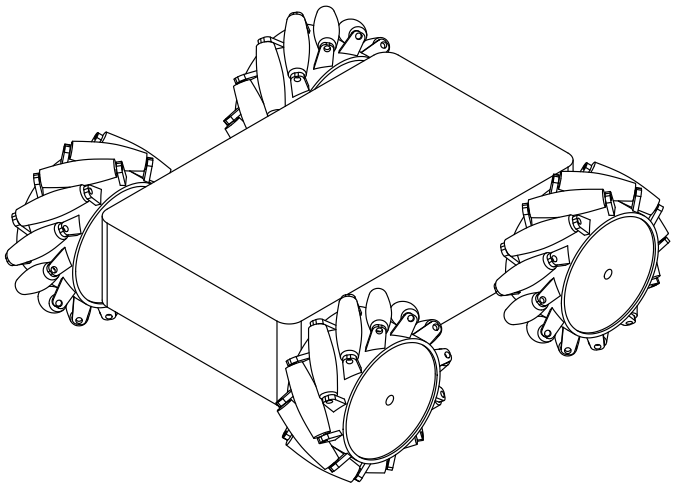

Figure 2.6: Vehicle with swedish wheels

posed using Swedish wheels to build mobile robots with isotropic dynamic properties [75]. KAMRO, a large Mobile robot with two PUMA 260 manipulators designed for flexible automation of industrial processes, was presented by Paromtchik and Rembold in 1994 [66]. A holonomic wheelchair was promoted by Hoyer in 1995 [38]. With a long development

program beginning in 1982, a large working prototype for shipboard munitions transport has been in development in the U.S. Navy Omni Directional Vehicle (ODV) program and has proven that a Swedish wheeled vehicle can traverse some real world obstacles and inclines [57]. Recent development using Swedish wheels, springing from this project has led to the introduction in 1999 of a holonomic forklift vehicle [59].

Swedish wheels have the same problems as the previous universal wheels—the small diameter of the roller, especially near the ends of the rollers, is limiting; and vibration caused by wheel speed variation, as explained in the previous section.

2.3.4 Tracks of Rollers

Treads allow linear motion and have been used to create two-DOF vehicles such as bulldozers and tanks. A holonomic vehicle can be produced by adding elements which allow motion orthogonal to the tread.

Treads made of rollers were introduced by Hirose in the VUTON mechanism [33]. The treads are driven along their length and have a passive freedom transverse to their length. The treads of rollers are assembled into a vehicle much as universal wheels are mounted, with three or four treads arranged symmetrically about the robot. This robot was touted for its large payload capability due to the multiple cylindrical rollers which give a large contact area.

A novel robot by West and Asada is a tank-like vehicle with rows of spheres that are pushed the length of the track by paddles while being simultaneously driven transversely by rollers [91]. It is a complex mechanism which uses three motors to power the rows of spheres which must also be retained within the tracks. This results in poor ground clearance.

Another design which attempts to address some of the ground clearance issues was proposed by Isoda, *et. al.* [41].

2.3.5 Orthogonal Wheel

Another contender in the Navy ODV development program used wheels which are truncated spheres [68, 51]. The mechanism acquired the name orthogonal wheels because of

the relationship of the two wheels in each wheel module. Orthogonal wheels can be arranged as radial pairs or tangential pairs. While the radial pair arrangement is somewhat mechanically simpler, it suffers from vibration due to wheel speed variation as in the double universal wheel.

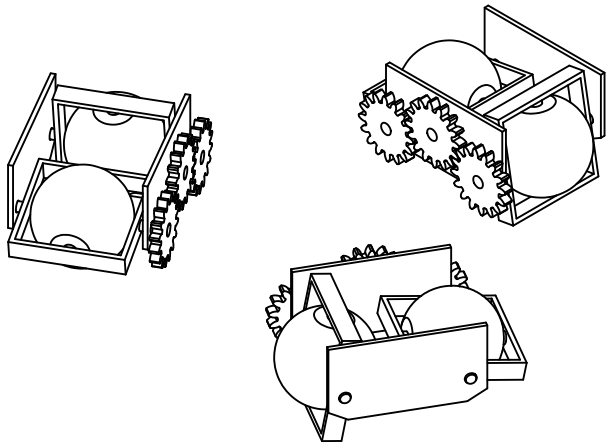

Figure 2.7: Tangential orthogonal wheel arrangement

The proper wheel speed for tangential pairs of orthogonal wheels is independent of which wheel of the pair is in contact with the ground. Robots with tangential pairs of orthogonal wheels have been recreated by other researchers with similar results [81]. More recently, a holonomic wheelchair design with orthogonal wheels was introduced [22].

In 1995 at Stanford, I was involved in the design and development of a pair of mobile manipulation systems, Romeo and Juliet, for the Stanford Assistant Mobile Manipulator, or SAMM, project. We modified and used tangential orthogonal wheel mechanisms which were designed and produced by Killough *et. al.* at Oak Ridge National Labs. I completed the mechanical design of the body, and—with great assistance from Nomadic Technologies—our research group produced the two robots in less than six months from start to finish. Romeo and Juliet, (see Figure 2.8), experimentally proved the benefits of having a holonomic mobile base for mobile manipulation [47, 50, 49, 45]. The SAMM robots had large reflected inertias which limited the achievable acceleration. They had terrible ground clearance and were not capable of traversing a door threshold. They were

uncomfortably unstable on their three wheel modules, often beginning to tip during normal acceleration or braking. These limitations gave a large incentive for the development of a better holonomic mobile robot for use in mobile manipulation systems.

Figure 2.8: Stanford Assistant Mobile Manipulator (SAMM) with orthogonal wheels

2.3.6 Ball Wheel

It has long been recognized that, kinematically, the ball wheel can be used to build a holonomic mobile robot. There have not been many attempts to build a mobile robot with ball wheels because of the difficulties in confining and powering a sphere. This problem was addressed in the orthogonal wheel design by affixing a rigid axis through the sphere which introduced a singularity at the pole of the axis and led to the orthogonal wheel design. Muir and Neuman had earlier noted that “a ball wheel could be implemented with a steered omniwheel” [64].

In 1993, Koshiyama and Yamafuji presented an "omnidirectional" spherical robot using the ball wheel as the body of the robot, with drive system and electronics included internally. They only included two actuators, however, so this design was still not holonomic [52]. In 1994, West and Asada undertook the design of a holonomic mobile robot with ball wheels. Their solution used active and passive rollers to guide and power the motions of the ball. The result behaved much like an omniwheel with a driven direction of motion and a passive direction of motion. Since their design had to address the special problems of driving a wheel without a direct connection such as an axle, they found that it was important to maximize the amount of friction between the driven rollers and the ball wheel [92, 93, 94]. In 1997, Mascaro, Spano, and Asada adapted the ball wheel design to serve as a reconfigurable bed/wheelchair [55]. This research was extended, in 1998, by Wada and Asada into a bed/wheelchair with four ball wheels in a mechanism with an actively reconfigurable footprint to adjust for situations such as narrow passage-ways or increased stability [83].

The ball wheel mobile robot is capable of smooth rolling motion with no wheel gaps and a smoothly varying wheel speed.

2.4 Holonomic Vehicles with Conventional Wheels

All of the designs discussed up to this point have used wheels with multiple rolling elements per wheel module. The multiple rollers are most obvious in the universal wheel and more subtly hidden in the ball wheel mechanisms. Because researchers have, in the last thirty years, used the bare term *wheel* for all rolling support bodies, we have been left with the awkward terminology *conventional wheel* or *normal wheel* to describe what is commonly known and readily available as a *wheel*. For simplicity in the remainder of this dissertation I will reclaim the use of the single word wheel to mean a wheel in the common, ordinary sense and refer to the more complex mechanisms reviewed in the previous sections either collectively as *compound wheels* or individually by their specific names. It is important to the contributions of this thesis to make a clear distinction between the common wheel and the more complex *compound wheel*.

A *wheel* has only a single roll axis that defines a single roll direction. This allows

a conventional wheel to be supported and driven much more easily than is possible for compound wheels with two roll axes. A wheel rolls smoothly and continuously on a single rolling surface, uninterrupted by supporting structure or bearings. One may ask: what was known about using a wheel to create holonomic motion?

The research can be broken into two groups which I will call "steered wheels" and "caster wheels." *Steered wheels* have intersecting roll and steer axes. This configuration creates a singularity in the mechanism (see Chapter 3). While caster wheels are also "steered" they are fundamentally different enough to classify them separately. *Caster wheels* have non-intersecting roll and steer axes, no singularity, and lead to the creation of a truly holonomic vehicle.

2.4.1 Steered Wheels

While, strictly speaking, mobile robots with steered wheels are nonholonomic mobile robots, they are capable of quite general motions. They are included here because of the contributions and importance of this research in improved mobility in mobile robots. These vehicles were studied to create a more maneuverable robot with three degrees-of-freedom.

In 1983 a team lead by Moravec at Carnegie Mellon University built the CMU Rover, a.k.a. Pluto, with the goal of building a robot base with "a full three degrees of freedom." It had three pairs of wheels and six motors. Each pair of wheels was independently steered and contained a differential between the two wheels which was driven by another motor. The wheels were arranged so that the steering axis of each wheel intersected the roll axis. Disappointingly, the robot moved unsteadily and with oscillations [61].

In the pursuit of a more maneuverable mobile robot, many other robots have been built more recently with steered and driven wheels with intersecting roll and steer axes. These robots have met with somewhat more success than the Rover due largely to improvements in computing power and control electronics.

Hirooka, Katanaya, and Tanaka developed a omnidirectional vehicle with steered and driven wheels for use as an AGV in flexible manufacturing in 1992. This included a special lift mechanism to pick up and transport pallets within a factory [32]. In 1993, Mehrabi and Hemami reported on their results with CONIC III, which had two driven and steered

wheels [58]. Similarly, Burke and Durrant-Whyte used driven and steered wheels as the basis for a modular mobile robot with distributed control [10].

In 1994 Kanayama introduced the kinematic concept of a *general motion* which can be performed by a robot with steered and driven wheels [42]. The general motion concept was proposed as a way to handle the singularities inherent in robots with driven and steered wheels. Later, in 1996, he revealed a relatively large, slow vehicle funded by the U.S. Military with indications it could be used as a turret-less tank, using the wheels to aim the muzzle [43].

Mori, Nakano, Takahashi, and Takayama constructed a mobile robot in 1996 with driven and steered wheels, but without motors on the steer axes. Instead, they installed a brake on each steer axis to lock-in one particular steering configuration during motion. Although the mechanism is similar to the others, the method of control relies on the wheel motors to reconfigure the steer angles with the robot at rest, and effectively reduces the robot to a one-DOF system during motion [62, 80].

In 1996, "Fatboy," a four-wheel mobile robot with driven and steered wheels, was demonstrated by Slater, Slater, and Legrand of Nomadic Technologies, Inc. [79]. This prototype proved the ability to control eight motor axes in a coordinated manner, and, in spite of the overconstrained nature of the system, to produce stable, graceful motions. The success of this prototype led directly to the formation of a project to produce a wheeled, *holonomic* mobile robot, the Nomad XR4000. I joined the XR4000 project early-on as the lead mechanical designer.

One interesting, related concept, the Cobot, was introduced in 1996. [67, 90, 28] Cobots have steered wheels which are *not* driven, but roll passively. Cobots are steered to enforce a desired path, but are passively powered by the operator along the path. They make use of the nonholonomic constraints to develop large forces normal to the path. Because the steer and roll axes intersect and the power used along the path is supplied by a human operator, no work is done by the actuators (with respect to the robot body); hence the steering actuators can be small and light. The large forces generated by the nonholonomic constraints—which pose problems for robots with driven and steered wheels (*eg.* the CMU Rover)—are used advantageously by Cobots.

2.4.2 Caster Wheels

In 1986 in their study of Wheeled Mobile Robots (WMR's), Muir (a recent graduate from the Rover project with Moravec) and Neuman noted specifically about the CMU Rover [64]:

> Rover can be redesigned to operate as an omnidirectional WMR by constructing the steering links so that the wheels are non-redundant. Since there are six actuators, the redesigned actuation structure will not be robust and will allow actuator conflict.

In more general terms they laid out the requirements for holonomic motion from a Wheeled Mobile Robot (WMR) [64]:

> An omnidirectional WMR design must thus consist of ball, omnidirectional, or *non-redundant conventional wheels* to allow three DOF motion [Italics added].

And most generally [64]:

> The kinematic design of a WMR allows three degrees of freedom if and only if all of the wheels possess three DOFs.

As we will see in Chapter 3, a steered wheel with intersecting roll and steer axes has only two DOF. Therefore, none of the mobile robot designs with this mechanism are holonomic. What is needed is a wheel mechanism with three DOF, such as the omniwheel or ball wheel, which has two roll DOF and one twist DOF. A caster is a steered wheel with skew roll and steer axes; and is therefore "non-redundant" as called for by Muir and Neuman. It has three DOF with the three freedoms described by the twist axis, roll axis, and steer axis. A holonomic mobile robot can be constructed with casters for locomotion.

It is interesting to note that Muir and Neuman acknowledge the possibility of holonomic motion using casters, which they call non-redundant conventional wheels. They dismiss the usefulness of this configuration and do not show it as one of their many examples, however, because as they continue: "We require that the actuator structure satisfy the *robust actuation criterion* shown [earlier in their paper] to avoid actuator conflict."

Along the way, other researchers concurred. In classifying all wheeled mobile robots into five classes, Campion, Bastin, and d'Andréa-Novel described one class of robot which is holonomic and contains designs with casters [11]:

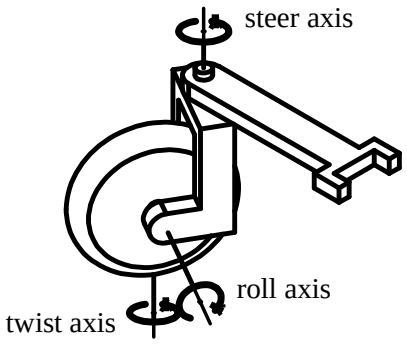

Figure 2.9: Caster

> These robots have *no* conventional fixed wheels and *no* conventional centered orientable wheels. Such robots are called *omnidirectional*.... In contrast, the other four types of robot have a restricted mobility.

West and Asada acknowledged and clarified the holonomic nature of mobile robots with only casters as they presented the design of a ball wheel mobile robot [92]:

> If all the wheels of a vehicle are casters, i.e. wheels held with an offset swivel axis, then full mobility is obtained (Campion, Bastin, and d'Andréa-Novel 1993). However, actuation is complicated. Consequently, casters usually only provide passive full mobility, as in office chairs for example.

and also [94]:

> An "actuated caster" design can provide full-mobility (Campion et al., 1993), but the kinematics are configuration dependent and actuation is difficult to implement (Alexander and Maddocks, 1989).

The ability to use actuated casters was established in the research community, yet no prototype was built until recently.

After completing the SAMM holonomic mobile manipulator robot systems (see Figure 2.8) in July, 1995, in a discussion with Dr. Jeff Kerr, I became aware of the possible use of casters to create a vehicle mechanism with holonomic motion. Later that year,

Wada, Tominaga, and Mori published work with an early one-wheeled powered-caster prototype [86]. Independent of Wada, *et. al.*, in 1995 Nomadic Technologies, Inc. began designing a new generation robot with modular steered and driven wheels. I joined Nomadic in 1996 to design the mechanism for a steered and driven powered-caster mobile robot. The results and extensions of this project, first presented to the public as the Nomad XR4000 in 1997 [78], are presented in the remainder of this dissertation.

Wada and Mori followed the single wheel prototype the next year by a powered-caster vehicle mechanism with two powered-casters and two passive casters [84]. About this same time, Ferrière, Raucent, and Fournier published a study of powered-caster design trade-offs [27].

2.5 Mobile Manipulation

The use of both nonholonomic and holonomic mobile robots as the basis for a mobile manipulation system had been studied in our laboratory. It was determined that it was necessary to use a holonomic mobile robot in order to implement many of the useful control strategies which had been developed in our group. Indeed, Moravec *et. al.* had recognized the same thing, that a holonomic mobile robot would be enabling for mobile manipulation, when they attempted the first conventional wheeled holonomic mobile robot [61].

> The usefulness to a manipulator would be enhanced if the base could move with a full three degrees of freedom. Most straightforward seemed to be to make all the wheels of the vehicle steerable.

Experimental results in our lab using the SAMM robots, Romeo and Juliet, have begun to show the value and effectiveness of using a holonomic mobile robot as the basis of a mobile manipulation [47, 50, 46, 45].

2.6 Dynamic Modeling

There are several approaches which are taken to derive the equations of motion which embody the dynamics of a system. The choice of method can influence the effort needed to

model the system and affect the efficiency of the solution. In one example, the dynamics of a wheeled mobile robot are derived to address issues including the controllability of the system, and computational efficiency is not a factor [18]. However, the computational complexity of the solution is important when computing the dynamics in real-time, as needed for the control of a PCV. Wheeled mobile robots have two attributes which complicate the modeling and computation of their dynamics beyond the complexity faced when working with serial and branching manipulators. Wheeled mobile robots are both nonholonomic dynamic systems and parallel chain dynamic systems.

Nonholonomic dynamic systems are characterized by the existence of constraint equations involving functions of the system's generalized velocities which cannot be integrated to yield equations involving only generalized coordinates. Parallel chain dynamic systems are characterized by a greater number of kinematic joint DOFs than there are DOFs in the system. The extra DOFs can be resolved using loop-closure constraint equations of the in-parallel paths from the ground to the body of the robot. The loop-closure constraint equations are typically non-linear and often cannot be solved in closed form for the joint variables. The inextricable joint variables in the loop-closure equations are often found throughout the expressions which describe the dynamics, and thus greatly increase the complexity of the solution.

Thanjavur and Rajagopalan, in a survey of the study of dynamics of Wheeled Mobile Robots for model based control application [82], report finding derivations of the equations of motion done with either the Newton-Euler method or the Lagrangian approach. They give examples for both approaches, many of which are of particular interest here [71, 17, 100, 76, 4].

In the Newton-Euler method, the model of the mechanical system is decomposed into its various rigid bodies and constraint forces are introduced where connections had been. The solution includes finding the constraint forces which cause the system to behave identically to the original articulated system. Solving for constraint forces, which are of little interest from the control standpoint, increases the complexity of the equations.

For holonomic systems, Lagrange's extension to the Newton-Euler framework eliminates the need to find the constraint forces by projecting the dynamics into the space defined by the system's generalized coordinates and speeds. For a nonholonomic system with

fewer DOFs than generalized speeds, the extra equations are eliminated by the introduction of Lagrange multipliers. The equations describing the Lagrange multipliers are generally coupled differential equations which need to be solved simultaneously with the dynamic equations, again increasing the complexity of the solution. Whereas the extra constraint forces of the Newton-Euler approach represent the internal forces of the mechanism responsible for the reduction in DOF due to holonomic constraints, the Lagrange multipliers and associated equations represent the constraint forces which are responsible for the further reduction in DOFs due to the nonholonomic constraints [60].

The use of Kane's method [44] offers advantages over Newton-Euler and Lagrangian methods when modeling nonholonomic and closed-chain systems.[1] Kane's approach is based on the concept of virtual power, rather than virtual work. This method focuses on the system's degrees of freedom by working with equations based on the generalized speeds rather than generalized coordinates. In this way, the modeling of nonholonomic systems is simplified because the nonholonomic constraints can be directly incorporated since they are functions of the generalized speeds already. The modeling of closed-chain mechanisms is also simplified, as the derivatives of the loop-closure equations are used and yield constraint equations which are linear in the generalized speeds, and thus the variables of interest are easily separable.

[1] Kane's methods have directly influenced my approach, as I was fortunate to have studied dynamics with Professor Kane during my coursework at Stanford.

Chapter 3

Kinematics

3.1 The Powered-Caster Vehicle

We have seen in Chapter 2 that it was understood, at least on a kinematic level, that a holonomic mobile robot could be created using normal wheels rather than compound wheels. Holonomic mobile robots with normal wheels are required to have wheel mechanisms which are "non-redundant" or "orientable." I will use the word *caster* henceforth to describe such a mechanism, because it is intuitive and descriptive. A caster, as shown in Figure 2.9, is a common type of wheel mechanism found on shopping carts, differential drive mobile robots, and rolling office chairs. A caster is a three DOF mechanism; much like a three DOF serial robot manipulator, which gives the endpoint of the manipulator three DOF, provided there are no singularities.

A practical example is the common rolling office chair (see Figure 3.1). It has four or five legs, each of which ends in a caster. If you have moved yourself from one spot to another while sitting in such a chair, you have experienced the holonomic mobility this mechanical arrangement provides. Move left, move back, rotate, one-to-the-next in any order—all without having to worry about maximum/minimum steering angle, or current configuration. We could not do this pushing a model car around on a desktop nor moving a child about in wagon for these mechanisms, in contrast, are nonholonomic vehicles.

This simple office chair example gives us an intuitive pathway to the invention of a caster-based holonomic vehicle. Push a rolling office chair across the floor in an arbitrary

Figure 3.1: A well known holonomic vehicle

path while recording the the motions of each wheel. Next, return the chair to its original starting configuration, and playback the motion of each wheel with appropriately mounted actuators. The chair will traverse the same path as before, but this time under its own power. By powering and controlling each caster, we can execute any motion through which an unpowered chair can be pushed. Such a mechanism is a *powered-caster vehicle* or *PCV* which can be used as the basis of a holonomic mobile robot. This dissertation will describe the existence, construction, and control of a PCV.

3.2 Robot Geometry

A PCV is composed of a *body* to which n powered-casters are attached. In this chapter, the powered-casters will be represented kinematically. The details of how the casters are physically powered will be discussed in Chapter 4. The spatial position of the PCV in the world can be described by the global vector, ${}^{\circ}\mathbf{x}$, from the fixed world frame, $\mathbf{O}$, to the local

vehicle frame, $\mathbf{V}$, where (as shown in Figure 3.2)

$$ {}^{\mathsf{O}}\mathbf{x} = \begin{bmatrix} x \\ y \\ \theta \end{bmatrix} \tag{3.1} $$

The elements x and y describe the position of the origin of the vehicle coordinate system, and θ indicates the orientation of the vehicle frame. Thus, as a mobile robot, three coordinates fully define the configuration of the PCV in the world.

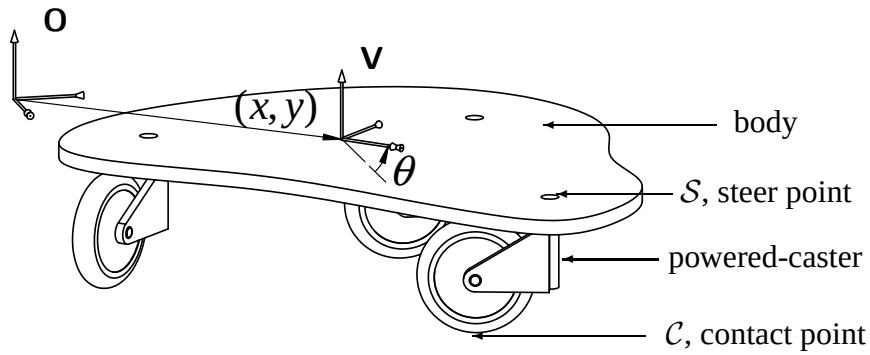

Figure 3.2: PCV position

The geometry of the PCV will be described in the vehicle coordinate system, $\mathbf{V}$. Since this coordinate system is used for the majority of the work presented, it will be assumed that all quantities will be expressed in $\mathbf{V}$ unless explicitly noted. The origin of the frame $\mathbf{V}$ is designated as, $\mathbf{V}_{\oplus}$; and the origins of other frames will be shown with the same subscript. Spatial vector quantities can be translated from/to the global frame with a rotation, ${}^{\mathsf{O}}_{\mathsf{V}}R$, or its inverse which is simply the transpose:

$$ {}^{\mathsf{O}}_{\mathsf{V}}R = \begin{bmatrix} \cos(\theta) & -\sin(\theta) & 0 \\ \sin(\theta) & \cos(\theta) & 0 \\ 0 & 0 & 1 \end{bmatrix} \tag{3.2} $$

$$ {}^{\mathsf{O}}\dot{\mathbf{x}} = {}^{\mathsf{O}}_{\mathsf{V}}R\,\dot{\mathbf{x}} \tag{3.3} $$

$$ \dot{\mathbf{x}} = {}^{\mathsf{O}}_{\mathsf{V}}R^{\mathsf{T}}\,{}^{\mathsf{O}}\dot{\mathbf{x}} \tag{3.4} $$

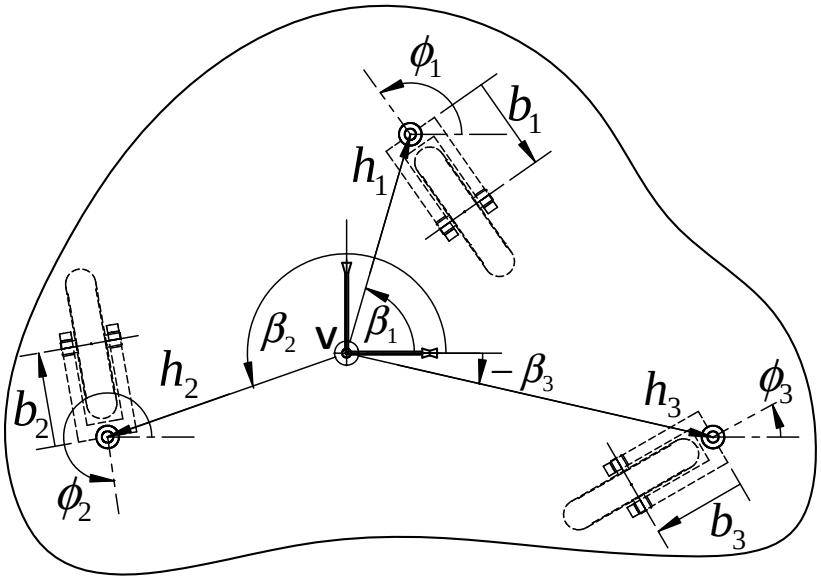

Figure 3.3: PCV geometry

The $\mathfrak{n}$ casters of the robot are attached at their respective *steer points*, $\mathcal{S}_i$, with $i = 1 \ldots \mathfrak{n}$. We define the location to the steer point by the vector $\mathbf{h}_i$ from the vehicle origin, $\mathbf{V}_{\oplus}$, to the i^{th} steer point, $\mathcal{S}_i$. Since it simplifies the presentation, I will often use the polar form of the vector:

$$\mathbf{h}_i = (h_i, \beta_i) \tag{3.5}$$

The magnitude is h, and the direction, β, is given by the angle from $\hat{\mathbf{v}}_x$ to line from $\mathbf{V}_{\oplus}$ to $\mathcal{S}_i$. The location of the wheel axis is given by the vector $\mathbf{b}$, from steer axis to roll axis. The components in polar form are

$$\mathbf{b}_i = (-b_i, \phi_i) \tag{3.6}$$

From the wheel axis, the wheel contact point, $\mathcal{C}$, is a distance r found by the vector

$$\mathbf{r}_i = -r_i\, \hat{\mathbf{v}}_z \tag{3.7}$$

3.3 Rolling Wheel Kinematics

Before looking at the mechanisms which will make up our mobile robot, it will be instructive to review the kinematics of a rolling wheel. We will restrict the wheel to remain vertical and to have a single point contact with the ground. We are interested in the instantaneous motions possible for the wheel. The nonholonomic constraints which define rolling were given in Chapter 1 in global coordinates. The rolling motion constraints (see Figure 3.4) for the motion of the wheel contact point, $\mathcal{C}$, in coordinates of the local fork frame, F are

$$^{\mathsf{F}}\dot{x}_{\mathcal{C}} = r\dot{\rho} \tag{3.8}$$

$$^{\mathsf{F}}\dot{y}_{\mathcal{C}} = 0 \tag{3.9}$$

leaving the two DOF, $\dot{\rho}$ and $\dot{\sigma}$.

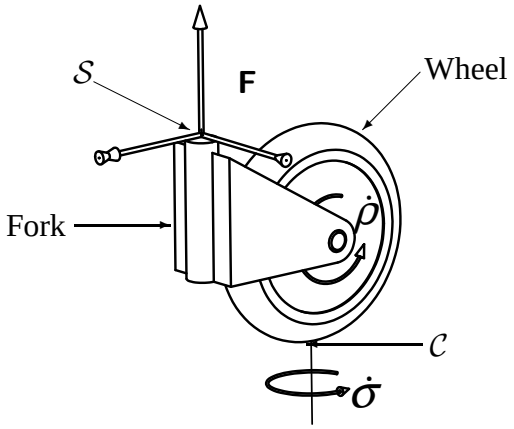

Figure 3.4: Degrees of freedom for a rolling wheel

One major difference between holonomic and nonholonomic systems involves the effect the path taken between two joint configurations has on the final Cartesian configuration. In a holonomic system the path taken does not affect the final global position. In a nonholonomic system, however, the path will affect the final position of the mechanism. For a system with two joints, two different paths between a pair of joint configurations could be elementary as moving the first joint first and the second joint next for one path,

versus moving the second joint first and the first joint next for the other path. When studying the instantaneous motion properties of a mechanism, the order in which joint motions occur is no longer important; regardless if the system is holonomic or not. This can be a confusing point, but when all displacements are infinitesimal, the second order effects introduced by reordering the motions vanish.

We can now demonstrate what elemental Cartesian motions are generated by combinations of motions of the wheel DOFs. Begin by observing the steer point, $\mathcal{S}$, of the caster because this point will remain coincident with a point on a body carried by the caster. A small rolling motion, $\delta\rho$, will produce a motion in the x direction. A small twisting motion, $\delta\sigma$, will produce a motion in the y direction in addition to the rotation, $\delta\sigma$. The two resultant linear motions of $\mathcal{S}$, generated by $\delta\rho$ and $\delta\sigma$, are always orthogonal and, provided that $r > 0$ and $b > 0$, always span the motion space for this point (see Figure 3.5). Since the

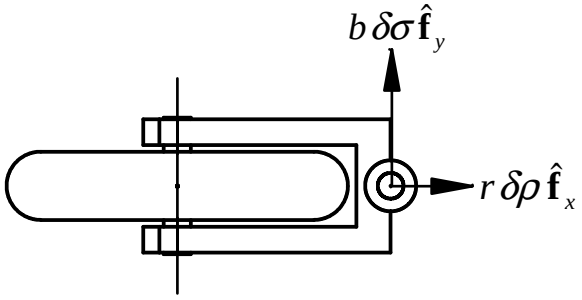

Figure 3.5: Elemental displacements

order in which infinitesimal motions are executed does not affect the final position of the mechanism, we can execute each motion independently with consistent results. Dividing by the time over which these displacements occur, in the limit, these displacements yield the velocity of $\mathcal{S}$. Using spatial notation, the local velocity of $\mathcal{S}$ is

$$\dot{\mathbf{x}}_{\mathcal{S}} = \begin{bmatrix} r\dot{\rho} \\ b\dot{\sigma} \\ \dot{\sigma} \end{bmatrix} \tag{3.10}$$

3.4 Caster Kinematics

As shown in Figure 3.6, a caster mechanism is a simply an upright wheel with an offset pivot attached to the body of the vehicle. The caster is the fundamental mechanism of a PCV and it is important to understand its kinematics. A caster mechanism has three DOF: twisting about the contact point, rolling, and steering. What is important for this dissertation is how we view the caster DOFs.

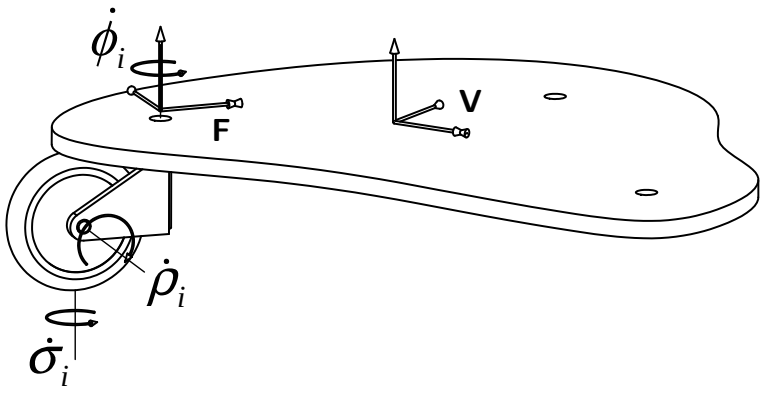

Figure 3.6: Degrees of freedom for a caster

Many of the ideas in this dissertation are rooted in the literature and terminology of serial and parallel chain robot manipulators.[1] In the remainder of this dissertation I will approach the caster mechanism as a three DOF serial chain manipulator which is fixed to the ground at the contact point and is used to control the manipulator endpoint, which will be coincident with origin of the vehicle coordinate frame, **V**. As shown in Figure 3.7, the caster mechanism can rotate about the twist axis which passes through the contact point; it can translate by rotation of the wheel about the roll axis; and the body of the caster mechanism (Figure 3.6), a.k.a. the arm of the manipulator (Figure 3.7), can rotate about the steer axis. The three revolute freedoms are the *joints* of PCV mechanism.

[1]The dissertation presented here is the second topic I studied in depth during my years at Stanford. The approaches I take here show the influence of my earlier research. Prior to the study of mobile robot design, I outlined the design of a 10 DOF high performance robot arm, ARTISAN; built a one DOF prototype actuator mechanism for the parallel end effector; and conceived and built a two DOF wrist prototype with high-ratio one-stage evoloid gearing and novel, asymmetric, integrated joint torque sensing. [34]

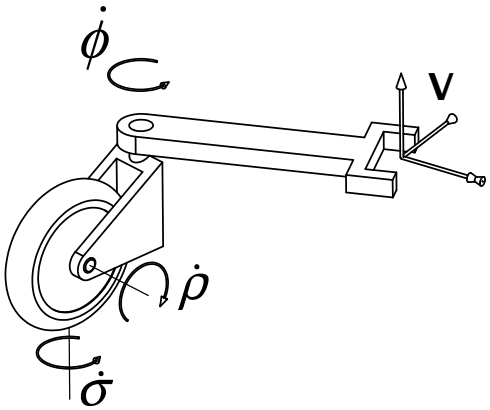

Figure 3.7: A powered-caster "manipulator"

To facilitate the understanding of the caster kinematics, we can represent the nonholonomic caster system with an instantaneously equivalent holonomic representation (see Figure 3.8). This holonomic representation is useful to picture the velocity relationships between the joint speeds and the endpoint speeds of the arm. The relations between the two sets of speed can be written as a Jacobian matrix, J_i.

When using the holonomic representation, we must remember that it is valid for infinitesimally small displacements. If we were allowed to reconfigure the holonomic representation, it may be possible to introduce a singularity. When $\sigma = \pm 90^\circ$, the holonomic mechanism is in a singularity and loses a DOF. However, the model is kinematically similar to the nonholonomic mechanism only when $\sigma = 0^\circ$. In this configuration, the equations for rolling motion, eqn. 3.10, are valid.

Because at any instance we can construct a holonomic, serial chain *manipulator* representation of a caster module, some important theoretical kinematic and dynamic properties can be explored. It is in this context that many of the properties of a PCV will be derived.

Continuing with the terminology of serial chain robot manipulators, it is easy to see why a steerable wheel with zero caster distance was called redundant by Muir and Neuman. This form of the mechanism is singular since the $\dot{\sigma}$ and $\dot{\phi}$ rotations are co-axial. It has lost a degree of freedom at the endpoint and gained an internal degree of freedom. We can demonstrate this singularity: as the endpoint is held fixed in location and orientation, it

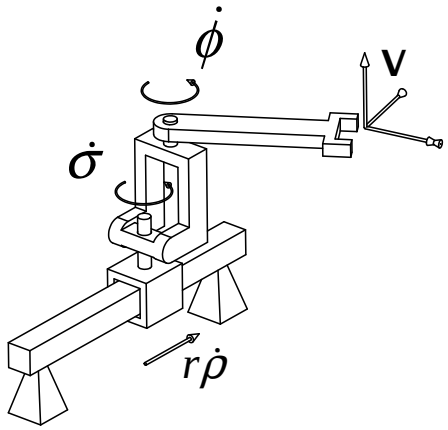

Figure 3.8: An instantaneous holonomic caster representation

is still possible to steer the wheel and internally reconfigure the mechanism. While it is less obvious because of the coupling introduced, a steered wheel with intersecting roll and steer axes is still singular even when the steer axis does not pierce the contact point. We can, as before, demonstrate the redundancy by holding the endpoint fixed and observing the ability of the wheel to continue to roll around an internal DOF without affecting the endpoint position or orientation.[2] Since each wheel of a holonomic mobile robot must have three DOF, a PCV must always have a non-zero caster distance.

The kinematics of a manipulator define the relationships between the speeds of the joints of the manipulator and the Cartesian speeds of the end effector or more precisely, the *operational point*. So as we treat each caster as a manipulator—beginning at the wheel contact points, $\mathcal{C}_i$, and propagating forward just as with any serial chain mechanism, we easily find the *wheel Jacobian,* J_i, which relates the three wheel joint speeds, $\dot{\mathbf{w}}_i$, and the operational point speeds, $\dot{\mathbf{x}}$.

$$\dot{\mathbf{w}}_i = \begin{bmatrix} \dot{\phi}_i \\ \dot{\rho}_i \\ \dot{\sigma}_i \end{bmatrix} \tag{3.11}$$

$$\dot{\mathbf{x}} = \mathsf{J}_i \, \dot{\mathbf{w}}_i \tag{3.12}$$

[2]This is precisely the effect which is exploited by syncro-drive mobile robots to steer in place.

As shown in Figure 3.7, $\dot{\phi}$ is the steering rate, $\dot{\rho}$ is the angular speed of rolling, and $\dot{\sigma}$ is the angular twist rate at the wheel contact. With the planar workspace of our manipulators, the operational speeds are expressed:

$$\dot{\mathbf{x}} = \begin{bmatrix} \dot{x} \\ \dot{y} \\ \dot{\theta} \end{bmatrix} \tag{3.13}$$

Because of the parallel nature of the final mechanism, it will be more useful to work with the *wheel constraint matrix*, J^{-1}. The wheel constraint matrix is the relationship between operational and joint speeds, the opposite relationship of the Jacobian. It can be computed by symbolically inverting the wheel Jacobian from eqn. 3.12, or derived directly by inspection. The wheel constraint matrix of a caster is always rank three—full rank for its size, and the motion space to which the PCV is confined.

$$\dot{\mathbf{w}}_i = \mathsf{J}_i^{-1}\, \dot{\mathbf{x}} \tag{3.14}$$

$$\mathsf{J}_i^{-1} = \begin{bmatrix} -\mathrm{s}\phi/b & \mathrm{c}\phi/b & h[\mathrm{c}\beta\mathrm{c}\phi + \mathrm{s}\beta\mathrm{s}\phi]/b - 1 \\ \mathrm{c}\phi/r & \mathrm{s}\phi/r & h[\mathrm{c}\beta\mathrm{s}\phi - \mathrm{s}\beta\mathrm{c}\phi]/r \\ -\mathrm{s}\phi/b & \mathrm{c}\phi/b & h[\mathrm{c}\beta\mathrm{c}\phi + \mathrm{s}\beta\mathrm{s}\phi]/b \end{bmatrix} \tag{3.15}$$

As written here, the scalars $\phi,\ b,\ r,\ h,\ \beta$ are assumed to be the i^{th} scalar which belongs to the i^{th} module, and are shown without their subscripts for compactness. For compactness we use $\mathrm{s}\cdot$ and $\mathrm{c}\cdot$ as shorthand for $\sin(\cdot)$ and $\cos(\cdot)$.

The kinematic dual of eqn. 3.14 describes the relationships between joint torques, $\mathbf{\Gamma}_i$, and operational point forces.

$$\mathbf{\Gamma}_i = \begin{bmatrix} \Gamma_{\phi i} \\ \Gamma_{\rho i} \\ \Gamma_{\sigma i} \end{bmatrix} \tag{3.16}$$

$$\mathbf{F} = \mathsf{J}_i^{-\mathsf{T}}\, \mathbf{\Gamma}_i \tag{3.17}$$

The joint torque, $\Gamma_{\phi i}$, is the steer actuator; the torque, $\Gamma_{\rho i}$, is the roll actuator; and $\Gamma_{\sigma i}$ is the

twist actuator. The spatial representation of the Cartesian forces at the operational point is

$$\mathbf{F} = \begin{bmatrix} F_x \\ F_y \\ M_z \end{bmatrix} \tag{3.18}$$

with F_x and F_y two linear forces, and M_z a moment on the vehicle body in the direction of the vehicle z-axis.

It is interesting to note that the first two rows of the wheel constraint matrix, J^{-1}, express the nonholonomic constraints due to ideal rolling, while the third row is a holonomic constraint, that when integrated becomes:

$$\theta = \sigma - \phi \tag{3.19}$$

3.5 Inverse Kinematics

A powered-caster vehicle can be viewed as a collection of cooperating, powered-caster manipulators which all are attached to the same operational point. The PCV is expected

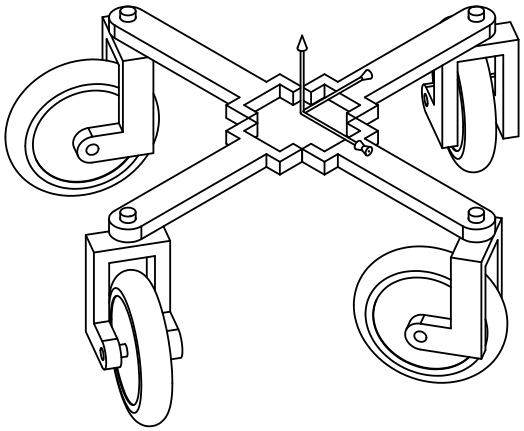

Figure 3.9: Cooperating caster manipulators

to have exactly three freedoms, regardless of the number of wheels in the mechanism. We

can show this using the planar form of Grübler's formula [16].

$$F = 3(l - j - 1) + \sum_{i=1}^{j} f_i \tag{3.20}$$

$$F = 3(2 + 2\mathfrak{n} - 3\mathfrak{n} - 1) + 3\mathfrak{n} = 3 \tag{3.21}$$

The number of links is $l = 2+2\mathfrak{n}$, with 1 link for the robot body, 1 link for the ground, and $2\mathfrak{n}$ links for the $\mathfrak{n}$ wheels and $\mathfrak{n}$ forks. The number of joints, $j = 3\mathfrak{n}$, is three joints per wheel module: steering, rolling, and twisting at the contact point. Finally, $f_i = 1$, since each joint has 1 DOF. This results in exactly three DOF (eqn. 3.21) the same number of variables as needed to describe the vehicle coordinates (Figure 3.2), as would be expected for a holonomic mechanism.

Ultimately, we would like to control the position, velocity, and acceleration of the PCV using the actuators and encoders in the powered-casters. Because of the nonholonomic constraints at the wheels, it is not possible to get a relationship between the joint positions and the robot positions. We can derive, however, a simple relationship between the joint velocities and the robot velocities.

In a PCV there are nonholonomic rolling constraints which reduce the number of degrees-of-freedom to be less than the number of generalized coordinates. The general form of the constraint equations express the dependence of some joint speeds, $\dot{\mathbf{q}}_{p+1}, ..., \dot{\mathbf{q}}_n$, on a set of independent, generalized speeds, $\dot{\mathbf{q}}_1, ... , \dot{\mathbf{q}}_p$, where p is the number of generalized speeds, and n is the total number of speeds. The generic constraint equations can be written with the dependent joint speeds expressed as linear combinations of the independent generalized speeds

$$\dot{\mathbf{q}}_r = \sum_{s=1}^{p} A_{rs}\dot{\mathbf{q}}_s + B_r \qquad (r = p + 1, ..., n) \tag{3.22}$$

where A_{rs} and B_r can be functions of the configuration variables but contain no speeds.

The PCV is a parallel mechanism—it has multiple contacts with the ground which attach through multiple paths to the end effectors which hold the same operational point

attached to the vehicle body. It is easy to derive the inverse kinematics for a parallel mechanism. The inverse kinematics tell us what joint velocities result from a given operational point velocity. Starting with an arbitrary robot velocity, $\dot{\mathbf{x}}$, we can use the results of the previous section to write the corresponding caster module joint speeds. The inverse kinematics of the PCV can be expressed as a collection of wheel module kinematics. Using $\dot{\mathbf{w}}_i$ from eqn. 3.11, J_i^{-1} from eqn. 3.15, and $\mathbf{\Gamma}_i$ from eqn. 3.16

$$\dot{\mathbf{w}} = \begin{bmatrix} \dot{\mathbf{w}}_1 \\ \dot{\mathbf{w}}_2 \\ \vdots \\ \dot{\mathbf{w}}_n \end{bmatrix} \quad ; \quad \mathsf{J}^{-1} = \begin{bmatrix} \mathsf{J}_1^{-1} \\ \mathsf{J}_2^{-1} \\ \vdots \\ \mathsf{J}_n^{-1} \end{bmatrix} \quad ; \quad \mathbf{\Gamma} = \begin{bmatrix} \mathbf{\Gamma}_1 \\ \mathbf{\Gamma}_2 \\ \vdots \\ \mathbf{\Gamma}_n \end{bmatrix} \tag{3.23}$$

the full inverse kinematics are:

$$\dot{\mathbf{w}} = \mathsf{J}^{-1}\,\dot{\mathbf{x}} \tag{3.24}$$

$$\mathbf{F} = \mathsf{J}^{-\mathsf{T}}\,\mathbf{\Gamma} \tag{3.25}$$

3.6 Robot Inverse Kinematics

Because, mechanically, it would be difficult, if even possible, to directly sense the twist DOF, $\dot{\sigma}$, we would prefer to eliminate the use of this variable from the control and sensing of the PCV. Taking advantage of the system's redundancy, we can eliminate these quantities. Thus, we will express the sensed joint speeds, which we will call the *robot joint speeds*, $\dot{\mathbf{q}}$, as including only the steer and roll DOFs, $\dot{\phi}$ and $\dot{\rho}$:

$$\dot{\mathbf{q}}_i = \begin{bmatrix} \dot{\phi}_i \\ \dot{\rho}_i \end{bmatrix} \quad ; \quad \dot{\mathbf{q}} = \begin{bmatrix} \dot{\mathbf{q}}_1 \\ \dot{\mathbf{q}}_2 \\ \vdots \\ \dot{\mathbf{q}}_n \end{bmatrix} \tag{3.26}$$

Similarly, it would be difficult to actuate the twist DOF, so it is useful to eliminate them and express the relationships between the operational space forces and the torques at the

actuated joints, or *robot joint torques*, $\mathbf{\Gamma}$, where

$$\mathbf{\Gamma}_i = \begin{bmatrix} \Gamma_{\phi i} \\ \Gamma_{\rho i} \end{bmatrix} \quad ; \quad \mathbf{\Gamma} = \begin{bmatrix} \mathbf{\Gamma}_1 \\ \mathbf{\Gamma}_2 \\ \vdots \\ \mathbf{\Gamma}_n \end{bmatrix} \tag{3.27}$$

We can express the sensed joint speeds in terms of the vehicle speeds by using the two equations which describe the nonholonomic constraints at each contact point to form the *wheel constraint matrix*, C_i.

$$\mathsf{C}_i = \begin{bmatrix} -\mathrm{s}\phi/b & \mathrm{c}\phi/b & h[\mathrm{c}\beta\mathrm{c}\phi + \mathrm{s}\beta\mathrm{s}\phi]/b - 1 \\ \mathrm{c}\phi/r & \mathrm{s}\phi/r & h[\mathrm{c}\beta\mathrm{s}\phi - \mathrm{s}\beta\mathrm{c}\phi]/r \end{bmatrix} \tag{3.28}$$

$$\dot{\mathbf{q}}_i = \mathsf{C}_i \, \dot{\mathbf{x}} \tag{3.29}$$

The scalars $\phi,\ b,\ r,\ h,\ \beta$ are again shown without their assumed i subscripts for compactness. Gathering the equations from each caster to form a complete description of the PCV we get

$$\mathsf{C} = \begin{bmatrix} \mathsf{C}_1 \\ \mathsf{C}_2 \\ \vdots \\ \mathsf{C}_n \end{bmatrix} \tag{3.30}$$

$$\dot{\mathbf{q}} = \mathsf{C} \, \dot{\mathbf{x}} \tag{3.31}$$

$$\mathbf{F} = \mathsf{C}^\mathsf{T} \, \mathbf{\Gamma} \tag{3.32}$$

The matrix, C, in eqn. 3.31, is the *robot constraint matrix*. It describes the relationships between the $2n$ sensed joint speeds, $\dot{\mathbf{q}}$ and the 3 operational speeds, $\dot{\mathbf{x}}$; as well as the relationships between the $2n$ torques, $\mathbf{\Gamma}$, of the actuated joints and the 3 operational forces, $\mathbf{F}$, of the robot body.

The *robot constraint matrix*, C, is a type of Jacobian matrix as it describes the mapping from robot Cartesian speeds to robot joint speeds, a mapping opposite that of the traditional

Jacobian. The robot constraint matrix is found directly from the kinematics of the PCV and is not an algebraic inversion of the more usual Jacobian, written J, as in: $\dot{\mathbf{x}} = J\dot{\mathbf{q}}$, and so is represented without using the 'inverse' notation; as, C, not, J^{-1}.

Chapter 4

Design

4.1 PCV Design Goals

The design evolution of a mechanical system is highly dependent upon the mechanism's desired tasks and operating environment. To keep the discussion in this chapter finite, I will focus upon the design of the PCV which is optimized for use as an "office" robot. An office-type robot has been the most common goal of previous holonomic vehicle designs and so will lend itself most readily to direct comparisons. The mobile robot being designed here will have two primary uses: as a mobile agent which will maneuver throughout a building, and as a mobile platform integrated into a mobile manipulation system. It should be noted that the issues examined in this chapter are important to the design of all PCVs and will be relevant to the PCV designer with different design goals than those presented. This chapter will explore the mechanical design of the powered-caster vehicle or PCV, detail its advantages, and show the important design decisions for an indoor mobile robot. This concept germinated and was nurtured at Nomadic Technologies, Inc. where much of the design work discussed in this dissertation took place. The result of this design has grown into the commercially available Nomad XR4000 produced by Nomadic Technologies.

4.1.1 Holonomic Mobility

The primary goal when designing a holonomic mobile robot is to produce a vehicle body which moves equally well in each of its three degrees of freedom. The user of the holonomic mobile robot should be able to treat the robot as if it were "floating" across the ground; the workings of the particular mechanism used to create motion should be transparent with respect to the control of the vehicle.

A big advantage that a holonomic vehicle has over a nonholonomic vehicle is that the controller, and consequently the planner, do not have to understand the state of the system. In a nonholonomic system such as a car, the current vehicle orientation as well as the steering angle dictate which motions are possible at any given instant. In a PCV the knowledge of the system's steer angles is only needed at the lowest controller level as is discussed in this work. Those who wish to build a system onto a PCV will be able to use a decoupled controller—including the case of mobile manipulation where holonomic mobility is especially important.

4.1.2 Smooth Motion

As seen in Chapter 2, a wide variety of mechanisms have been developed to create a holonomic wheeled vehicle. One common fault these designs all share is that they all experience vibrations during motions due to the way that holonomic motion is achieved. The quality of motion of a wheeled mobile robot is dependent on a lack of vibrations.

The PCV, in contrast, because it employs round, normal wheels, produces smooth rolling motions with no mechanical source of vibrations. On any given wheel there is one contact point which moves in a smooth, continuous manner, and thus vibrations from shifting support points or discontinuous wheel velocities are not created. Another improvement is that the location of each contact point is well known so that control is more exact. Also, because there are no passive bodies, and, more importantly, no unmeasured bodies in a powered-caster design, the dynamics of the system can be fully and accurately modeled.

Each wheel mechanism contains a single nonholonomic wheel which is large enough for good ground clearance [86]. A PCV is the only holonomic mechanism which can be designed to effectively use currently available pneumatic tires. The benefits of using

pneumatic tires are well understood and include traction, suspension, vibration control, noise abatement, and the ability to use a wide variety of off-the-shelf components.

4.1.3 Control vs. Design

The design of a powered-caster vehicle is unique among holonomic vehicle designs because the required control is configuration dependent and time-varying. Upon examining the designs in Chapter 2, it can be shown that other holonomic vehicles, in contrast, were designed for ease of control. All of the designs were controllable with no knowledge of the internal configuration of the robot mechanism, and no designs required a time-varying control for a constant desired motion in local coordinates. Unfortunately, other desirable qualities such as smooth motion and the ability to surmount floor irregularities were sacrificed.

Because the use of computers for the control of complex, configuration and time dependent systems is well established, it is not necessary to limit the abilities and qualities of a holonomic vehicle to simplify the control of the vehicle. We can therefore design a holonomic vehicle using the concept of powered-casters which addresses all of the shortcomings of previous holonomic vehicle designs.

4.1.4 Mobile Manipulation

One of the criteria for the design of a PCV in the context of the Stanford Robotics Laboratory “manips” research group is that it should be a capable platform for mobile manipulation. In order to build a prototype mobile manipulation system, I limited my search of manipulators to currently available industrial robot arms with the following qualifications:

- at least six degrees of freedom
- adequate control bandwidth for experiments in dynamic control
- a reach of about a meter for interaction with people
- ability to use 50 volts direct-current for power
- availability of an open architecture controller

The only readily available robot arm in the United States which meets these criteria is the PUMA 560, and so it was decided that the PCV would need to support this manipulator. The need to support a 130 lb. manipulator which can draw 20 Amperes of electrical current restricts the minimum size which a vehicle can safely be. The effects of this decision can been seen in many of the following discussions.

4.2 Geometry, Layout, and Component Selection

The geometry, layout, and component selection for the mechanical design of the PCV determines the suitability of the vehicle for its environment and intended tasks. These factors determine the robot size and shape, the composition of the caster modules, and the relative distribution of the components in the robot.

4.2.1 Size

A mobile robot which will work in an office environment with people should not be too small nor too large. A robot which is too large could fill a hallway so that no people could pass, at least not comfortably. At a maximum, a mobile robot will must be able to pass through a standard doorway or else it will not be able to maneuver throughout the building. In the United States the opening of a standard doorway, including the width taken by the open door, is approximately 30 inches, or about 76 cm. In other parts of the world it can be slightly smaller. Leaving at least several centimeters of clearance per side as a reasonable precaution, the size of a doorway limits the maximum width of an office mobile robot to 68 cm or less.

Yet, a robot which is too small will likely be stepped on, damaging the robot or possibly injuring its assailant. A mobile robot which is at least as large as a child should be easily recognizable and so avoid the danger of being overlooked.

A larger practical minimum size limitation is presented when it is required (see Section 4.1.4) that the mobile robot be capable of carrying a manipulator arm for research in dynamic control of mobile manipulation systems. Some of the aspects of the PUMA 560 manipulator which directly affect the necessary size of the mobile robot follow. A PUMA 560

manipulator is relatively tall and heavy, so the stability of the system is a concern during the design of the PCV. The support of the electrical requirements of the manipulator in addition to those of the PCV require a substantial volume to house the lead-acid batteries which are to be the power source. While batteries which are large enough to supply the system inflate the size of the PCV, if carefully arranged (see Section 4.2.5) they also act as ballast, increasing the stability of the mobile manipulation system.

4.2.2 Shape

A holonomic mobile robot has, by definition three independent DOFs. Because I wish to exploit the decoupled nature of the DOFs of a holonomic mobile robot, the robot should be designed so that it does not have a preferred direction of travel due to the robot shape. For example, the motion of a rectangular mobile robot must be designed such that the orientation of the robot body is considered for each motion executed. Specifically, a rectangular mobile robot may need to have its orientation DOF restricted to pass down a hallway without collision. This restriction adds a form of coupling between the linear and rotational DOFs. The independence of the three DOFs can be assured by choosing a circular shape for the robot body. A holonomic mobile robot that has a circular shape can always reorient regardless of its position and linear velocity in its environment.

The holonomic robot should also not have a preferred direction due to the configuration of the drive system. The position and orientation of the drive elements should not require, for example, motion on the local frame x-direction to assure the greatest obstacle traversal ability. The design of the drive system must allow equal ability to move in an arbitrary direction at any time.

A faceted shape which closely approximates a cylinder can be used with equal geometric utility. The facets can be used to hold an array of skin-mounted sensors at well-defined orientations and this shape is easier to manufacture than a pure cylinder. A drawing of the XR4000 hull, Figure 4.1, shows the facets, upper and lower sensor rings, and approximately cylindrical shape. The “smile” on the front of the robot is a window for a laser rangefinder sensor.

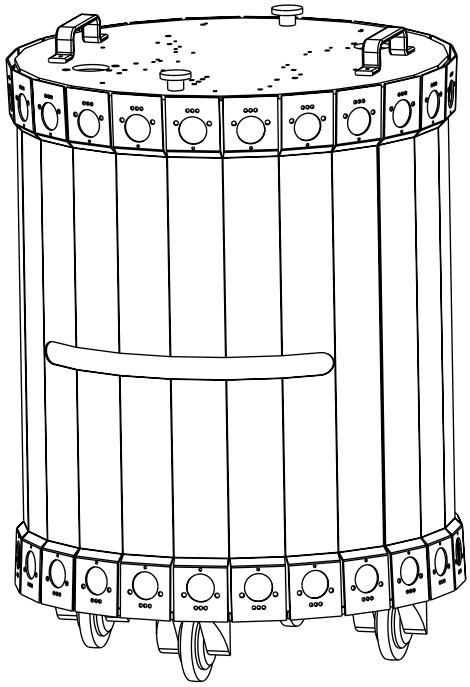

Figure 4.1: Nomadic Technologies XR4000 robot

4.2.3 Modularity

The definition of the PCV encompasses systems with two or more, possibly unique, powered-caster modules. Each powered-caster could theoretically have different motors, its own wheel radius and caster offset, and an arbitrary location on the robot. It is not clear what benefit would be gained by mixing different sized components in a holonomic mobile robot since each module will be performing a similar task. We consider a modular PCV design in which all caster modules are similar and can replace one another without changing the nature of the robot. Repeatedly using the same module design, with common geometry and actuators, has several important benefits. It simplifies the theoretical discussion; many of the indexed values such as wheel radius and caster offset lose their indices and become a single constant. The practical issues of component design, production, and maintenance are all simplified when a single module design is used for each desired wheel. A common caster module design has desirable dynamic properties, enhancing the isotropic nature of

the mechanism, as will be shown later. Therefore, without loss of generality, this thesis will focus on and highlight PCVs composed of identical powered-caster units.

A PCV consists of n driven and steered wheel modules, known as *powered-casters*, and a main body to which the powered-casters are attached as in Figure 4.2. A modular

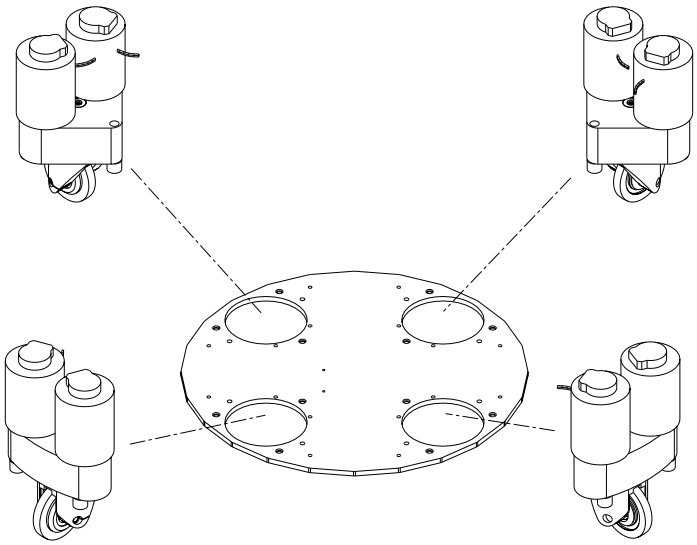

Figure 4.2: A PCV base with four powered-caster modules (exploded view)

approach simplifies the layout of the internal structure of the robot. It is mechanically much simpler than traditional robots which used syncro-drive mechanisms that use transmission belts or linkages and tie all the wheels together at several different levels. Since only electrical connections are needed to couple the caster modules together, the modules can be placed about the robot as desired and the spaces between the modules need only have a small amount of space reserved for these few wires.

4.2.4 Symmetry

The scheme of the mobile robot can be simplified by only considering symmetric designs. A symmetric design places all the, n, module steer-points equispaced on a circle of radius

h with all the location angles, β_i such that

$$\beta_i = \frac{(i-1)}{\mathfrak{n}} \, 2\pi \tag{4.1}$$

A symmetric, holonomic mobile robot makes intuitive sense since the robot may move in any direction. There is no "front" to the robot, and, as stated in Section 4.2.2, there should be no preferred direction due to the robot structure.

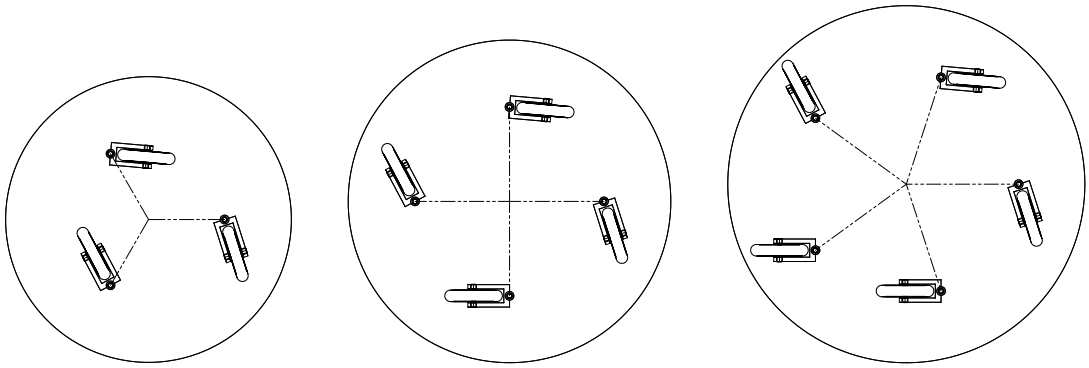

Figure 4.3: Symmetric PCVs with 3, 4, and 5 powered-casters

Using a symmetric design is also beneficial for dynamic reasons. It is a good strategy for assuring that the motor torques will be distributed evenly, and it leads to nearly isotropic acceleration abilities and nearly isotropic reflected mass properties.

4.2.5 Packaging

Many geometric factors affect the simple packaging of the components. The layout of the caster modules defines the space remaining, primarily for the batteries. With the casters and batteries packed in tightly, the minimum size of the robot may be limited.

As the robot is made more compact, the motors crowd together and threaten to protrude from the robot outline. At the same time, it is desirable to design the PCV so that the wheel cannot protrude from the outline of the robot either. To ensure that at all times the wheels

remain under a circular robot the following inequality must be obeyed

$$R > h + b + r \tag{4.2}$$

where R is the radius of the robot, h is the distance from the center to the steer axis, b is the caster offset, and r is the wheel radius.

Because, as will be shown later, we cannot control the positions of the caster joints, we will need to insure that the swept volume of each caster does not intersect any other caster's swept volume. Values for theses geometric parameters must be selected so that

$$h \tan\left(\frac{\pi}{\mathfrak{n}}\right) - b - r > 0 \tag{4.3}$$

assuming that the wheels are symmetrically arranged about the PCV. The structure of the PCV itself should be designed to allow the casters unrestricted motion as well.

This is balanced by the desire to increase the wheel radius so that the wheels can be large enough to surmount anticipated obstacles. The PCV design can be optimized to find a good compromise in wheel size which gives a smooth ride and can traverse office-type obstacles, while still fitting within the robot and not interfering. Other types of holonomic mobile robots with passive rollers tend to have small rollers or rollers which taper down to have a small cross section near the ends, and hence have poor performance when negotiating the same obstacles which are handled by the larger normal wheels of a PCV.

4.2.6 Suspension

Most vehicles have some type of suspension—typically either pnuematic tires, sprung wheels, or both. A PCV is unique among holonomic vehicle designs in that it can readily accommodate both types of suspension. Pneumatic wheels, or tires, provide excellent vibration dampening, traction, and wear properties. They are readily available and well understood.

Because of the modularity of the PCV powered-casters, each powered-caster can be isolated from the main body of the vehicle by a spring/damper arrangement. There is no mechanical linkage between modules as in many other mobile robot designs, so each

module can move independently. The addition of vertical travel to the modules provides increased isolation from the terrain irregularities.

4.2.7 Number of Wheels

A PCV can mathematically be constructed of two or more caster modules. For a vehicle rolling on the ground, however, two wheels are not enough to form a stable platform which will not fall over. In choosing how many powered-caster modules to use, the designer should balance the tradeoffs of load capacity, stability, and packaging.

A larger number of wheels will improve the load capacity of the robot by distributing the weight over a greater number of wheels. A greater number of wheels will also tend to increase the stability of the robot. As the number of caster modules is increased, however, implementation becomes less practical due to increased complexity, robot weight, and lack of space to accommodate the greater number of modules.

If the goal is to design and *build* a PCV, then in order to minimize wasted space, one very practical consideration cannot be avoided: "Batteries are square." A close packing of rectangular objects (lead-acid batteries) favors robot layouts with multiples of four wheels. A PCV with four caster modules, rather than eight or twelve, was chosen as a good compromise which minimizes robot complexity and weight while providing good stability and load capacity.

4.3 Module Structure

4.3.1 Powered-Caster Module Design Issues

A PCV is composed of powered-caster modules; an example of a powered-caster module is one which I designed for the Nomad XR4000 mobile robot as shown in Figure 4.4. The design goals for the powered-caster module must support the design goals for the robot as discussed in Section 4.1.

To achieve those goals the powered-caster modules must be compact. Using a gearing arrangement with vertically oriented motors gives a more compact design than one in which the motors are sticking out horizontally from the gearbox. Vertically oriented motors

benefit the design by allowing the use of helical gearing at their output, rather than bevel gearing. Helical gears are stronger, smoother, quieter, and less expensive than bevel gears.

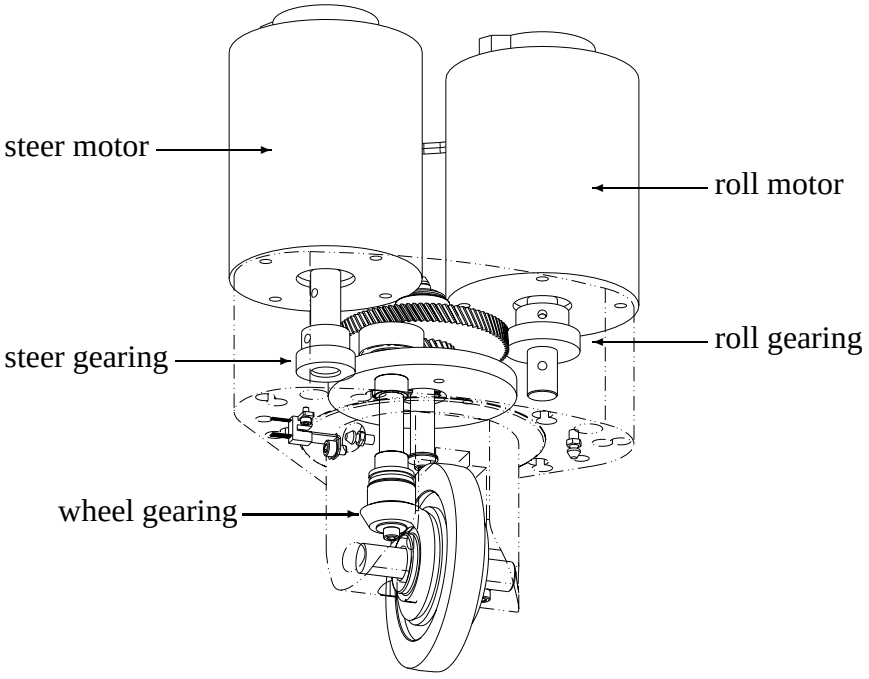

Figure 4.4: Powered-caster module

The gearbox arrangement is designed to allow continuous steering, a feature which is required by the PCV concept. All the gears used are low-ratio helical or spiral-bevel gears and are are fully back-driveable which greatly improves the suitability of the mechanism for use with a force based controller.

Since no real surface is perfectly flat, the wheels should be designed to be large enough to roll over small bumps, divots, and obstacles [87, 26]. The wheel size is soon limited, however, by the interactions between wheel modules as discussed earlier. I found that a 11 cm diameter gives a good balance so that a compact overall robot size is maintained with larger, smooth-rolling wheels.

4.3.2 Gearbox Kinematics

The kinematic and dynamic models of the PCV are developed using the joint coordinates and speeds of the caster modules. As in most robots, the actuators and encoders of the PCV are isolated from the joints by a gearbox. It is important to understand the gearbox relationships to analyze and implement a complete solution.

We begin with the motor speeds, $\dot{\mathbf{w}}$, composed of the steer motor speed $\dot{\mathrm{w}}_{i,\mathrm{steer}}$, and roll motor speed, $\dot{\mathrm{w}}_{i,\mathrm{roll}}$, for each powered-caster module.

$$\dot{\mathbf{w}} = \begin{bmatrix} \dot{\mathbf{w}}_1 \\ \dot{\mathbf{w}}_2 \\ \vdots \\ \dot{\mathbf{w}}_\mathrm{n} \end{bmatrix} \quad ; \quad \dot{\mathbf{w}}_i = \begin{bmatrix} \dot{\mathrm{w}}_{i,\mathrm{steer}} \\ \dot{\mathrm{w}}_{i,\mathrm{roll}} \end{bmatrix} \tag{4.4}$$

Likewise, the motor torques, $\boldsymbol{\tau}$, are made up of the steer motor torque, $\tau_{i,\mathrm{steer}}$, and roll motor torque, $\tau_{i,\mathrm{roll}}$, for each powered-caster module.

$$\boldsymbol{\tau} = \begin{bmatrix} \boldsymbol{\tau}_1 \\ \boldsymbol{\tau}_2 \\ \vdots \\ \boldsymbol{\tau}_\mathrm{n} \end{bmatrix} \quad ; \quad \boldsymbol{\tau}_i = \begin{bmatrix} \tau_{i,\mathrm{steer}} \\ \tau_{i,\mathrm{roll}} \end{bmatrix} \tag{4.5}$$

The relationship between the joint speeds, $\dot{\mathbf{q}}$, and the motor speeds, $\dot{\mathbf{w}}$, can be given simply as:

$$\dot{\mathbf{w}} = \mathbf{N}\,\dot{\mathbf{q}} \tag{4.6}$$

while its dual, relating the motor torques, $\boldsymbol{\tau}$, and the joint torques, $\boldsymbol{\Gamma}$, is:

$$\boldsymbol{\Gamma} = \mathbf{N}^\mathsf{T}\,\boldsymbol{\tau} \tag{4.7}$$

The gearbox matrix, $\mathbf{N}$, is block diagonal with repeated powered-caster module gearbox

matrices, $\mathbf{N}_0$.

$$\mathbf{N}_0 = \begin{bmatrix} -\eta_s & -\eta_r \\ 0 & \eta_r\eta_w \end{bmatrix} \quad ; \quad \mathbf{N} = \begin{bmatrix} \mathbf{N}_0 & & 0 \\ & \ddots & \\ 0 & & \mathbf{N}_0 \end{bmatrix} \tag{4.8}$$

The individual terms can be expressed using the individual gear ratios described in Table 4.1 and shown in Figure 4.4. The actual values or the Nomad XR4000 are also given in Table 4.1.

Table 4.1: Gear parameters

Description	Parameter	XR4000
Gear ratio of roll gearing	η_r	2.36
Gear ratio of steer gearing	η_s	3.32
Gear ratio of wheel gearing	η_w	2.00

4.4 Performance

The performance of a mobile robot, as for any robot, can be expressed in terms of position, velocity, and acceleration properties. Position performance is related to the quality of the mobile robot odometry. The odometry performance will be discussed later in the control section.

Velocity performance measures the top speeds attainable. The faster the robot can move; ideally, the more work the robot can complete. However, since this mobile robot is being designed to work where people are present, it is possible to have too high of a performance. For safety, a mobile robot which will be used around people should not be capable of speeds much above a walking pace. The maximum speed goal for the PCV is therefore between 1.0 m/s and 1.5 m/s.

Acceleration performance is measured by the peak accelerations achievable, and the quality of the acceleration is measured by the acceleration isotropicity. A robot which is

able to accelerate equally well in all directions, with similar units, has isotropic acceleration capabilities. Since, at each instant, the robot could be called upon to accelerate in any direction, isotropic acceleration capabilities are ideal. Just as it is desirable for the acceleration capabilities to be constant with respect to direction, it is ideal that the acceleration capabilities remain constant over time, independent of the robot state.

The achievable acceleration will ultimately be limited by the coefficient of friction of the wheels on the ground. Manipulators which are rigidly bolted to the floor are capable of several G's endpoint acceleration. High performance vehicles, however, begin to lose traction before reaching 1 G of acceleration. An ambitious acceleration goal for a mobile robot would be 0.5 G's with a more realistic goal of 0.2 G's or 2.0 m/s^2. Adding a manipulator on top of the PCV, especially a PUMA 560, encourages limiting the maximum acceleration capability so as to not tip over during peak acceleration.

The quality of the PCV as a base for mobile manipulation is affected by the shape of the reflected mass. A constant, isotropic reflected mass is ideal.

4.4.1 Speed

One fundamental design goal for a mobile robot is the ability to translate and rotate with sufficient speed. The PCV is designed to achieve the specified speed performance goals. The design criteria include top linear speed, top rotational speed, and required combinations of linear and angular speeds.

A battery driven PCV which is powered by mechanically commutated, brushed DC motors has theoretical top speeds which are limited by the available DC voltage, $\mathcal{E}_{\mathrm{b}}$, the voltage of the batteries. The torque, τ, produced by brushed DC motors is proportional to the current, i, flowing through the motor according to the motor's torque constant, $\mathcal{K}$.

$$\tau = \mathcal{K} i \tag{4.9}$$

A spinning brushed DC motor produces a back-EMF voltage, $\mathcal{E}_{\mathrm{emf}}$, proportional to the motor's speed, $\dot{\mathbf{w}}$, according to the *back-EMF constant*. Both the *torque constant* and the *back-EMF constant* are typically published, in appropriate units, in the specifications for motors made in the U.S.A. according to Imperial units. When using metric units, however,

the two constants are theoretically identical and in practice only differ by a few percent. Thus, we use the metric system, and can use the same symbol, $\mathcal{K}$, to represent both constants. The relationship between motor speed, $\dot{\mathbf{w}}$, and back-EMF becomes:

$$\mathcal{E}_{\text{emf}} = -\mathcal{K}\dot{\mathbf{w}} \tag{4.10}$$

Since the battery voltage is opposed by the back-EMF, the maximum speed that the motor can achieve occurs when the magnitude of the back-EMF equals the battery voltage, $|\mathcal{E}_{\text{emf}}| = \mathcal{E}_{\text{b}}$. At this point the current through the motor is zero, no torque is created, and thus, the motor cannot speed up further.

With knowledge of the gear ratios, and the geometry of the robot, we can translate top achievable motor speeds into top speeds for the robot. There are two conditions which limit the top speeds of the PCV. The first is the condition when the wheels are rolling. It is the most prevalent condition for the wheels of the robot. Using the maximum motor speed, the gear ratios in the transmission, and the kinematics of the caster mechanisms, we get the maximum theoretical speed at which the PCV can roll in a straight line.

$$v_{\text{max\_roll}} = \frac{r}{\eta_r \eta_w} \frac{\mathcal{E}_{\text{b}}}{\mathcal{K}} \tag{4.11}$$

With the wheels rolling at the same speed, but tangent to a circle instead of parallel to one another, the PCV is rotating in-place and the maximum rolling rotational speed is:

$$\dot{\theta}_{\text{max\_roll}} = \frac{1}{\sqrt{h^2 - b^2}}\, v_{\text{max\_roll}} \tag{4.12}$$

The linear and rotational conditions can be geometrically combined to determine the range of combined linear and rotational speeds which are possible under rolling wheel conditions. If we set the ratio of maximum linear speed to maximum rotational speed as, ϵ, with, $0 \leq \epsilon \leq 1$, then

$$v_{\epsilon\text{\_roll}} = \epsilon\, v_{\text{max\_roll}} \tag{4.13}$$

$$\dot{\theta}_{\epsilon\text{\_roll}} = (1 - \epsilon)\, \dot{\theta}_{\text{max\_roll}} \tag{4.14}$$

The second condition which affects top speeds of the PCV is the ability to use the steer

axis at speed when a wheel is transitioning from leading to trailing, *i.e.* executing a ***flip***. As wheel speeds increase it becomes less likely that a wheel will attain a leading configuration. This condition is a weaker limitation because it is not likely that all the wheels will flip together at top speed. In the event that one wheel exceeds its ability, the other wheels can compensate and are still sufficient to control the PCV through the quick transition. Still, it is instructive to understand the limitations imposed by the kinematics of the PCV. One maneuver which does routinely include wheel flips is when the PCV reverses directions. During this maneuver, even when accelerating to top speed, the wheel flips occur well before top speed is reached. The maximum linear speed for controlled wheel flip depends on both the steering and, because of gearbox coupling, translation motors:

$$v_{\max\_\text{steer}} = \min\left(\frac{b}{\eta_s}\frac{\mathcal{E}_\text{b}}{\mathcal{K}}\ ,\ \frac{b}{\eta_r}\frac{\mathcal{E}_\text{b}}{\mathcal{K}}\right) \tag{4.15}$$

It follows that the maximum rotational speed for controlled wheel flip is

$$\dot{\theta}_{\max\_\text{steer}} = \frac{1}{h}\, v_{\max\_\text{steer}} \tag{4.16}$$

Again, the linear and rotational conditions can be geometrically combined to determine the range of combined linear and rotational speeds which are possible during a well controlled wheel flip. If we set the ratio of maximum linear speed to maximum rotational speed as, ϵ, with, $0 \leq \epsilon \leq 1$, then

$$v_{\epsilon\_\text{steer}} = \epsilon\, v_{\max\_\text{steer}} \tag{4.17}$$

$$\dot{\theta}_{\epsilon\_\text{steer}} = (1-\epsilon)\, \dot{\theta}_{\max\_\text{steer}} \tag{4.18}$$

Using the parameters for the XR4000, the expected top speed performance limits are given in Tables 4.2 and 4.3 at a theoretical efficiency of 85%. We can see that the experimental values are only slightly lower than the computed values indicating that the actual robot drivetrain efficiency was slightly lower than assumed. Although the "max_steer" speeds are only half of the rolling speeds, they are adequate due to the reasons discussed previously. Careful selection must be made in order to obtain a mechanism which has the ability to reach the desired top speed while maintaining good acceleration properties. At the same time, by choosing components so that motor and gearbox speeds are kept low,

Table 4.2: Maximum linear speed

	Theoretical $(\frac{m}{s})$	Experimental $(\frac{m}{s})$
$v_{\text{max\_roll}}$	1.44	1.30
$v_{\text{max\_steer}}$	0.74	

Table 4.3: Maximum rotational speed

	Theoretical $(\frac{rad}{s})$	Experimental $(\frac{rad}{s})$
$\dot{\theta}_{\text{max\_roll}}$	6.69	6.50
$\dot{\theta}_{\text{max\_steer}}$	3.46	

mechanical noise due to high component speeds can be minimized, resulting in longer component life and an improved robot aesthetic.

The tradeoffs in top linear and rotational speeds expressed in eqns. 4.13 – 4.14 have been plotted on Figure 4.5 to show the total operating range of the XR4000 PCV. The end-points of the boundary line, shown as triangles, are given, on the x-axis, by the maximum linear speed, and on the y-axis by the maximum rotational speed. The motion of the robot for which the maximum linear speed, point 'A', was recorded is shown in Figure 4.6. The motion of the robot for which the maximum rotational speed, point 'D', was recorded is shown in Figure 4.7.

The robot was also commanded to execute several motions with combined linear and rotational speeds. During these motions the robot moves in a straight line while rotating. We call this motion a "Frisbee" motion because it is kinematically similar to the motion of a flying disk. The motion of the robot at a linear speed of 1.0 m/s with a rotational speed of 1.57 rad/s, point 'B', is shown in Figure 4.8. The motion of the robot at a linear speed of 0.5 m/s with a rotational speed of 4.0 rad/s, point 'C', is shown in Figure 4.9.

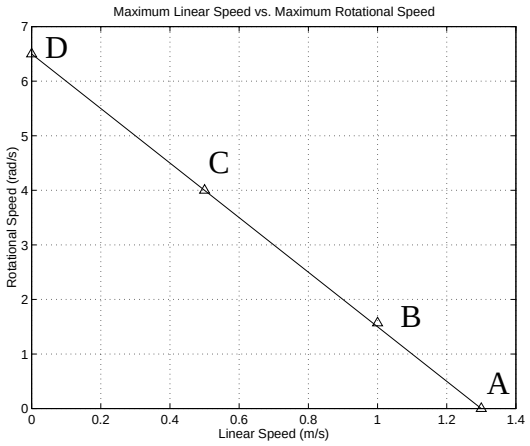

Figure 4.5: Maximum linear speed vs. maximum rotational speed

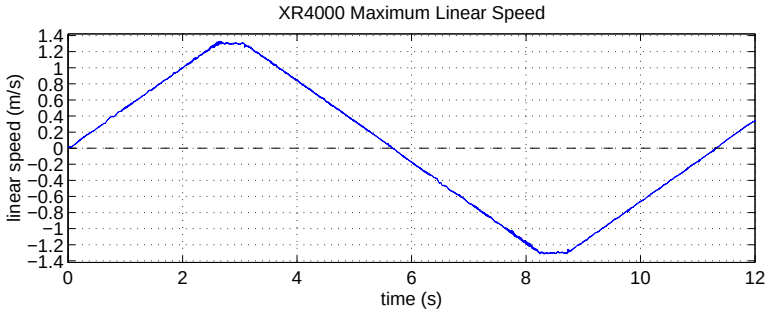

Figure 4.6: Maximum linear speed: point ‘A’

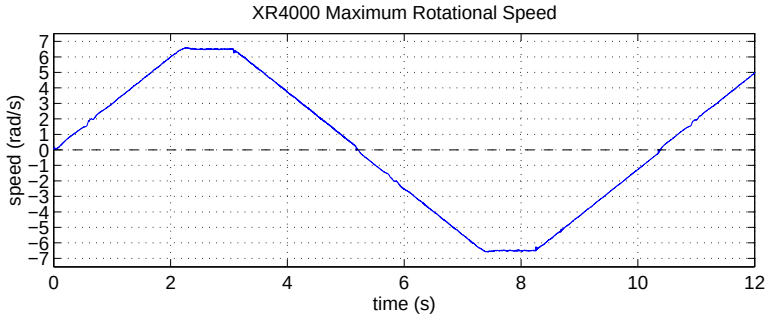

Figure 4.7: Maximum rotational speed: point ‘D’

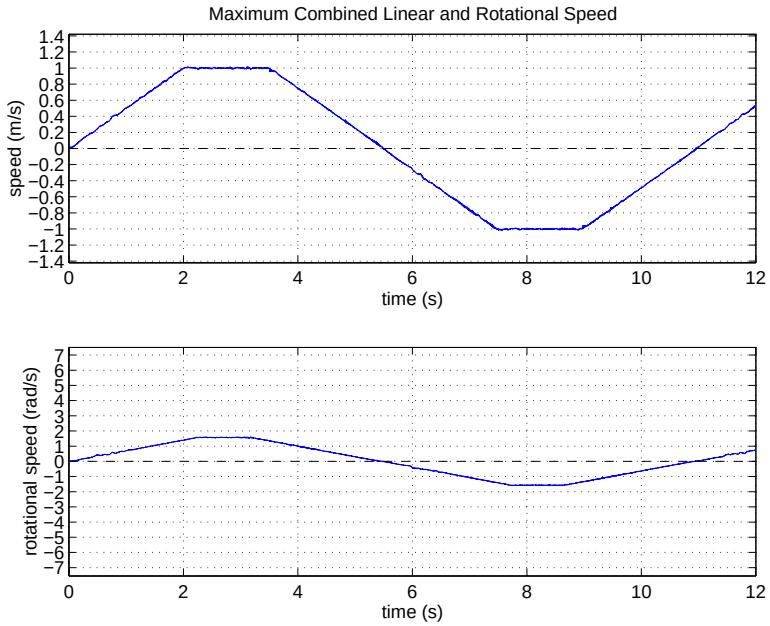

Figure 4.8: Maximum combined speed: point ‘B’

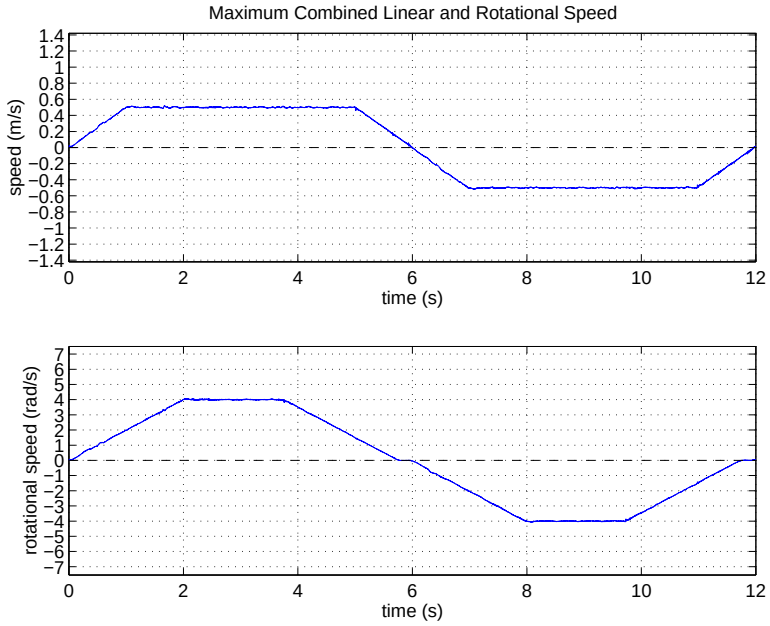

Figure 4.9: Maximum combined speed: point ‘C’

4.4.2 Acceleration

A holonomic mobile robot is distinguished by its ability to instantly accelerate in any direction. It is important that the acceleration ability is nearly isotropic and not greatly affected by the mechanism's changing configuration.

Design for the desired acceleration properties involves trade-offs with many factors, primarily the speed performance of the previous section. As before, the geometry, motor parameters, and gearing are central to the determination of the acceleration performance.

The acceleration of the PCV is governed primarily by two factors: the mass of the robot, which includes both the robot body mass and the reflected mass from the motors and gearing, and the torque capacity of the motors. The brush DC motors produce torque proportional to the current in the windings, as shown in eqn. 4.9. The maximum torque of the motors is determined by the maximum current, $i_{\max}$, which can be delivered by an amplifier to the motor.

$$\tau_{\max} = \mathcal{K} i_{\max} \tag{4.19}$$

With a symmetric design we can study the possible accelerations by analyzing one wheel module and one $\mathfrak{n}^{\text{th}}$ of the robot. Looking at the extreme cases which form a basis for an arbitrary acceleration, we have linear and angular acceleration accelerating with only the *roll* motors or only the *steer* motors. The inertia parameters, $\mathcal{I}$, are described in Table 4.4. The maximum linear acceleration, from rest, accelerating only the roll motors

Table 4.4: Inertia parameters of dynamic model

Description	Parameter	XR4000 (Kg m^2)
Inertia of fork and wheel, about steer axis	$\mathcal{I}_f$	$3.3\ 10^{-3}$
Inertia of roll motor rotor and pinion	$\mathcal{I}_r$	$2.6\ 10^{-4}$
Inertia of steer motor rotor and pinion	$\mathcal{I}_s$	$2.5\ 10^{-4}$
Inertia of translation gearing	$\mathcal{I}_g$	$4.9\ 10^{-4}$
Inertia of wheel, about roll axis	$\mathcal{I}_w$	$3.8\ 10^{-4}$
Inertia of robot body, about central vertical axis	$\mathcal{I}_R$	7.0

is:

$$a_{\max\_\text{roll}} = \tau_{\max\_\text{roll}} \frac{\eta_r \eta_w}{r} \left(\frac{\eta_r^2 \eta_w^2 \mathcal{I}_r + \eta_w^2 \mathcal{I}_g + \mathcal{I}_w}{r} + \frac{m}{\mathfrak{n}} \right)^{-1} \tag{4.20}$$

The maximum linear acceleration, from rest, accelerating only the steer motors is:

$$a_{\max\_\text{steer}} = \tau_{\max\_\text{steer}} \frac{\eta_s}{b} \left(\frac{\eta_s^2 \mathcal{I}_s + \mathcal{I}_f}{b} + \frac{m}{\mathfrak{n}} \right)^{-1} \tag{4.21}$$

The robot has this same acceleration capability in the direction perpendicular to a straight linear motion since that is also only dependent on the same parameters. For isotropic acceleration properties, $a_{\max\_\text{roll}}$ and $a_{\max\_\text{steer}}$ ideally should be approximately equal.

The maximum angular acceleration, from rest, accelerating only the roll motors is:

$$\alpha_{\max\_\text{roll}} = \tau_{\max\_\text{roll}} \frac{\eta_r \eta_w \sqrt{h^2 - b^2}}{r} \left((h^2 - b^2) \frac{\eta_r^2 \eta_w^2 \mathcal{I}_r}{r} + \frac{\mathcal{I}_R}{\mathfrak{n}} \right)^{-1} \tag{4.22}$$

The maximum angular acceleration, from rest, accelerating only the steer motors is:

$$\alpha_{\max\_\text{steer}} = \tau_{\max\_\text{steer}} \frac{\eta_s h}{b} \left(h^2 \frac{\eta_s^2 \mathcal{I}_s}{b} + \frac{\mathcal{I}_R}{\mathfrak{n}} \right)^{-1} \tag{4.23}$$

4.4.3 Stability

The stability of a vehicle determines under what conditions the vehicle will remain upright and under what conditions a vehicle will tip over. There are two types of stability criteria which are inherent in the design of a PCV: static stability and dynamic stability.

While static stability is not a function of acceleration, it is included in this section to unify the discussion of stability issues. In a symmetric PCV, static stability is affected by the number of wheels, the amount of caster offset of each wheel, and the location of the vehicle center of gravity. Due to the issues of symmetry and packaging in Sections 4.2.4 and 4.2.5, all PCVs with a central center of gravity that have four or more powered-casters will be statically stable. (It is possible to construct a PCV with three wheels that is in danger of falling over in some configurations as evidenced by the three-wheeled PCV in Figure 4.3.) The static stability for a symmetric design is described by the polygon of support. To determine the static stability of a symmetric PCV, the center of mass can be

displaced no more than a distance r_{CG} from the robot centroid, which is the centroid of the caster modules:

$$r_{\mathrm{CG}} < h \cos\left(\frac{\pi}{\mathfrak{n}}\right) - b \tag{4.24}$$

where h is the distance from the robot centroid to the caster module, $\mathfrak{n}$ is the number of caster modules, and b is the caster offset distance. A negative result for the right hand side of eqn. 4.24 (as may be the case for some three-wheeled PCVs) indicates that, regardless of the position of the center of gravity, there are wheel configurations for which the robot will tip.

Once static stability is established, the robot may still become unstable and tip over during operation due to acceleration induced forces. To ensure the motions executed with desired performance will "keep all the wheels on the ground," the maximum allowable acceleration, $a_{\max}$, can be computed:

$$|a_{\max}| = \left[h \cos\left(\frac{\pi}{\mathfrak{n}}\right) - b\right] \frac{g}{z_{\mathrm{CG}}} \tag{4.25}$$

where the geometric parameters are the same as in the previous equation and g is the value of the gravitational acceleration, or 9.81 m/s^2 for earth-bound robots. By keeping the height of the center of gravity, z_{CG}, low to the ground we can greatly increase the performance of the robot. Increasing the number of wheels beyond five, however, leads to very minimal gains in stability.

4.4.4 Isotropicity

Holonomic motion is a kinematic concept. By virtue of being holonomic, a holonomic mobile robot has the *ability* to accelerate in an arbitrary operational space direction. This does not address the magnitudes of achievable accelerations in different directions. A robot which can accelerate equally in its operational space DOFs, with similar units, is said to have *isotropic acceleration* capability. In addition to having isotropic acceleration capabilities in each configuration, it is desirable that the acceleration capabilities remain constant across different configurations. Robot manipulators are notorious for having wildly varying acceleration abilities that can easily differ by an order of magnitude, both directionally

and between configurations.

In a PCV, the configuration of the casters affects the isotropic quality of the robot, the magnitude of maximum acceleration, and the reflected endpoint mass and inertia. An effective measure of the isotropic quality of a mechanism is the value of the reflected endpoint mass and inertia. Values for the reflected x and y masses are shown in Figure 4.10, and

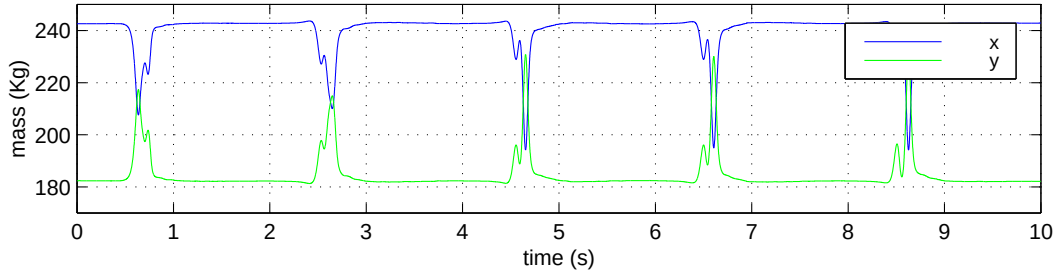

Figure 4.10: XR4000 operational space reflected mass values

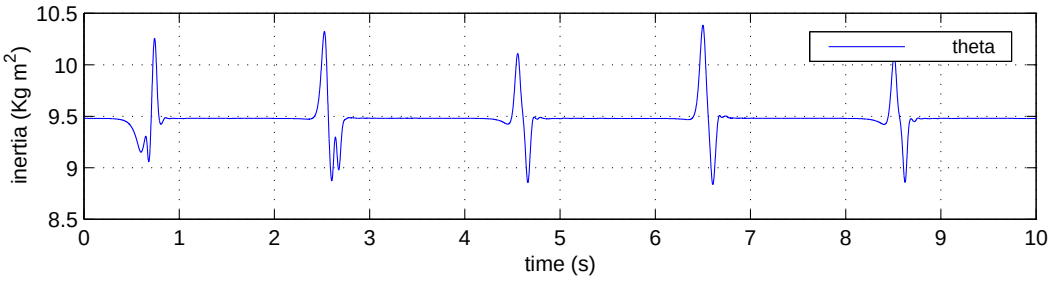

Figure 4.11: XR4000 operational space reflected inertia value

values for reflected rotational inertia are shown in Figure 4.11. These values were gathered during a pacing motion of the robot moving back-and-forth along the y-axis. During this motion the casters all flip directions so that the mechanism is repeatedly swept through a wide range of configurations. The reflected mass values are especially meaningful measures of the isotropic acceleration ability of the XR4000 PCV since it uses eight identical actuators.

The important point to note from the above plots is that the XR4000 mechanism is inherently very isotropic. The reflected mass values differ only by about 30% between forward motion (shown as the y-axis values here) where the wheels are trailing, and sideways motion (shown as the x-axis values here). Likewise, the reflected inertia values only vary by about 10% over the wide range of configurations encountered.

One common approach during control is to approximate the configuration-dependent reflected mass and inertia values by constants. This works quite well for the XR4000 PCV, as an average value of 215 Kg for the two mass values and 9.5 Kg·m^2 for the reflected inertia value will give results which are always within 15%.

Chapter 5

Dynamic Modeling

5.1 Background

5.1.1 Motivation

Robots are non-linear dynamic systems which are not well controlled using fixed gain controllers. It is well understood in the control of robot manipulator arms that the changing robot configuration causes large changes in mass and inertia of a robot mechanism as perceived at the actuators. The changing reflected masses and inertias change the effective gain of the controller, create disturbance forces to the controller, and change the gravity-induced biases of the system. The results of the dynamic disturbance forces and system changes are degradation in the accuracy and performance of the controller. This situation often limits the use of high controller gains due to instabilities caused by too large of a system gain in some configurations.

One approach to reduce the impact of many dynamic effects is to design the robot mechanism to be as symmetric as possible. The powered-casters in a PCV, however, are intentionally asymmetric to provide smooth, singularity-free motion capability. Consequently, the eccentricity of the mass and interaction forces with the ground produce dynamic coupling forces which affect the motion of the vehicle. For example, shortly after the PCV has begun simply reversing directions, the casters will flip around to regain their trailing posture. During this transition, the forks and components associated with the steering axes will

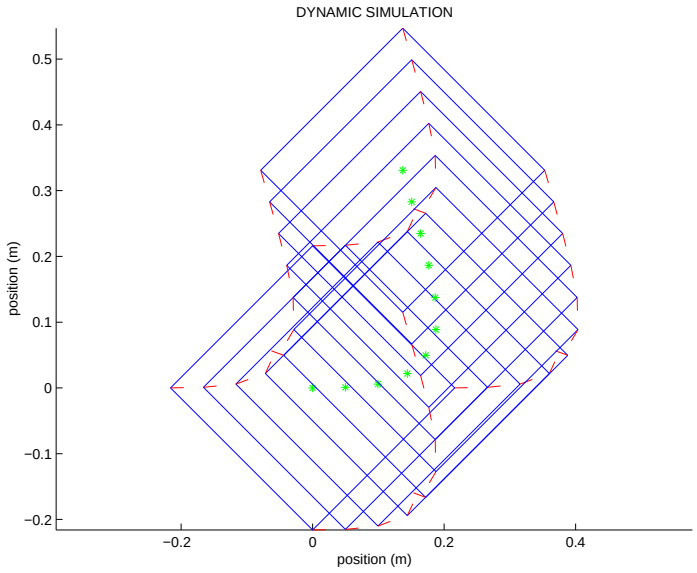

Figure 5.1: Dynamic simulation with $\dot{x}|_0 = 0.5$ m/s, $\boldsymbol{\phi}|_0 = [181\ 181\ 181\ 181]^{\mathsf{T}}$ deg

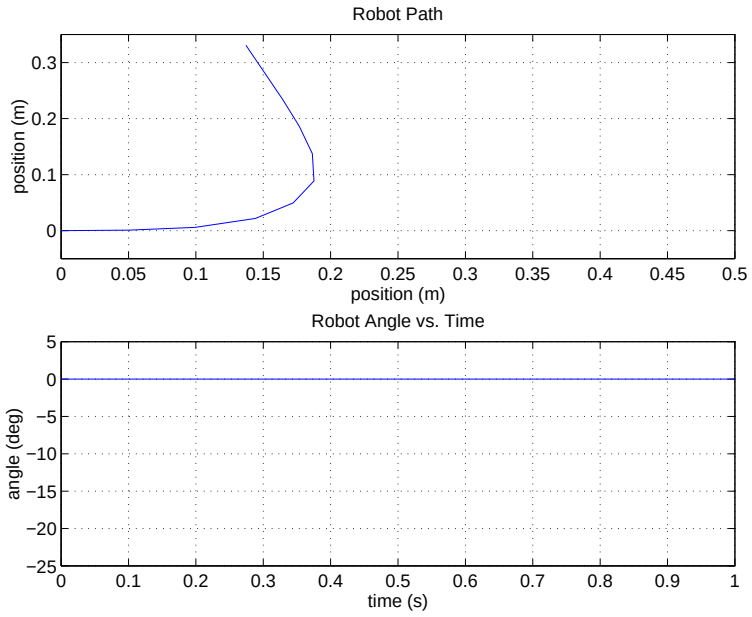

Figure 5.2: Robot path x vs. y, and robot orientation θ vs. time

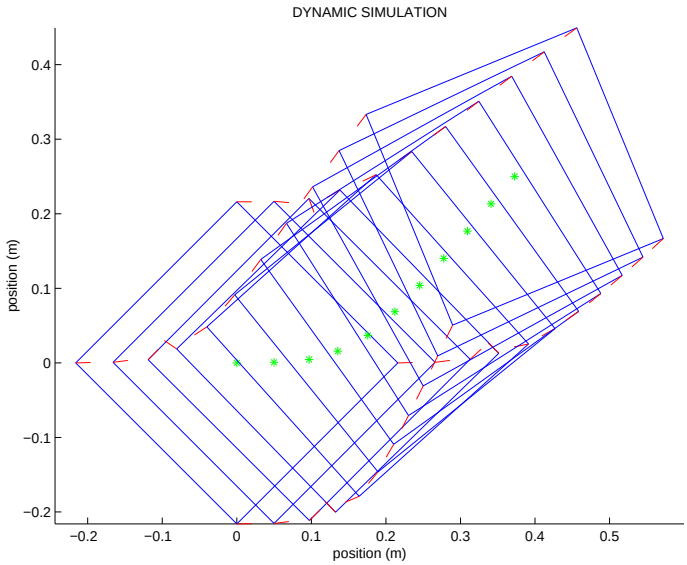

Figure 5.3: Dynamic simulation with $\dot{x}|_0 = 0.5$ m/s, $\boldsymbol{\phi}|_0 = [181\ 180\ 181\ 181]^\mathsf{T}$ deg

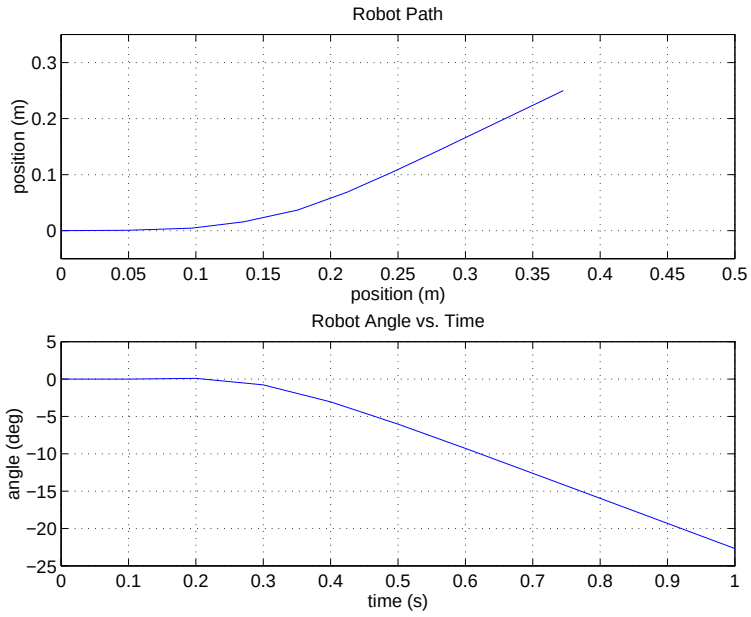

Figure 5.4: Robot path x vs. y, and robot orientation θ vs. time

accelerate and then decelerate while the wheels and components associated with the roll axes will decelerate and then accelerate. To illustrate the consequences, consider a passive (*i.e.* uncontrolled), four-caster robot which is moving to the right with a velocity of 0.5 m/s. Also suppose that the wheels of this robot are all in an "upstream" configuration—a possible configuration if the robot has recently begun moving in the x direction. Figures 5.1 – 5.4 show two simulations with slightly different initial conditions. These simulations demonstrate that the dynamic effects of the PCV mechanism can be significant; and that the dynamic effects are quite sensitive to the robot configuration.

5.1.2 Dynamic Decoupling

Dynamic decoupling is a common technique used to improve dynamic performance and simplify the control of complex robotic systems [16, 48]. By understanding the nature of the dynamic forces generated during any motion of the robot, we can effectively cancel these forces, and linearize the dynamic system to be controlled. The approach begins with the modeling of the mechanical dynamics of the robot. The mechanical dynamics are generally the dominant non-linear component of the robot system.[1] Dynamic modeling of serial chain and branching, tree-like robot manipulators is well understood and has been solved using many methods. The most efficient methods are based on recursive, Newton-Euler and D'Alembert formulations [24, 54, 14].

To implement dynamic decoupling, the joint forces which will compensate for the dynamic effects need to be computed. Estimates of the dynamic properties, $\hat{A}$, $\hat{\mathbf{b}}$, $\hat{\mathbf{g}}$, can be used to compute the control torque values, $\mathbf{\Gamma}_c$, required to produce the control acceleration, $\ddot{\mathbf{q}}_c$, which is used as the input to the system.

$$\mathbf{\Gamma}_c = \hat{A}\,\ddot{\mathbf{q}}_c + \hat{\mathbf{b}} + \hat{\mathbf{g}} \tag{5.1}$$

When the control torque is applied to the physical robot, as represented by the dynamic

[1] With modern components, other dynamics including the electromagnetic dynamics of the motors and the electrical dynamics of the motor amplifiers, are very linear in the range of frequencies in which robot control is desired. Thus, as is typical, the high frequency dynamics of these components will be ignored.

equation

$$A\,\ddot{\mathbf{q}} + \mathbf{b} + \mathbf{g} = \mathbf{\Gamma} \tag{5.2}$$

and the estimates of the dynamic parameters are exact, the result is that the dynamically decoupled manipulator behaves according to

$$\ddot{\mathbf{q}} = \ddot{\mathbf{q}}_c \tag{5.3}$$

and the actual acceleration is precisely what is commanded by the controller. The important point here is that eqn. 5.1 gives a formula to directly compute the joint torques, $\mathbf{\Gamma}$, which, when applied, will dynamically decouple the robot.

A PCV is not a serial chain robot, however; it is a parallel robot with multiple mechanical paths from the ground to the operational point. The dynamics can be represented by the constrained system:

$$C^{\mathsf{T}} A'\,\ddot{\mathbf{q}} + C^{\mathsf{T}}\mathbf{b}' + C^{\mathsf{T}}\mathbf{g}' = C^{\mathsf{T}}\mathbf{\Gamma} \tag{5.4}$$

where C describes the loop-closure constraint equations which project the unconstrained dynamics into a constrained sub-space [73]. In the classical dynamic approaches, the particular choice of subspace is selected arbitrarily by the system designer and may not have intuitive meaning. Because the constraint matrix, C, is not invertible, eqn. 5.4 cannot be solved for the joint torque information needed to dynamically decouple this model.

5.1.3 Operational Space Dynamic Model

Using the *operational space dynamic formulation*, the dynamics of a robot mechanism can be represented as single rigid body with the same set of DOFs as the task. By representing the properties of the mechanism at a chosen point, called the *operational point*, and with the same DOF's as the task, the operational space dynamic formulation yields an intuitive representation of the system's complex dynamic properties. The most common, general basis chosen is Cartesian coordinates. For a general mechanism, including a robot manipulator, there are three linear DOFs and three rotational DOFs in Cartesian space. For a given coordinate frame choice, the DOF's are represented by linear speeds along the x, y, and z axes and angular speeds about the same three axes.

The operational space dynamics are written as a relationship involving the operational point spatial accelerations, $\ddot{\mathbf{x}}$, and the spatial forces, $\mathbf{F}$, acting on the operational point. The dynamic properties of the mechanism at the operational point are represented by the equation

$$\Lambda\,\ddot{\mathbf{x}} + \boldsymbol{\mu} + \mathbf{p} = \mathbf{F} \tag{5.5}$$

with the mass, Λ, the velocity coupling terms, $\boldsymbol{\mu}$, and the gravity terms, $\mathbf{p}$.

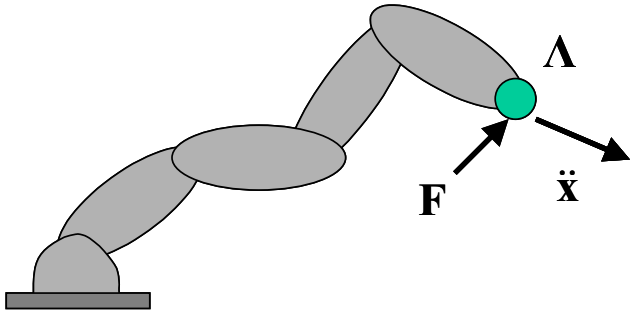

Figure 5.5: Manipulator operational space representation

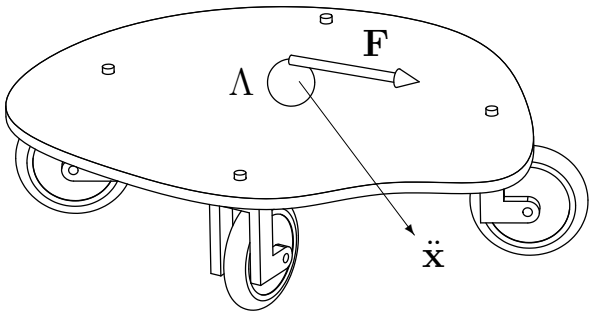

Figure 5.6: Mobile robot operational space representation

A holonomic mobile robot is constrained to move upon a plane surface and the description of the Cartesian space has three DOFs, with two linear and one rotational. This

gives

$$\ddot{\mathbf{x}} = \begin{bmatrix} \ddot{x} \\ \ddot{y} \\ \ddot{\theta} \end{bmatrix} \qquad and \qquad \mathbf{F} = \begin{bmatrix} f_x \\ f_y \\ m_\theta \end{bmatrix} \tag{5.6}$$

The operational point is typically chosen to be the centroid of the vehicle, but can be chosen arbitrarily—even outside the physical dimensions of the vehicle. The choice of an operational point gives a good way to describe the motion of the three DOF vehicle with respect to an x, y, θ system of freedoms. The overall dynamic equation of motion can still be represented by eqn. 5.5 with 3x1 and 3x3 components.

5.1.4 Augmented Object Model

The augmented object model is an extension of the operational space model which is applied to multiple robot systems. By representing the effective dynamics of each individual robot in a common frame of reference, at a common operational point; the augmented object model states that the dynamics of the composite system are found by summing the operational space dynamics of the load and each robot. In Figure 5.7 the representations of

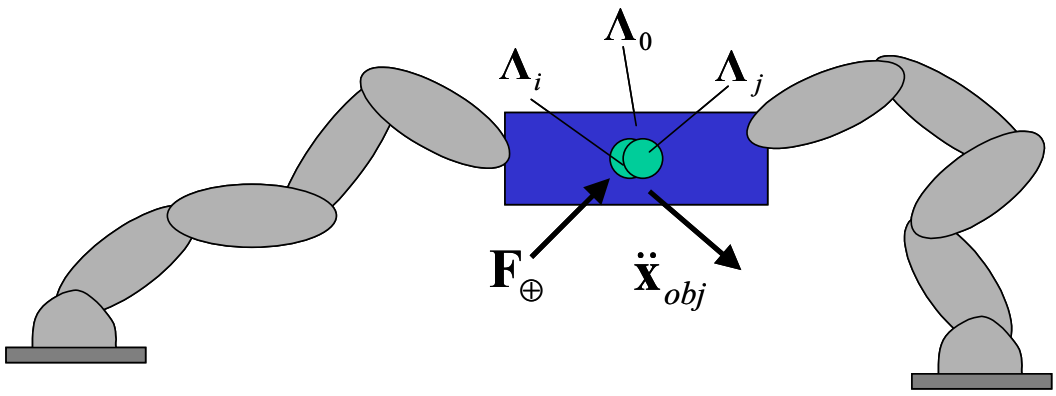

Figure 5.7: Augmented object representation of cooperating manipulators

the dynamics of the load, Λ_0, and the dynamics of the m manipulators, Λ_i, Λ_j, etc., can be

summed

$$\Lambda_{\oplus} = \sum_{k=0}^{m} \Lambda_k \tag{5.7}$$

$$\boldsymbol{\mu}_{\oplus} = \sum_{k=0}^{m} \boldsymbol{\mu}_k \tag{5.8}$$

$$\mathbf{p}_{\oplus} = \sum_{k=0}^{m} \mathbf{p}_k \tag{5.9}$$

to give the dynamics of the *augmented object*, from which the method derives its name.

$$\Lambda_{\oplus}\, \ddot{\mathbf{x}} + \boldsymbol{\mu}_{\oplus} + \mathbf{p}_{\oplus} = \mathbf{F} \tag{5.10}$$

As shown in Chapter 3, the PCV can be viewed as a collection of cooperating manipulators—just the situation which the augmented object model describes. In the remainder of this chapter I will show how the augmented object model can be applied to a PCV.

5.1.5 Closed-Chain Dynamics

Typically, the dynamic equations of motion for a parallel system with nonholonomic constraints such as a PCV are formed in one of two ways: the unconstrained dynamics of the whole system can be derived and the constraints are applied to reduce the number of degrees of freedom [11]; or the system is cut up into pieces, the dynamics of these subsystems are found, and the loop closure equations are used to eliminate the extra degrees of freedom.

For a four-wheeled XR4000 robot, using the first method treating the robot as a "free-flying" unconstrained system, we will obtain three equations for the DOFs of the robot body, one equation for each steer DOF, and one equation for each roll DOF; for a total of 11 equations. The robot is not hovering above the ground, however, and the constraints imposed by the wheel contacts can be described, for each wheel, by one equation for the rolling constraint, and one equation for the lateral constraint; giving 8 constraints. This system of 19 equations must be reduced to three independent equations which describe the dynamics of the vehicle.

Using the same example of an XR4000 robot, the second method begins with equations of simple closed loops, such as are present from one wheel contact point, through the wheel and caster, across the robot body, down another caster to its wheel contact point, and across the ground back to the original wheel contact point. Each loop has three DOF and there are four such loops for a total of 12 equations. The separate mechanisms described by each set of loop equations can be constrained with the introduction of three constraint equations per pairs of mechanisms. By constraining three pair of mechanisms, the mathematically cloven robot is unified, with a total of 9 constraint equations. Using this method, 21 equations must be reduced to three independent equations to describe the dynamics of vehicle.

The equations of motion generated either way must give the same numerical results—there is only one right answer. Ideally, both these methods would yield the same minimal set of symbolic dynamic equations, but in practice it is difficult to reduce the proliferation of terms that are introduced in a large number of equations. Thus, the method used to generate the equations of motion can significantly affect the efficiency of the real-world solution.

5.2 Single Wheel Dynamics

To get a more efficient form of the dynamic equations of motion, we will use a method which uses compatible 3 DOF systems. Let us first decompose the PCV into modules by separating it into modular pieces, where each includes one wheel, its fork, and the actuation mechanisms for that wheel and fork. We will also include the *operational point*, $P_{\oplus}$, we have chosen for the vehicle, in every module.

A single module is a serial chain "manipulator" mechanism, which can be modeled without the use of loop-closure constraint equations. I assume that the constraints will be satisfied and proceed to model one wheel module from the ground to the center of the robot. We are interested in finding the relationships between the applied actuator torques and the motions of the bodies which make up our manipulator.

We can model the PCV as a collection of cooperating manipulators such as shown in Figure 3.9. The dynamic equations of motion for this three DOF serial manipulator can be

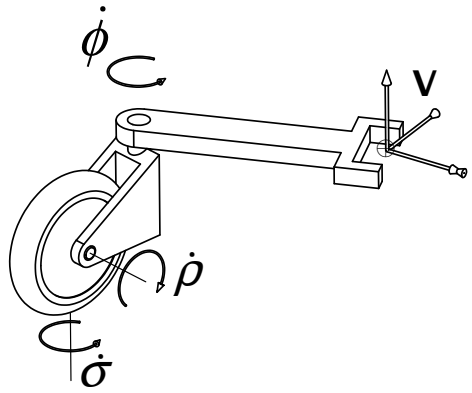

Figure 5.8: Single wheel manipulator

written [16],

$$A_i(\mathbf{q}_i)\,\ddot{\mathbf{q}}_i + \mathbf{b}_i(\mathbf{q}_i, \dot{\mathbf{q}}_i) = \mathbf{\Gamma}_i \tag{5.11}$$

where $\mathbf{q}$ and its derivatives are the joint positions, velocities, and accelerations, A is the symmetric mass matrix, and $\mathbf{b}$ is the vector of centrifugal and Coriolis coupling terms. We assume that the PCV is on level ground and have dropped the effects of gravity.

Using the joint space dynamics from eqn. 5.11 and the Jacobian in eqn. 3.14, we can express the operational space dynamics [48] of the i^{th} manipulator as

$$\Lambda_i(\mathbf{q}_i)\ddot{\mathbf{x}} + \boldsymbol{\mu}_i(\mathbf{q}_i, \dot{\mathbf{x}}) = \mathbf{F}_i \tag{5.12}$$

with

$$\Lambda_i = \mathsf{J}_i^{-\mathsf{T}} A_i \mathsf{J}_i^{-1} \tag{5.13}$$

$$\boldsymbol{\mu}_i = \mathsf{J}_i^{-\mathsf{T}} \left(A_i \dot{\mathsf{J}}_i^{-1} \dot{\mathbf{x}} + \mathbf{b}_i \right) \tag{5.14}$$

where Λ is the operational space mass matrix, $\boldsymbol{\mu}$ is the operational space vector of centrifugal and Coriolis terms, and $\mathbf{F}_i$ is the force/torque vector at the origin of the end effector coordinate system. Since our manipulator is simple and not redundant, we compute J^{-1} directly, thus avoiding an inversion operation which is traditionally required. Also note that as expressed here, $\boldsymbol{\mu}_i$ is a function of $\mathbf{q}_i, \dot{\mathbf{q}}_i$ and $\dot{\mathbf{x}}$. This representation allows us to use exact local information, such as the rolling speed of the wheel, which is measured directly, and

to use the best estimates of the base speeds which were developed in the previous section.

Examples of the dynamic parameters generated with the program AUTOLEV are shown in Table 5.1 for one caster module and represent the size and complexity of the dynamic terms. The joint coordinates σ and ϕ are here `Q1` and `Q3`, while the joint speeds $\dot{\sigma}$, $\dot{\rho}$, and $\dot{\phi}$ are here `U1`, `U2`, and `U3`. The wheel, with mass `MW`, is modeled as symmetric, with the center of mass on the x-axis of the caster, and a polar inertia of `IW`. The fork, with mass `MF`, is modeled as symmetric side-to-side, with a center of mass on the x-axis a distance of `CGFX` from the steer axis and with a central inertia of `IF`. The "arm" of the caster/manipulator, with mass `MR`, has an inertia of `IR` as seen at the endpoint of the arm.

Table 5.1: Automatically generated dynamic parameter examples

```
-> LAMBDA[1,1] = MF + MR + MW + IW/R^2 + H*MR*SIN(Q3)*(SIN(Q1)-SIN(Q1-2*Q3)-2
        *SIN(Q3)*COS(Q1-Q3))/B - (MF+MW+IW/R^2-(IFZ+MF*(B+CGFX)^2)/B^2)*SIN(Q3)^2


-> MU[1] = TT*COS(Q3)/R + CGFX*MF*COS(Q3)*U3^2 + 2*MF*R*SIN(Q3)*U2*U3 +
        3*MR*R*SIN(Q3)*U2*U3 - (B*TG*SIN(Q3)+B*TS*SIN(Q3)-IFZ*R*SIN(Q3)*U2*U3-
        2*MF*B^3*COS(Q3)*U3^2-2*MR*B^3*COS(Q3)*U3^2-MW*B^3*COS(Q3)*U3^2-2*B*CG
        FX*MF*R*SIN(Q3)*U2*U3-IW*B^3*COS(Q3)*U3^2/R^2-MF*R*(B+CGFX)^2*SIN(Q3)*
        U2*U3)/B^2 - H*(MF*COS(Q1)*U3^2+MR*COS(Q1)*U3^2+MW*COS(Q1)*U3^2+MF*
        SIN(Q3)*SIN(Q1-Q3)*U3^2+MW*SIN(Q3)*SIN(Q1-Q3)*U3^2+IW*(COS(Q1)*U3^2+
        SIN(Q3)*SIN(Q1-Q3)*U3^2-COS(Q1)*U1*U3-SIN(Q3)*SIN(Q1-Q3)*U1*U3-COS(Q3)*
        COS(Q1-Q3)*(U1-U3)^2)/R^2-MF*COS(Q1)*U1*U3-MR*COS(Q1)*U1*U3-MW*COS(Q1)*
        U1*U3-MF*SIN(Q3)*SIN(Q1-Q3)*U1*U3-MW*SIN(Q3)*SIN(Q1-Q3)*U1*U3-MF*COS(Q3)*
        COS(Q1-Q3)*(U1-U3)^2-MW*COS(Q3)*COS(Q1-Q3)*(U1-U3)^2-SIN(Q3)*SIN(Q1-Q3)*
        (IFZ*U3^2+MF*(B+CGFX)^2*U3^2-IFZ*U1*U3-IFZ*(U1-U3)^2-MF*(B+CGFX)^2*
        U1*U3-MF*(B+CGFX)^2*(U1-U3)^2)/B^2)
```

5.3 Vehicle Dynamics

By modeling the parts of the PCV as manipulators, we can use the augmented object model, presented earlier, to form the system dynamics of the entire mobile robot. The augmented object model assumes that all of the manipulators are fixed to the ground and are grasping a common object. A PCV fits this description because, at any given instant, the PCV caster

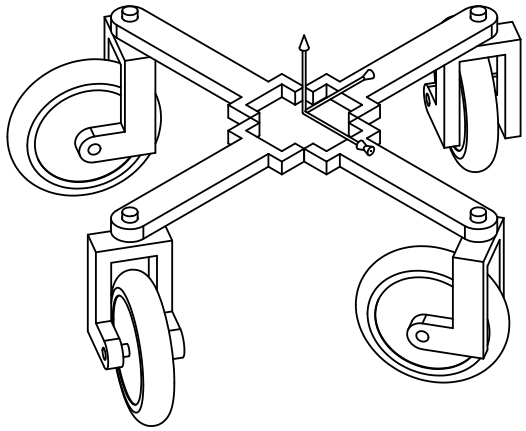

Figure 5.9: Cooperating caster manipulators

"manipulators" are fixed to the ground at the contact point since the relative velocity of the wheel on the ground is zero.

To simplify the notation, and to emphasize the unifying nature of the solution, I will drop the use of the augmented object notation, $\oplus$, and use only the variable names without subscripts. Using the results of the simple dynamics for a single caster wheel mechanism found in Section 5.2, the total vehicle dynamics become:

$$\mathbf{F} = \Lambda\, \ddot{\mathbf{x}} + \boldsymbol{\mu} \tag{5.15}$$

The dynamic elements are the summation of the elements from the separate mechanisms.

$$\Lambda = \sum_{i=1}^{n} \Lambda_i \tag{5.16}$$

$$\boldsymbol{\mu} = \sum_{i=1}^{n} \boldsymbol{\mu}_i \tag{5.17}$$

Note that, regardless of number of casters, eqns. 5.16 – 5.17 have a fixed size of 3x3. There are no matrix inversions which need to be computed. The dynamics of a system are dependent on the positions and velocities of the mechanism at any given instance. The solution found by this method is consistent with the constraints, but does not enforce the

constraints. The information of the global constraints is not encoded in this solution, and so this computation is efficient.

Chapter 6

Control

6.1 Introduction

Due to the nonholonomic nature of the PCV mechanism it is not possible to independently control the joint axes of the robot. The controllable subspace is nicely characterized by the DOFs of the robot body, or vehicle. One common description of the vehicle DOFs, and one that will be used here, is the coordinates and freedoms of the (x, y, θ) operational space description. All approaches to control will deal with controlling the vehicle's motions as defined by the motions of the vehicle's origin in the world.

6.2 Joint Control

Joint level control has been proposed by Wada and Mori for control of a PCV [85]. It is designed to indirectly control only the velocities of the three degrees of freedom $(\dot{x}, \dot{y}, \dot{\theta})$ of the PCV. Their approach is based on control of the velocities of the caster steer points. To outline their approach:

1. Generate a desired vehicle velocity to which to servo.
2. Compute the desired steer point velocities.
3. Use a pseudo-inverse matrix to map the desired steer point velocities to desired roll and steer speeds.

4. Use an axis-by-axis velocity controller to servo the roll and steer axes to the desired speeds.

5. Use the measured roll and steer speeds to compute the twist angles of the wheels in absolute coordinates, as these values are used in various matrices throughout.

6. Use a matrix based on the constraint of the distance between steer points to compute the absolute velocity and rotation rate of the vehicle.

The approach by Wada and Mori raises some important issues and at the same time adds unnecessary confusion in the profusion of steps used. Item 1 is a consequence of the nonholonomic elements in the PCV. The nonholonomic constraints, by nature, are non-integrable and no symbolic solution exists for control of the vehicle positions, x, y, θ, by controlling the mechanism joint positions, ρ_i, ϕ_i. Thus, we cannot directly control the location of the robot by controlling the robot joint coordinates as is done for many mechanisms. For any motion of the vehicle, a trajectory of desired velocities must be generated if joint velocity control is to be used. There are many types of control for which generating a trajectory of desired velocities is either inconvenient or impossible. For example, controllers which minimize a functional of the sensor input, or controllers which are reactive, cannot easily generate a trajectory of velocities.

Items 2 and 3 can be accomplished more succinctly and without the use of a pseudo-inverse. Beginning with the desired vehicle speeds, $\dot{\mathbf{x}}_d$ from item 1, we can use the constraint matrix, C from eqn. 3.31, to compute the desired joint velocities directly.

$$\dot{\mathbf{q}}_d = \mathsf{C}\,\dot{\mathbf{x}}_d \tag{6.1}$$

Using eqn. 6.1, as in item 4, we can use a PD type controller to generate torque or PWM signals, $\mathbf{\Gamma}$, to the joint actuators

$$\mathbf{\Gamma} = -k_p(\dot{\mathbf{q}} - \dot{\mathbf{q}}_d) - k_v(\ddot{\mathbf{q}} - \ddot{\mathbf{q}}_d) \tag{6.2}$$

$$\mathbf{\Gamma}_i = \begin{bmatrix} \Gamma_{i\phi} \\ \Gamma_{i\rho} \end{bmatrix} \quad ; \quad \mathbf{\Gamma} = \begin{bmatrix} \mathbf{\Gamma}_1 \\ \mathbf{\Gamma}_2 \\ \vdots \\ \mathbf{\Gamma}_n \end{bmatrix} \tag{6.3}$$

With a large enough proportional gain, this controller will cause the robot to move, more or less, in the desired direction. A controller of this type relies on the error signal between the actual and desired velocities to generate a signal for the actuators and so will always have some error. This error will cause the PCV to lag the desired trajectory and to not follow the desired generated path. One standard approach to improving a situation with constant error in the controller is to integrate the error and compute a correction. Integrating the joint error will yield poor corrections, however, because the joint-by-joint integrals will not have been subject to the constraints of the mechanism and thus are sure to violate the rolling constraints of the wheels. As a practical issue, it can be difficult to create a stable controller using a velocity signal which is created by digitally differentiating the position signal of an encoder (or worse a potentiometer). Many times the difficulty of relying on velocity estimates is circumvented by using a joint-level trajectory generator. Infinitesimally the next desired joint position is akin to the next desired velocity. Small errors introduced by the finite step size between the trajectory positions can lead to large internal forces as the constraints, which are only instantaneously valid, are no longer satisfied.

Item 5 calculates the wheel orientations in absolute world coordinates. While some knowledge of the wheel orientation is needed, it is generally better to use the directly measured steer angles, ϕ_i, as shown in eqn. 3.28. The steer angles also have the advantage that they are measured with respect to the vehicle and will not accumulate error, or *drift*, over time.

The odometry calculation in item 6 is actually a generalized inverse which is a least squares fit of the calculated steer point velocities to obtain a set of vehicle speeds. Wada and Mori do not recognize their matrix as a generalized inverse and so squander an opportunity to meaningfully optimize this inverse. An example of a more meaningful generalized inverse which is used for the PCV odometry is discussed later in Section 6.4.1.

A joint velocity controller was implemented on the XR4000 following the framework of eqns. 6.1 – 6.2 . It was used to servo the robot's velocity according to commands given by a user via a joystick. In this application, the robot moved in the direction indicated by the joystick with a velocity proportional to the joystick deflection. The controller was successful in this task, since the results were only measured by the perceptions of the joystick operator. Results for dead reckoning using this controller were poor due to the inherent error discussed previously.

6.3 Operational Space Control

6.3.1 Kinematic Control

Instead of controlling the PCV joint axis velocities, $(\dot{\phi}_i, \dot{\rho}_i)$, using a *joint velocity controller* we can choose to directly control the operational variables of interest, namely the position and orientation of the robot body, x, y, θ, using an *operational space controller*. This straightforward approach restores our ability to control the system's position coordinates, a luxury we had abandoned in the previous section. To implement an operational space controller, we must be able to calculate the operational space coordinates of the robot "end effector," and we must know how to apply operational space forces to the robot end effector. Viewing the PCV as an augmented object system (see Figure 3.9), the end effector is actually the robot body; moving the end effector is equivalent to moving the robot.

Assuming for a moment that we know the robot position and velocity, $\mathbf{x}$ and $\dot{\mathbf{x}}$, we can use, for example, a PD controller with acceleration feed forward (eqn. 6.4), to compute an operational space force which will cause the state of the system to converge to the desired state, $\mathbf{x}_d, \dot{\mathbf{x}}_d, \ddot{\mathbf{x}}_d$

$$\mathbf{F} = -K_p(\mathbf{x} - \mathbf{x}_d) - K_v(\dot{\mathbf{x}} - \dot{\mathbf{x}}_d) + \ddot{\mathbf{x}}_d \tag{6.4}$$

with K_p, K_v the position and velocity gains, and $\mathbf{x}_d$ and its derivatives the desired position, velocity, and acceleration. Using eqn. 6.4, we have a controller that will stably deliver the vehicle to any desired operational position or velocity. Because of the scaling effects of the structurally and configuration dependent mechanism masses and inertias, the gains need to be set differently for each axis.

The output of this controller, as is typical of operational space controllers, is an operational space force, $\mathbf{F}$, which is made up of the two linear forces and one moment as applied to the PCV operational point.

$$\mathbf{F} = \begin{bmatrix} F_x \\ F_y \\ M_z \end{bmatrix} \tag{6.5}$$

6.3.2 Dynamically Decoupled Control

The direct application of operational space control can be improved with the knowledge of the dynamics from Chapter 5. One of the more effective techniques for controlling a coupled non-linear system such as the PCV is the *nonlinear dynamic decoupling approach* [48]. Nonlinear dynamic decoupling in operational space is obtained by the selection of the following control structure:

$$\mathbf{F} = \Lambda\, \mathbf{F}^* + \boldsymbol{\mu} \tag{6.6}$$

where $\mathbf{F}$, as in eqn. 6.4, is the operational space force which is to be applied to the PCV; and $\mathbf{F}^*$ is the control force for a linearized unit mass system. As an example, we can again choose to implement a simple PD controller with acceleration feed forward,

$$\mathbf{F}^* = -k_p(\mathbf{x} - \mathbf{x}_d) - k_v(\dot{\mathbf{x}} - \dot{\mathbf{x}}_d) + \ddot{\mathbf{x}}_d \tag{6.7}$$

with k_p, k_v the position and velocity gains, but this time for an ideal, isotropic unit-mass, unit-inertia system.

6.4 Closing the Loop

The use of operational space control requires the ability to measure or compute:

1. the operational space velocity, $\dot{\mathbf{x}}$, and

2. the joint torques, $\boldsymbol{\Gamma}$, which will yield a given set of operational space forces, $\mathbf{F}$.

In a serial chain robot, such as a PUMA 560 manipulator, the Jacobian matrix, J_{manip}, can be used to compute $\dot{\mathbf{x}}$ in Item 1 from the measured joint velocities, $\dot{\mathbf{q}}$

$$\dot{\mathbf{x}} = J_{manip}\, \dot{\mathbf{q}} \tag{6.8}$$

and to compute $\mathbf{\Gamma}$ in Item 2 from the operational force, $\mathbf{F}$, which is the output of the controller.

$$\mathbf{\Gamma} = J_{manip}^{\mathsf{T}}\, \mathbf{F} \tag{6.9}$$

In a PCV, because of the nature of the parallel mechanism, no Jacobian matrix is available. Further complicating matters is the fact that the PCV has both measured and unmeasured joints, and both actuated and unactuated joints. From the analysis of the kinematics in Chapter 3, we have shown that the *constraint matrix*, C, relates the quantities of interest. The non-square constraint matrix, however, cannot be used directly to compute the necessary values since it is not invertible.

In an ideal robot, a generalized inverse of the constraint matrix, $\mathsf{C}^{\#}$, can be used to find the needed solutions.

$$\dot{\mathbf{q}} = \mathsf{C}^{\#}\, \dot{\mathbf{x}} \tag{6.10}$$

$$\mathbf{\Gamma} = \mathsf{C}^{\#\mathsf{T}}\, \mathbf{F} \tag{6.11}$$

While the results of using an arbitrary generalized inverse for an ideal robot will be consistent, the use of a generalized inverse in a real robot with measurement, calibration, and parameter errors and uncertainties can greatly affect the quality of the generated motions. I will now detail several good choices of generalized inverses and describe the implications of each choice.

6.4.1 Odometry

Since the constraint matrix is not square with size $2\mathfrak{n} \times 3$, it is not invertible. For our over-constrained system with more measurements than operational velocities, we can use a generalized inverse of the constraint matrix, $C^{\#}$, to give results we desire. For an ideal robot with no measurement error, using any arbitrary left inverse will yield the same results.

However, when there is unmodeled slippage at the wheel contacts along with the ever present measurement errors of real hardware, the particular choice of generalized inverse will yield different results.

One common choice of generalized inverse is the Moore-Penrose pseudo-inverse [64]. This leads to an $\dot{\mathbf{x}}$ which minimizes, in a least-squares manner, the joint velocity differences between the measured system and the consistent set of joint velocities associated with the corresponding robot velocity. The physical meaning of fitting a solution to the joint velocities is elusive.

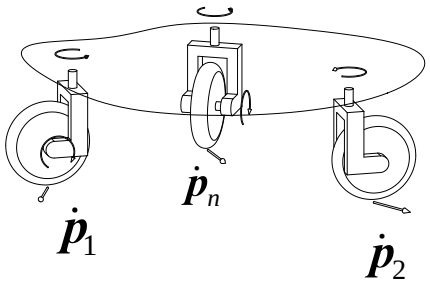

Figure 6.1: Contact point velocities

A more physically meaningful solution can be found by looking at the set of wheel velocities at the contact points, $\dot{\mathbf{p}}$, as shown in Figure 6.1. It may be easiest to visualize the contact point velocities as speeds the contact points would have in the world if the robot body were held fixed and the wheels were not in contact with the ground. The sensed contact points velocities can be calculated from the measured joint speeds with the one-to-one mapping below where C_q is square, full rank, block diagonal, and invertible.

$$\dot{\mathbf{q}} = C_q \, \dot{\mathbf{p}} \tag{6.12}$$

When the robot obeys the ideal rolling assumptions, there exists a robot velocity where the sensed contact speeds, $\dot{\mathbf{p}}$, are identical to the consistent set of contact speeds, or *ideal speeds*, $\dot{\check{\mathbf{p}}}$, found with the kinematic relationship

$$\dot{\check{\mathbf{p}}} = C_p \, \dot{\mathbf{x}} \tag{6.13}$$

However, as is to be expected, when there is some slippage and measurement noise, $\dot{\tilde{\mathbf{p}}} \neq \dot{\mathbf{p}}$. By using the Moore-Penrose pseudo-inverse of the non-square matrix C_p,

$$C_p^+ = (C_p^{\mathsf{T}} C_p)^{-1} C_p^{\mathsf{T}} \tag{6.14}$$

we find the PCV velocity, $\dot{\mathbf{x}}$ which minimizes, in a least-squares way, the differences between the sensed contact speeds and the ideal contact speeds.

$$\dot{\mathbf{x}} = C_p^+ \, \dot{\tilde{\mathbf{p}}} \tag{6.15}$$

This solution will therefore minimize the total perceived slip by minimizing the differences between $\dot{\mathbf{p}}$ and $\dot{\tilde{\mathbf{p}}}$.

We can use C_p^+ to build a generalized inverse of the constraint matrix by combining another one-to-one mapping. The mapping from the joint speeds to contact point speeds can be found by inverting eqn. 6.12 to find C_q^{-1}.

$$\mathsf{C}_{qp}^{\#} = C_p^+ C_q^{-1} \tag{6.16}$$

Our estimate of the robot velocity, assuming that slip is minimized, uses, $\mathsf{C}_{qp}^{\#}$, a generalized inverse of the constraint matrix to give the equation which is used for computing the PCV velocity, given the joint velocities.

$$\dot{\mathbf{x}} = \mathsf{C}_{qp}^{\#} \, \dot{\mathbf{q}} \tag{6.17}$$

We have tested the odometry of the Stanford XR4000 moving randomly for one minute in a 1.5m x 2.5m area and then returning to its starting position. When using the generalized inverse from eqn. 6.16, the dead-reckoning error was less than half as large as when the pseudo-inverse of the constraint matrix, C^+, was used.

6.4.2 Torque Distribution

The nonholonomic rolling constraints in a wheeled mobile robot are special in that they can be broken (or re-established) based on the frictional forces of contact. When the rolling constraints are broken, the wheels slide across the ground, a condition called *slip*, and robot

performance, accuracy, and controllability are degraded. Because of the zero-caster-offset used in the CMU Rover, a.k.a. Pluto, small errors in wheel heading caused large constraint forces to be developed. Muir and Neuman described the effect of these errors [64]:

> Pluto's drive system ... with six motors, is overdetermined (or overconstrained). In addition to moving the robot forward, sideways and spinning it about its axis, the individually driveable and steerable wheels are able to attempt to twist, compress and stretch the floor in various interesting ways.

The CMU Rover was generating forces which were not contributing to the commanded motion, but rather were introducing slip and error. A general PCV always has a greater number of actuators than degrees of freedom. There are many ways to distribute the effort among the joints to achieve a desired operational space force.

Distributed Traction

Just as the contact point velocities can be broken into components which contribute to the PCV motion and those that do not, the joint torques can be broken down into two components: a part which contributes to the motion of the PCV, and a part that contributes to internal forces.

The force/velocity duality combined with eqn. 6.17 is ideal for solving the problem of "stretching the floor." By distributing the joint torques using the transpose of the generalized inverse in eqn. 6.17

$$\mathbf{\Gamma} = C_{qp}^{\#^T}\ \mathbf{F} \tag{6.18}$$

we minimize, in a least squares way, the contact forces developed by the wheels. The consequence is that the tractive effort is spread as evenly as possible among the wheels and the tendency for any one wheel to lose traction is minimized.

Minimum Power

A second useful generalized inverse can be developed by mapping the measured velocities through the motor speeds to the operational velocities. This generalized inverse which I will call, $C_N^{\#}$, distributes the operational forces among the motors so that the total mechanical motor power used is minimized.

Again begin by mapping the operational velocities to the speeds of interest, this time the motor speeds. This can be thought of as a two-step process of mapping the operational speeds to joint speeds using eqn. 3.31 and then mapping the joint speeds to motor speeds using eqn. 4.6, which when combined give an expression for the ideal motor speeds, $\dot{\tilde{\mathbf{w}}}$, where

$$\dot{\tilde{\mathbf{w}}} = N\ \mathsf{C}\ \dot{\mathbf{x}} \tag{6.19}$$

The solution which minimizes the difference between the measured and estimated motor speeds uses the pseudo-inverse

$$(N\mathsf{C})^{+} = \left(\mathsf{C}^{\mathsf{T}} N^{\mathsf{T}} N \mathsf{C}\right)^{-1} \left(\mathsf{C}^{\mathsf{T}} N^{\mathsf{T}}\right) \tag{6.20}$$

$$\dot{\mathbf{x}} = (N\mathsf{C})^{+}\ \dot{\mathbf{w}} \tag{6.21}$$

We can use $(N\mathsf{C})^{+}$ to build a generalized inverse of the constraint matrix by combining another one-to-one mapping. The mapping from the joint speeds to motor speeds can be found by inverting eqn. 4.6 to find N^{-1}, giving the generalized inverse:

$$\mathsf{C}_N^{\#} = (N\mathsf{C})^{+} N^{-1} \tag{6.22}$$

This generalized inverse can be used to find the mapping from measured joint speeds to PCV operational speeds using ideal motor speeds.

$$\dot{\mathbf{x}} = \mathsf{C}_N^{\#}\ \dot{\mathbf{q}} \tag{6.23}$$

As an equation of odometry, this equation is not intuitive. The dual of this equation, however, gives the solution we seek—namely the minimum energy solution for the distribution of torques

$$\boldsymbol{\Gamma} = \mathsf{C}_N^{\#^{\mathsf{T}}}\ \mathbf{F} \tag{6.24}$$

6.4.3 Generalized Inverses

There have been problems with using generalized inverses of Jacobians in the past for manipulators because the meaning of minimizing quantities which have a combination of

linear and angular units is not well defined. The two proposed generalized inverses do not suffer from this problem because the velocity vectors of interest have consistent units. Only linear units are present in the vector of contact velocities from the first example, while the speeds of interest in the second example have only angular units.

Other useful, physically meaningful generalized inverses can be found using the same methodology as follows. A one-to-one mapping from the velocities of interest to the measured velocities is derived. A second mapping, which goes from the operational speeds to the velocities of interest is derived. The product of the two mappings must equal the constraint matrix, C. The new generalized inverse of the constraint matrix is then the pseudo-inverse of the second matrix times the direct inverse of the first matrix.

6.5 Results

The real-time operating system QNX was used to run the controller containing the full dynamics of PCV at 1000 Hz on an on-board 450 MHz Pentium II.

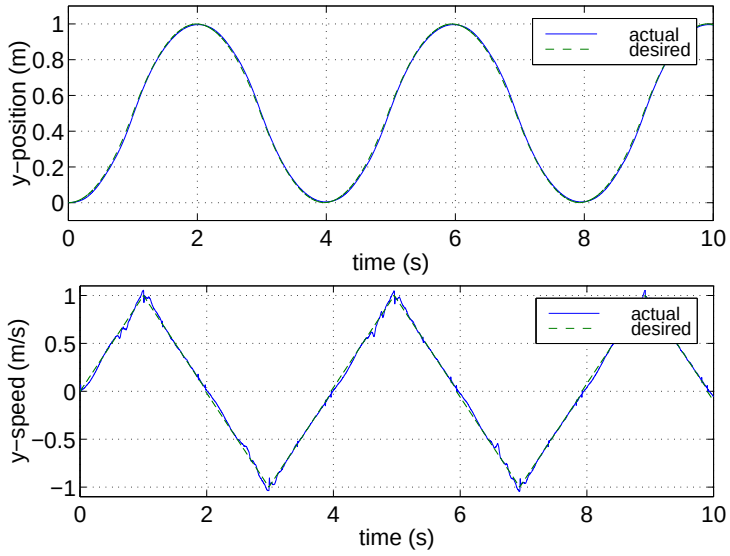

Figure 6.2: Position vs. time and velocity vs. time with dynamic compensation

To demonstrate the effectiveness of the proposed dynamic compensation, the XR4000

robot was commanded to move from zero to one meter in the y direction with 0.1 m/s^2 acceleration. The robot is to follow a straight line ($x = 0$) and to not rotate ($\theta = 0$). The gains used in these experiments were reduced by a factor of 10 from the gains used during normal motions so that dynamic disturbances would be more apparent. Each time the

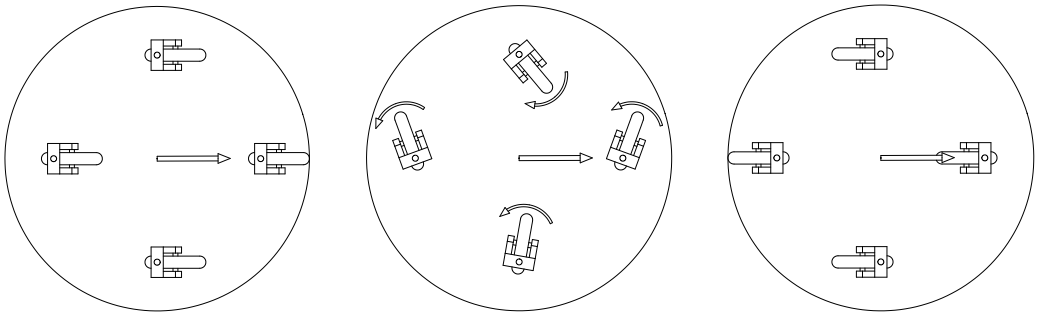

Figure 6.3: Wheel "flip" which leads to large dynamic disturbance forces

XR4000 moves in this task, all four wheels must flip directions, and cause large dynamic coupling forces as seen in Figure 6.4. Notice that the dynamic side forces reaches 400–600 Newtons and the dynamic coupling torque reaches 50–100 Newton-meters.

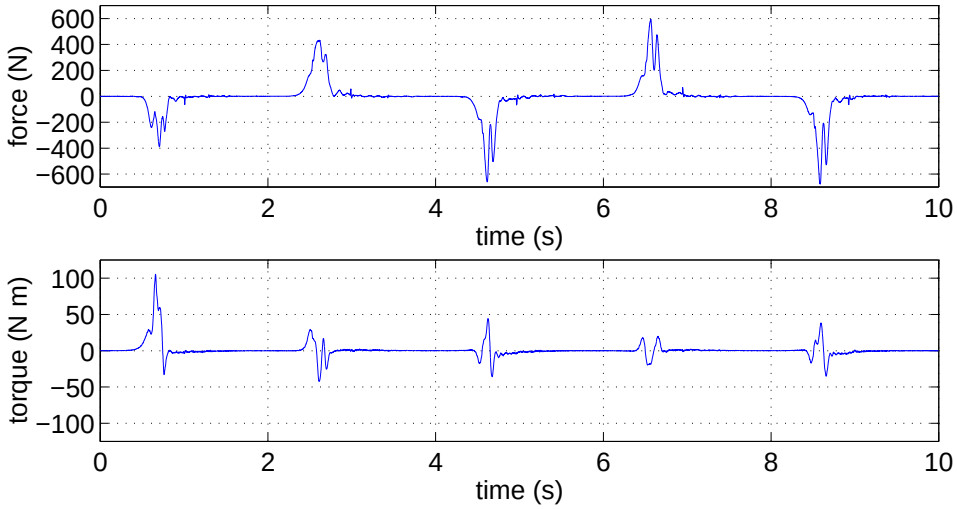

Figure 6.4: Coupling force compensation, x, and torque compensation, θ

In Figures 6.5 and 6.6 the disturbance effects of the dynamic forces are shown. In Figure 6.5 , the robot is run without using dynamic compensation and has position errors on the order of 30 mm and 3°. In Figure 6.6, the robot is run while implementing the proposed dynamic compensation and the errors are reduced to about 5 mm and 0.5°. The results are impressive when we consider the magnitude of the disturbances and the rapid rate at which the compensation must change.

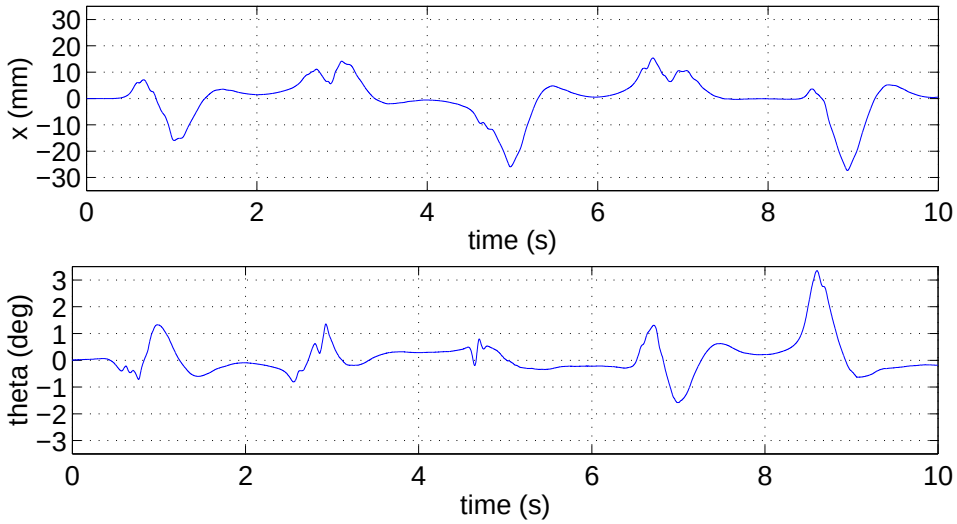

Figure 6.5: Position vs. time, without dynamic compensation

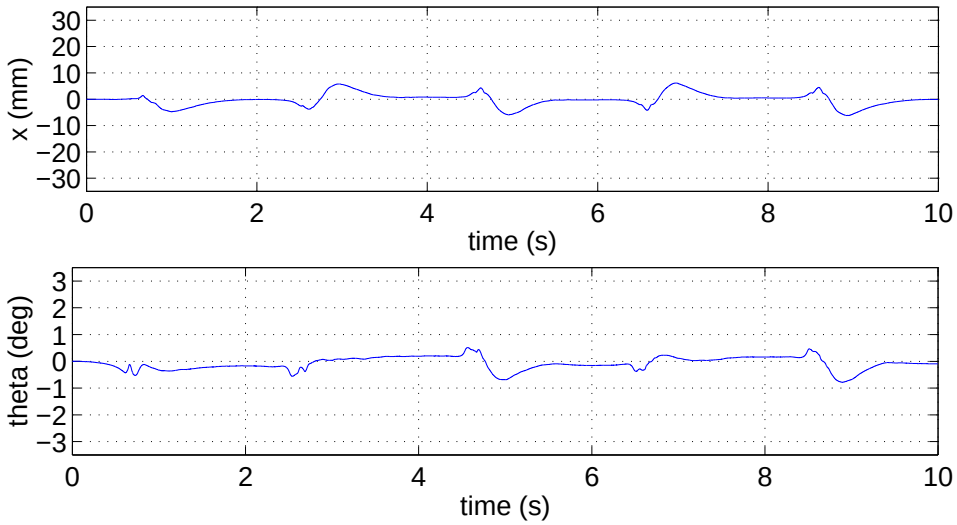

Figure 6.6: Position vs. time, with dynamic compensation

Chapter 7

Mobile Manipulation

7.1 PCV plus manipulator

One important use of a holonomic mobile robot is as the base of a mobile manipulator [35, 37]. Because of the holonomic nature of the mobile robot as a base, the combination of a PCV and manipulator produce a mobile manipulator which can be regarded as a single redundant manipulator with a very large workspace. Therefore, we do not need to plan separate trajectories for the arm and base individually. Rather, we can use the methods of operational space control for redundant manipulators. This allows direct endpoint control to achieve the exact desired task, while null-space behaviors can, for example, center the manipulator near the middle of its local workspace or perform obstacle avoidance of objects on the ground.

7.2 Dynamically Decoupled Joint Control

I have shown in Chapter 6 how to dynamically decouple a PCV. This is important so that the dynamic effects of the motions of the casters do not impart dynamic disturbance forces on the vehicle. In a mobile manipulation system the motion of the manipulator will also impart dynamic disturbance forces upon the vehicle. In order to compensate for the arm dynamic disturbance *forces*, the PCV controller must be capable of generating a desired force output. Since the force output of a nonholonomic wheeled vehicle cannot be fully

controlled due to the reduced number of degrees of freedom imposed by the nonholonomic constraints, a holonomic mobile robot is required. Using a holonomic mobile robot mechanism is not enough; the particular method of control is important. A PCV using a joint velocity controller cannot produce a specified force output, and so cannot be used in a mobile manipulation system which is to be dynamically decoupled [85]. One of the contributions of this dissertation is a controller which gives a method to produce a specified force output from the PCV, independent of the current PCV speed and acceleration [36].

Not only do the moving casters dynamically affect the motion of the robot, but the reaction forces from the manipulator affect the motion of both the robot body and the casters. Computing the reactions between the casters and the joints of the manipulator is difficult. We can instead resolve the reaction forces between the casters and the arm joints at the junction of the mobile base endpoint and the base of the manipulator arm.

When controlled via the dynamic decoupling described in the previous chapters the base appears to be an isotropic unit-mass, 3-DOF mechanism. Therefore, we can model the base as a single mass constrained by two orthogonal linear axes and one revolute axis. Proceeding from these three serial joints to the endpoint of the serial manipulator, we can use a fast dynamics algorithm (*eg.* Chang [14]) to efficiently compute the dynamics of the full mobile manipulator in real-time.

In more mathematical terms, we can treat a PCV/manipulator-arm, mobile manipulator system as a composite, macro-mini system, with composite dynamics:

$$\mathbf{A}\,\ddot{\mathbf{Q}} + \mathbf{b} + \mathbf{g} = \mathbf{T} \tag{7.1}$$

Throughout the following analysis the PCV is considered as the *base* and the related terms are shown with a b subscript. Likewise, the manipulator is considered the *arm* and the related terms are shown with an a subscript. The composite joint coordinates of the mobile manipulation system, $\mathbf{Q}$, are composed of the PCV operational coordinates, $\mathbf{x}_b$, and the arm joint coordinates, $\mathbf{q}_a$.

$$\mathbf{Q} = \begin{bmatrix} \mathbf{x}_b \\ \mathbf{q}_a \end{bmatrix} \tag{7.2}$$

The composite joint torques, $\mathbf{T}$, are composed of the PCV operational forces, $\mathbf{F}_b$, and the

arm joint torques, $\mathbf{\Gamma}_a$.

$$\mathbf{T} = \begin{bmatrix} \mathbf{F}_b \\ \mathbf{\Gamma}_a \end{bmatrix} \tag{7.3}$$

The forms of the individual terms in the dynamic equations are explored, with a non-holonomic vehicle, by Yamamoto and Yun [98]; and by my office-mate, Alan Bowling, using macro-mini robot systems, in his dissertation [6]. In the system presented here, the base "joint" coordinates are identical to the base operational coordinates. Also, there are no gravity effects of the base mechanism on the base joints because the PCV is assumed to be on level ground. Combining these principles, we get the form of parameters from the composite equations of motion:

$$\mathbf{A} = \begin{bmatrix} \Lambda_b + \Lambda_a & A_{ab} \\ A_{ab}^T & A_a \end{bmatrix} \quad ; \quad \mathbf{b} = \begin{bmatrix} \boldsymbol{\mu}_b + \mathbf{b}_{ba} \\ \mathbf{b}_{ab} + \mathbf{b}_A \end{bmatrix} \quad ; \quad \mathbf{g} = \begin{bmatrix} 0 \\ \mathbf{g}_a \end{bmatrix} \tag{7.4}$$

The $\mathbf{A}$ matrix is the system mass matrix. It contains, Λ_b, the PCV operational mass matrix. It is important to note here that the operational degrees of freedom for the PCV are being treated as the first three joint DOFs of the mobile manipulator system. The matrix Λ_a contains information about the base forces generated by the mass of the arm during accelerations of the base. The coupling mass matrix, A_{ab}, describes the reaction forces acting on the base due to joint accelerations of the arm, and its dual (the transpose), describes the equal and opposite effects the base accelerations have on the arm joint torques. Finally, the matrix, A_a, is the well known manipulator joint space matrix which describes the relationships between the arm joint torques and arm joint accelerations.

The centrifugal and Coriolis vector, $\mathbf{b}$, has four terms. It contains the PCV velocity coupling terms, $\boldsymbol{\mu}_b$ which are the base forces generated by the interactions of the base velocities. The cross-coupling terms describe the forces felt by the base, $\mathbf{b}_{ba}$, and by the arm joints, $\mathbf{b}_{ab}$, due to the combined velocities of the base and arm. The fourth term, $\mathbf{b}_a$, is the traditional centrifugal and Coriolis vector associated with a manipulator due to the interactions of the velocities of the manipulator joint speeds.

The gravity vector, $\mathbf{g}$, contains one zero vector due to the assumption that the PCV is on level ground. The second vector which is the typical manipulator gravity vector, $\mathbf{g}_a$,

describes the joint torques developed by the gravity loading on the manipulator.

Bowling demonstrates that it is difficult to find a symbolic solution for the terms Λ_a and Λ_{ab}, and shows a complex method for calculating $\mathbf{b}_{ba}$ and $\mathbf{b}_{ab}$. Since the values of these parameters will be used for control purposes, the efficiency of the solution is important. We can use the work of Chang as presented in his dissertation for fast computation of the **A**, **b**, and **g** parameters [14]. Chang specifically provides a method for computing the dynamics of serial, branching manipulators; and so his algorithm cannot be used to compute the PCV dynamics, Λ_b and $\boldsymbol{\mu}_b$, because of the parallel nature of the PCV. I will now show how to integrate the structure of Bowling with the methods of Chang in addition to methods presented in this thesis to produce a modular, efficient, real-time controller for a PCV-based mobile manipulator system.

To continue to use the fast algorithms of Chang, we express the kinematic freedoms of the PCV, which is the base, as a virtual serial mechanism in Cartesian coordinates. By setting the mass and inertia parameters of the base to zero for this computation, the kinematics of the base will be fully captured without incorrectly representing the dynamics. Thus, the dynamics of the manipulator will be properly projected onto the composite mechanism. The fast serial algorithm will then compute the full effects of the arm on the system, which can be seen by setting Λ_b and μ_b to zero to give the equations of motion:

$$\begin{bmatrix} \Lambda_a & A_{ab} \\ A_{ab}^T & A_a \end{bmatrix} \begin{bmatrix} \ddot{\mathbf{x}}_b \\ \ddot{\mathbf{q}}_a \end{bmatrix} + \begin{bmatrix} \mathbf{b}_{ba} \\ \mathbf{b}_{ab} + \mathbf{b}_A \end{bmatrix} + \begin{bmatrix} 0 \\ \mathbf{g}_a \end{bmatrix} = \begin{bmatrix} \mathbf{F}_{b,\text{ext}} \\ \boldsymbol{\Gamma}_a \end{bmatrix} \tag{7.5}$$

Now, in a modular fashion, use the dynamic equations of motion of the PCV from eqn. 5.15 with the addition of the external force, $\mathbf{F}_{b,\text{ext}}$, acting on the mechanism.

$$\Lambda_b \ddot{\mathbf{x}}_b + \mu_b + \mathbf{F}_{b,\text{ext}} = \mathbf{F}_b \tag{7.6}$$

It can be seen that the total dynamics of eqns. 7.1 – 7.4 are equivalent to the rearranged form in eqns. 7.5 – 7.6 . Written in the latter form, however, we can modularize the calculations to use first, the fast recursive serial dynamics of Chang; and second, the efficient parallel dynamics of the PCV presented earlier. The common quantity, $\mathbf{F}_{b,\text{ext}}$, in the two equations is the dynamic reaction force developed by the manipulator. The base controller

can directly compensate for the complex arm dynamic disturbances just by compensating for the reaction forces of the arm. This greatly simplifies the implementation since a controller designed for a stand-alone PCV can be used within a mobile manipulation system as long as it is capable of simply developing arbitrary operational forces in addition to the desired, dynamically decoupled, base accelerations for which it was primarily designed.

7.3 Experiment

These experiments use the same PCV, a Nomad XR4000, as in the previous experiments. In addition, a PUMA 560 is added on top of the PCV. The XR4000 is fitted with a PUMA

Figure 7.1: “Romeo,” a Nomad XR4000 and PUMA 560

controller and contains all the necessary hardware for fully autonomous motion and control. The system, shown in Figure 7.1, is 230 kg, has a one meter reach, and can operate for

more than five hours continuously without recharging. The computations for the control of all axes are handled by a single Pentium II with a 450 MHz processor speed. The QNX real-time operating system allows for precise real-time operation, and all experiments were carried out with a 1000 Hz servo rate.

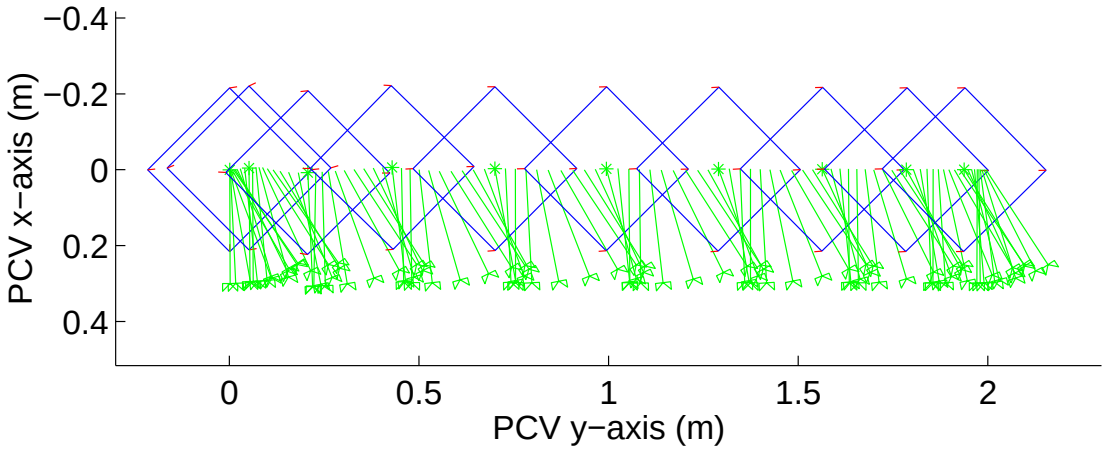

Figure 7.2: Path of robot and manipulator arm

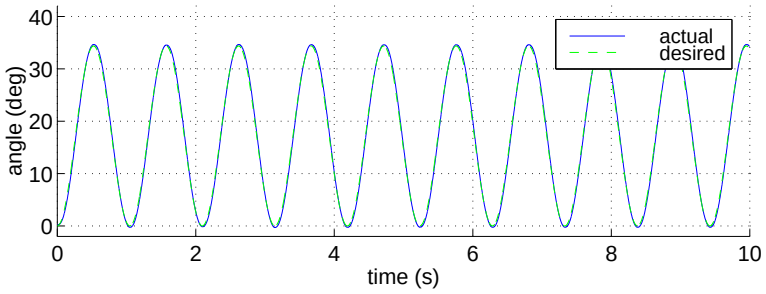

Figure 7.3: PUMA joint 1 angle vs. time

The experiment presented here shows the effectiveness of using dynamically decoupled, operational space control for XR4000 PCV when it is acting as the base "joints" of the mobile manipulator robot system. In this experiment the PCV, which we will call the *base* in this context, was commanded to travel from the original location, $(x, y, \theta) = (0, 0, 0)$, to two meters in the y direction, $(x, y, \theta) = (0, 2, 0)$. The PUMA 560 was configured to

begin in the "home" position with joint 2 level and pointing in the y direction and joint 3 vertical, pointing upward. When the motion was started, the PUMA was commanded to wave its arm by moving joint 1 (waist) between 0.0 and 0.6 radians (34.4°) at 0.95 Hz (6.0 rad/sec) in a sinusoidal trajectory. This trajectory is shown in Figures 7.2 and 7.3. Dynamic decoupling is used for the motions shown in these two figures.

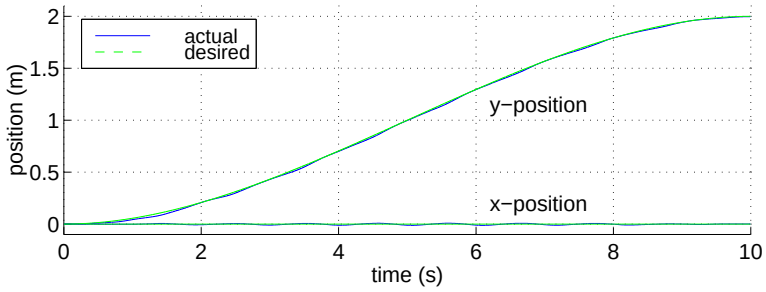

Figure 7.4: Base motion with no arm/base decoupling

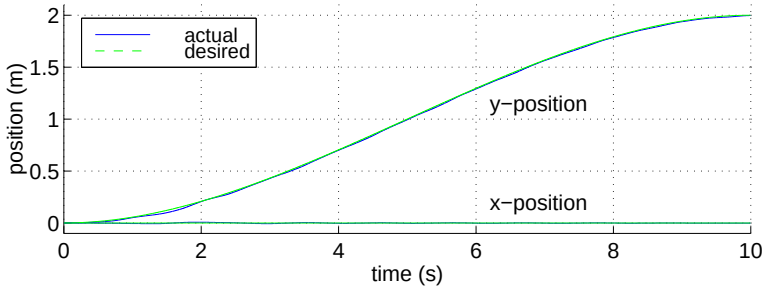

Figure 7.5: Base motion with arm/base decoupling

The rapid waving of the PUMA arm causes large dynamic disturbance torques particularly to the orientation of the base. The gains used in this experiment were reduced by a factor of 10 from the typical gains used during normal motions so that dynamic disturbances would be more apparent. The orientation errors of the base, when no dynamic decoupling between the manipulator and the base is used, are particularly large and are shown in Figure 7.6. Without dynamic compensation the orientation of the base has errors of about $\pm 6°$; while with dynamic compensation for the disturbance forces generated by the PUMA the orientation error is reduced to less than $\pm 1°$, as shown in Figure 7.7.

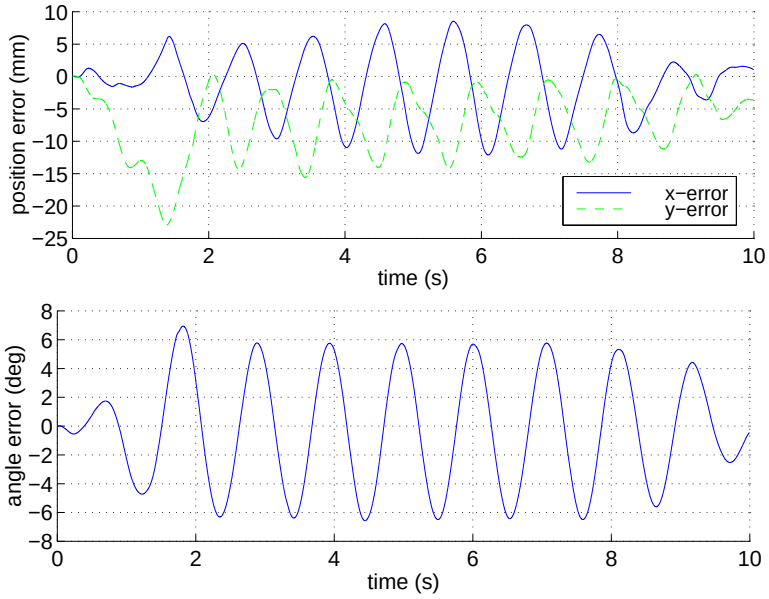

Figure 7.6: Base motion error with no arm/base decoupling

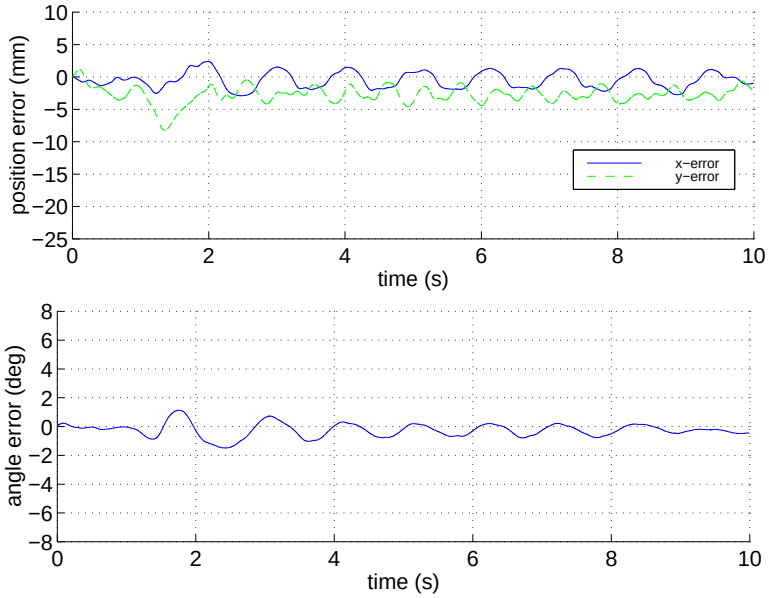

Figure 7.7: Base motion error with arm/base decoupling

Chapter 8

Future Work and Conclusions

8.1 Other Holonomic Mobile Robots

Since the term *holonomic mobile robot* has come to mean a robot which can instantly accelerate in an arbitrary direction, there are some interesting results which follow from this. Some common mobile robots which are regarded as nonholonomic robots can become holonomic robots with the addition of a simple rotational turret.

A differential drive robot, such as the Nomad Scout II, which I helped to design, could be easily transformed into a holonomic mobile robot by adding a turret with a vertical axis of rotation which did not intersect the common roll axis of the wheels. A differential drive robot can be viewed as a single powered caster kinematically. This "powered caster" is effectively actuated on the roll and twist DOFs, rather than the steer and roll DOFs of the powered caster which has been the subject of the preceding chapters. The transformation from nonholonomic robot to holonomic robot is accomplished, as with the PCV, by the introduction of the caster distance to the geometry of the robot. The caster distance here is the distance which separates the roll axis of the wheels and the orientation axis of the turret.

8.2 Vehicle Dynamics

One area of study which I have recently been introduced to is the study of vehicle dynamics [29]. Vehicle dynamics is an old discipline in which the analysis of the kinematic and dynamic properties of wheeled vehicles—typically restricted to cars, trucks, buses, etc.—has evolved to embody deep and insightful knowledge of rolling mechanisms. It is fascinating that the study of rolling motion is so refined when applied to automobiles and yet very little work has been done with robots.

Roboticists, lacking adequate "mapping" sensors, have intensely worked on improving the odometric capabilities of wheeled mobile robots [5, 15]. The researchers pursuing this type of work, until recently, assumed that the wheels of the robot are rigid bodies. Yet research in vehicle dynamics shows the important, large significance tire compliance has upon the behavior and path of any wheeled vehicle. Issues involving the study of the dynamics of robot tires and dynamic slip at the wheel/ground contact patch appear to be promising areas for research [77, 7]. It is an especially promising subject in conjunction with a PCV because of the redundant sensing (eight sensed axes for three DOF on a Nomad XR4000) which can be used to better compute the true interaction between the robot wheels and the floor. Further, slip information may be used to estimate the available traction and to characterize the surface which the robot is traversing [31].

8.3 Conclusions

I have presented the design of a new wheeled holonomic mobile robot, the *powered caster vehicle*, or PCV, which is being produced as the XR4000 mobile robot by Nomadic Technologies. The design of the powered caster vehicle provides smooth accurate motion with the ability to traverse the hazards of typical indoor environments. The design can be used with two or more wheels, and as implemented with four wheels provides a stable platform for mobile manipulation.

I have also described a new approach for a modular, efficient dynamic modeling of powered caster vehicles. This approach is based on the augmented object model originally developed for the study of cooperative manipulators. The actuation redundancy is resolved

to effectively distribute the actuator torques to minimize internal or antagonistic forces between wheels. This results in reduced wheel slip and improved odometry.

Using the vehicle dynamic model and the actuation and measurement redundancy resolution, I have developed a control structure that allows vehicle dynamic decoupling and slip minimization. The effectiveness of this approach was experimentally demonstrated for motions involving large dynamic effects.

The PCV dynamic model and control structure have been integrated into a new mobile manipulation platform integrating the XR4000 and a PUMA 560 arm. The experimental results on the new platform have shown full dynamic decoupling and improved performance.

Appendix A

The Virtual Linkage

The *virtual linkage* model was introduced by Williams as a physically meaningful representation of a system's DOFs which are not described by the motion of the payload [95, 96]. The model was introduced to represent the internal forces in a object grasped by multiple manipulators. The model can also be interpreted to represent the interaction forces which are exchanged between the various manipulators.

An arbitrary object has six degrees of freedom, three linear and three rotational. As multiple six-DOF manipulators grasp a common object or load, the degrees of freedom of the load remain six in number, while the number of DOFs of the system increase by six for each arm which grasps the load. The same principle can be applied to multiple three-DOF planar manipulators, all operating in a common plane, which are cooperatively manipulating a load that has three-DOF. As shown in Figure A.1, in the case of a PCV, the multiple three-DOF "manipulators" are the powered-casters, and the floor takes the place of the load which is being manipulated. This appendix will show a method of employing a virtual linkage representation for a PCV and how this representation is equivalent to the minimum slip odometry solution given in Chapter 6.

The PCV has $2n$ actuators and 3 DOF; therefore there are $2n-3$ forces which appear as tensions and compressions of the virtual actuators in the floor. For a four-wheeled Nomad XR4000 PCV, there are eight actuators, and three DOF for the robot body. This leaves five DOF which can be represented as five prismatic joints which form a quadrilateral with one diagonal.

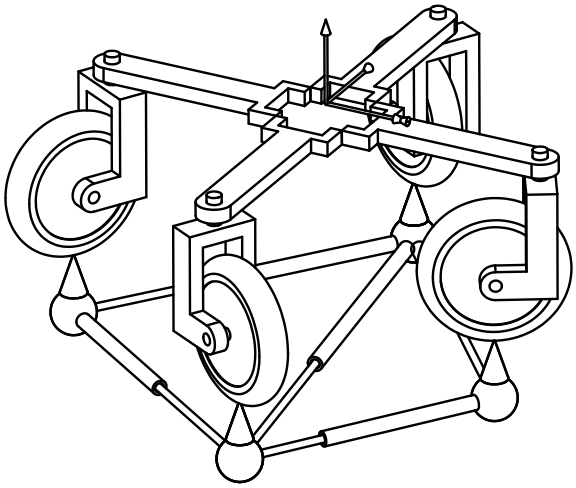

Figure A.1: PCV interacting with virtual linkage

The virtual linkage can be represented by the Jacobian mapping, E, from the Cartesian speeds of the grasp points to the internal speeds of the virtual actuators. For the PCV, the mapping is from the Cartesian speeds of the contact points, $\dot{\mathbf{x}}_c$, to the virtual speeds of the "truss" elements, $\dot{\boldsymbol{\varepsilon}}$.

$$\dot{\boldsymbol{\varepsilon}} = E\dot{\mathbf{p}} \tag{A.1}$$

A dual relationship also holds for the Cartesian contact forces, $\mathbf{f}_c$, and the virtual linkage forces, $\mathbf{t}$.

$$\mathbf{f}_c = E^{\mathsf{T}}\mathbf{t} \tag{A.2}$$

The matrix, E, can be expressed as a function of the directions of the virtual linkage elements, $\hat{\boldsymbol{\varepsilon}}$

$$E^{\mathsf{T}} = \begin{bmatrix} -\hat{\boldsymbol{\varepsilon}}_{12} & 0 & 0 & \hat{\boldsymbol{\varepsilon}}_{41} & \hat{\boldsymbol{\varepsilon}}_{31} \\ \hat{\boldsymbol{\varepsilon}}_{12} & -\hat{\boldsymbol{\varepsilon}}_{23} & 0 & 0 & 0 \\ 0 & \hat{\boldsymbol{\varepsilon}}_{23} & -\hat{\boldsymbol{\varepsilon}}_{34} & 0 & -\hat{\boldsymbol{\varepsilon}}_{31} \\ 0 & 0 & \hat{\boldsymbol{\varepsilon}}_{34} & -\hat{\boldsymbol{\varepsilon}}_{41} & 0 \end{bmatrix} \tag{A.3}$$

where the virtual linkage element vectors are functions of the wheel contact points, $\mathbf{p}$

$$\boldsymbol{\varepsilon}_{ij} = \mathbf{p}_j - \mathbf{p}_i \qquad ; \qquad \hat{\boldsymbol{\varepsilon}}_{ij} = \frac{\boldsymbol{\varepsilon}_{ij}}{|\boldsymbol{\varepsilon}_{ij}|} \tag{A.4}$$

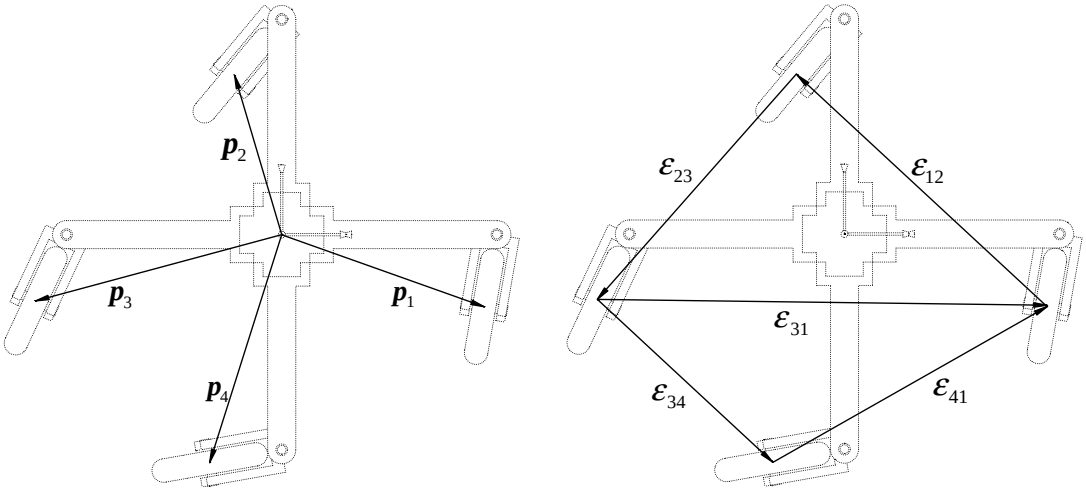

Figure A.2: Virtual linkage geometry

Ultimately the wheel contact point vectors, $\mathbf{p}_i$, are simply functions of the geometry:

$$\mathbf{p}_i = \mathbf{h}_i + \mathbf{b}_i \tag{A.5}$$

where $\mathbf{h}_i$ is the vector from the robot center to the i^{th} steer point and $\mathbf{b}_i$ is the vector from the i^{th} steer point to the i^{th} wheel contact point.

The Jacobian relating Cartesian robot velocities to wheel contact point Cartesian speeds is (see eqn. 6.13)

$$\dot{\mathbf{p}} = C_p\, \dot{\mathbf{x}} \tag{A.6}$$

where the mapping, C_p, is a function of the cross-product function of the wheel contact point vectors and can be expressed as:

$$C_p = \begin{bmatrix} \mathbf{I}_2 & \hat{\mathbf{p}}_1 \\ \vdots & \vdots \\ \mathbf{I}_2 & \hat{\mathbf{p}}_n \end{bmatrix} \qquad ; \qquad \hat{\mathbf{p}} = \begin{bmatrix} -p_y \\ p_x \end{bmatrix} \tag{A.7}$$

Both the robot Cartesian speeds, $\dot{\mathbf{x}}$, and the virtual actuator speeds, $\dot{\boldsymbol{\varepsilon}}$, can be projected

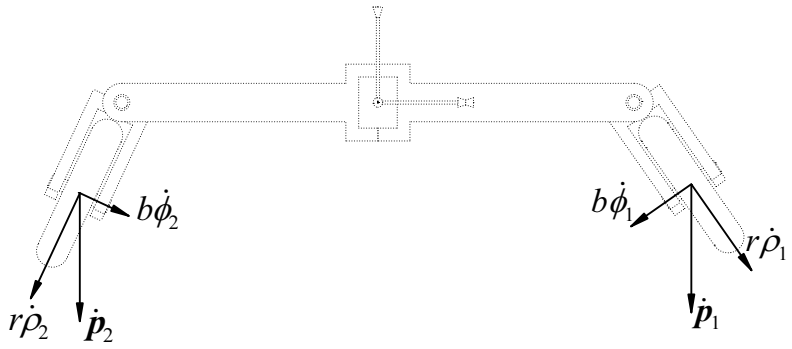

Figure A.3: External virtual velocities: y-axis robot velocity only

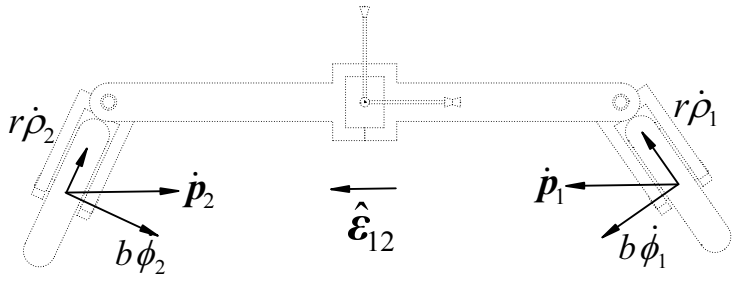

Figure A.4: Internal virtual velocities: virtual truss motion only

to the wheel contact Cartesian speeds. Combining eqn. A.1 and eqn. A.6 we get the composite PCV equation

$$\begin{bmatrix} \dot{\mathbf{x}} \\ \dot{\varepsilon} \end{bmatrix} = \begin{bmatrix} C_p^{\#} & E \end{bmatrix} C_q^{-1} \dot{\mathbf{q}} \tag{A.8}$$

The robot Cartesian velocities, $\dot{\mathbf{x}}$, and the velocities of the virtual linkage, $\dot{\varepsilon}$, span the space and are orthogonal to one another. The solution which causes zero slip (*i.e.* $\dot{\varepsilon} = 0$) is compatible with the solution for the robot Cartesian velocities in the top row, which is the same as given for minimum slip in Chapter 6.

Bibliography

[1] J. C. Alexander and J. H. Maddocks. On the kinematics of wheeled mobile robots. *The International Journal of Robotics Research*, 8(5):15–27, 1989.

[2] Hajime Asama, Masatoshi Sato, Luca Bogoni, Hayato Kaetsu, Akihiro Matsumoto, and Isao Endo. Development of an omni-directional mobile robot with 3 DOF decoupling drive mechanism. In *Proc. IEEE International Conference on Robotics and Automation*, volume 2, pages 1925–1930, Nagoya, Japan, 1995.

[3] D. Barrett, M. Grosenbaugh, and M. Triantafyllou. The optimal control of a flexible hull robotic undersea vehicle propelled by an oscillating foil. In *Proc. 1996 IEEE AUV Symp.*, pages 1–9, 1996.

[4] Alain Bétourné and Guy Campion. Kinematic modelling of a class of omnidirectional mobile robots. In *Proc. IEEE International Conference on Robotics and Automation*, volume 4, pages 3631–3636, Minneapolis, MN, April 1996.

[5] Johann Borenstein. The CLAPPER: a dual-drive mobile robot with internal correction of dead-reckoning errors. In *Proc. IEEE International Conference on Robotics and Automation*, volume 4, pages 3085–3090, San Diego, CA, May 1994.

[6] Alan Bowling. *Analysis of Robotic Manipulator Dynamic Performance: Acceleration and Force Capabiities*. PhD thesis, Stanford University, Stanford, California, U.S.A., June 1998.

[7] F. Demick Boyden and Steven A. Velinsky. Dynamic modeling of wheeled mobile robots for high load applications. In *Proc. IEEE International Conference on Robotics and Automation*, volume 4, pages 3071–3078, San Diego, CA, May 1994.

[8] Harold M. Bradbury. Omni-directional transport device. U.S. Patent #4223753, December 1977.

[9] R. A. Brooks. A robot that walks; emergent behaviors from a carefully evolved network. In *Proc. IEEE International Conference on Robotics and Automation*, pages 292–296, Scottsdale, AZ, May 1989.

[10] Thomas Burke and Hugh F. Durrant-Whyte. Kinematics for modular wheeled mobile robots. In *Proceedings of the IEEE/RSJ International Conference on Intelligent Robots and Systems*, volume 2, pages 1279–1286, Yokohama, Japan, 1993.

[11] Guy Campion, Georges Bastin, and Brigitte d'Andréa-Novel. Structural properties and classification of kinematic and dynamic models of wheeled mobile robots. In *Proc. IEEE International Conference on Robotics and Automation*, pages 462–469, Atlanta, GA, May 1993.

[12] Guy Campion, Georges Bastin, and Brigitte d'Andréa-Novel. Structural properties and classification of kinematic and dynamic models of wheeled mobile robots. *IEEE Transactions on Robotics and Automation*, 12(1):47–61, February 1996.

[13] Brian Carlisle. An omni-directional mobile robot. In Brian Rooks, editor, *Developments in Robotics*, pages 79–87. IFS Publications, Kempston, England, 1983.

[14] Kyong-Sok Chang. *Efficient algorithms for articulated branching mechanisms: dynamic modeling, control, and simulation*. PhD thesis, Stanford University, Stanford, CA, March 2000.

[15] Kok Seng Chong and Lindsay Kleeman. Accurate odometry and error modelling for a mobile robot. In *Proc. IEEE International Conference on Robotics and Automation*, volume 4, pages 2783–2788, Albuquerque, NM, April 1997.

[16] John J. Craig. *Introduction to Robotics*. Addison-Wesley, Menlo Park, CA, 2nd edition, 1989.

[17] Brigitte d'Andréa-Novel, Georges Bastin, and Guy Campion. Modelling and control of non holonomic wheeled mobile robots. In *Proc. IEEE International Conference*

on Robotics and Automation, volume 2, pages 1130–1135, Sacramento, CA, April 1991.

[18] Brigitte d'Andréa-Novel, Georges Bastin, and Guy Campion. Dynamic feedback linearization of nonholonomic wheeled mobile robots. In *Proc. IEEE International Conference on Robotics and Automation*, pages 2527–2532, Nice, France, May 1992.

[19] David J. Daniel, Bruce H Krogh, and Mark B. Friedman. Kinematics and open-loop control of an Ilonator-based mobile platform. pages 346–351, 1985.

[20] H.F.M. Van der Loos, S.J. Michalowski, and L.J. Leifer. Development of an omnidirectional mobile vocational assistant robot. In *Proc. ICAART*, pages 468–469, 1988.

[21] Stephen L. Dickerson and Brett D. Lapin. Control of an omni-directional robotic vehicle with mecanum wheels. In *National Telesystems Conference*, pages 323–328, Atlanta, GA, 1991.

[22] *Discover Magazine*. Turn and pivot of three: Oak ridge national laboratory's omnidirectional platform, July 1997.

[23] K. Dowling, R. Bennett, M. Blackwell, T. Graham, S. Gatrall, R. O'Toole, and H. Schempf. A mobile robot system for ground servicing operations on the space shuttle. In *Proceedings of SPIE - The International Society for Optical Engineering*, volume 1829, pages 298–309, Bellingham, WA, 1992.

[24] Roy Featherstone. *Robot Dynamics Algorithms*. Kluwer Academic Publishers, 1987.

[25] Dai Feng, Mark B. Friedman, and Bruce H. Krogh. Servo-control system for an omnidirectional mobile robot. In *Proc. IEEE International Conference on Robotics and Automation*, volume 3, pages 1566–1571, Scottsdale, AZ, May 1989.

[26] L. Ferrière, B. Raucent, and G. Campion. Design of omnimobile robot wheels. In *Proc. IEEE International Conference on Robotics and Automation*, volume 4, pages 3664–3670, Minneapolis, MN, April 1996.

[27] L. Ferrière, B. raucent, and A. Fournier. Design of a mobile robot equipped with off-centered orientable wheels. In *Proceedings of the Research Workshop of ERNET - European Robotics Network*, pages 127–136, Darmstadt, Germany, September 1996.

[28] R. Brent Gillespie, J. Edward Colgate, and Micheal Peshkin. A general framework for Cobot control. In *Proc. IEEE International Conference on Robotics and Automation*, Detroit, MI, May 1999.

[29] Thomas D. Gillespie. *Fundamentals of Vehicle Dynamics*. Society of Automotive Engineers, Inc., Warrendale, PA, 1992.

[30] Donald T. Greenwood. *Classical Dynamics*. Prentice-Hall, Inc., Englewood Cliffs, NJ, 1977.

[31] Fredrik Gustafsson. Monitoring tire-road friction using the wheel slip. *IEEE Control Systems Magazine*, pages 42–49, August 1998.

[32] Shigeru Hirooka, Ikuya Katanaya, and Shinobu Tanaka. Flexible automatic material handling system using guidless omni-directional vehicle. In *USA-Japan Symposium on Flexible Automation*, volume 2, pages 917–924, San Francisco, CA, 1992.

[33] Shigeo Hirose and Sinichi Amano. The VUTON: High payload high efficiency holonomic omni-directional vehicle. In 6^{th} *International Symposium on Robotics Research*, October 1993.

[34] Robert Holmberg, Sanford Dickert, and Oussama Khatib. A new actuation system for high-performance torque-controlled manipulators. In *RoManSy 9, Proceedings of the Ninth CISM-IFToMM Symposium on the Theory and Practice of Robots and Manipulators*, pages 285–292, Udine, Italy, September 1992.

[35] Robert Holmberg and Oussama Khatib. Development of a holonomic mobile robot for mobile manipulation tasks. In *FSR'99 International Conference on Field and Service Robotics*, Pittsburgh, PA, August 1999.

[36] Robert Holmberg and Oussama Khatib. A powered caster holonomic robotic vehicle for mobile manipulation tasks. In *RoManSy 2000, Proceedings of the Thirteenth*

CISM-IFToMM Symposium on the Theory and Practice of Robots and Manipulators, Zakopane, Poland, July 2000.

[37] Robert Holmberg and Oussama Khatib. Development and control of a holonomic mobile robot for mobile manipulation tasks. *The International Journal of Robotics Research*, to appear.

[38] H. Hoyer and U. Borgolte. OMNI - results and outlook: Conclusions from a successful project. In *Proceedings of the 1st MobiNet Symposium on Mobile Robotics Technology for Health Care Services*, pages 101–114, Athens, May 1997.

[39] Bengt Erland Ilon. Directionally stable self propelled vehicle. U.S. Patent #3746112, December 1971.

[40] Bengt Erland Ilon. Wheels for a course stable selfpropelling vehicle moveable in any desired direction on the ground or some other base. U.S. Patent #3876255, November 1972.

[41] Takashi Isoda, Peng Chen, Toshio Toyota, and Tatsuya Hirano. Omni-directional mobile robot for autonomic offroad running. In *IEEE International Workshop on Robot and Human Communication, RO-MAN*, pages 64–69, Sendai, Japan, 1997.

[42] Yutaka Kanayama. Two dimensional wheeled vehicle kinematics. In *Proc. IEEE International Conference on Robotics and Automation*, volume 4, pages 3079–3084, San Diego, CA, May 1994.

[43] Yutaka John Kanayama. Method of controlling a vehicle to make a combination of arbitrary translational and rotational motions. U.S. Patent #5719762, November 1995.

[44] Thomas R. Kane and David A. Levinson. *Dynamics: Theory and Applications*. McGraw-Hill, Inc., San Francisco, 1985.

[45] O. Khatib, O. Brock, K. Yokoi, and R. Holmberg. Dancing with juliet 1999. IEEE Robotics and Automation Conference Video Proceedings, 1999.

[46] O. Khatib, K. Yokoi, K. Chang, D. Ruspini, R. Holmberg, and A. Casal. 5^{th} IEEE international workshop on robot and human communication. In *Decentralized cooperation between multiple manipulators*, pages 183–188, 1996.

[47] O. Khatib, K. Yokoi, K. Chang, D. Ruspini, R. Holmberg, A. Casal, and A. Baader. Force strategies for cooperative tasks in mulitple mobile manipulation systems. In *International Symposium of Robotics Research*, Munich, October 1995.

[48] Oussama Khatib. A unified approach for motion and force control of robotic manipulators: The operational space formulation. *IEEE Journal of Robotics and Automation*, RA-3(1):43–53, February 1987.

[49] Oussama Khatib. Mobile manipuilator systems. In Anibal T de Alemeda and Oussama Khatib, editors, *Autonomous Robotic Systems*, pages 141–148. Springer-Verlag, London, 1998. presented at RoManSy '96: 11th CISM-IFToMM, Udine, Italy.

[50] Oussama Khatib, Kazuhito Yokoi, Kyong-Sok Chang, Diego Ruspini, Robert Holmberg, and Arancha Casal. Coordination and decentralized cooperation of multiple mobile manipulators. *Journal of Robotic Systems*, 13(11):755–764, 1996.

[51] Stephen M. Killough and François Pin. Design of an omnidirectional and holonomic wheeled platform prototype. In *Proc. IEEE International Conference on Robotics and Automation*, volume 1, pages 84–90, Nice, France, May 1992.

[52] Atsushi Koshiyama and Kazuo Yamafuji. Design and control of an all-direction steering type mobile robot. *The International Journal of Robotics Research*, 12(5):411–419, October 1993.

[53] W. H. T. La, T. A. Koogle, D. L. Jaffe, and L. J. Leifer. Toward total mobility: an omnidirectional wheelchair. In *Proc. 4th RESNA*, pages 75–77, Washington DC, 1981.

[54] Kathryn W. Lilly. *Efficient Dynamic Simulation of Robotic Mechanisms*. Kluwer Academic Publishers, 1992.

[55] Stephen Mascaro, Joseph Spano, and Haruhiko H. Asada. Reconfigurable holonomic omnidirectional mobile bed with unified seating (rhombus) for bedridden patients. In *Proc. IEEE International Conference on Robotics and Automation*, volume 2, pages 1277–1282, Albuquerque, NM, April 1997.

[56] Tad McGeer and Juris Vagners. Historic crossing: An unmanned aircraft's atlantic flight. *GPS World*, June 1999.

[57] Hillery McGowen. Navy omni-directional vehicle development. Brochure, Naval Surface Warfare Center Dahlgren Division, 6703 West Highway 98, Panama City, FL 32407-7001, September 1994. Code 2420.

[58] M. G. Mehrabi, R. M. H. Cheng, and A. Hemami. Dynamic modelling and control of wheeled mobile robots theory and experiment. In *Proceedings of the IEEE Conference on Control Applications*, volume 2, pages 659–665, Vancouver, Canada, 1993.

[59] *Modern Material Handling*. Forklift turns heads at ProMat 99, April 1999.

[60] Francis C. Moon. *Applied Dynamics: With Applications to Multibody and Mechatronic Systems*. John Wiley & Sons, Inc., New York, 1998.

[61] Hans P. Moravec. Three degrees for a mobile robot. In *Proceedings of the 1984 International Computers in Engineering Conference and Exhibit.*, volume 1, pages 274–278, Las Vegas, NV, 1984.

[62] Y. Mori, E. Nakano, T. Takahashi, and K. Takayama. A study on the mechanism and control of omni-directional vehicle. In *Proceedings of the IEEE/RSJ International Conference on Intelligent Robots and Systems*, volume 1, pages 52–59, Osaka, Japan, 1996.

[63] Patrick F. Muir and Chales P. Neuman. Kinematic modeling of wheeled mobile robots. *Journal of Robotic Systems*, 4(2):281–340, 1987.

[64] Patrick F. Muir and Charles P. Neuman. Kinematic modeling of wheeled mobile robots. Technical Report CMU-RI-TR-86-12, The Robotics Institute, Carnegie-Mellon University, Pittsburgh, PA, June 1986.

[65] Patrick F. Muir and Charles P. Neuman. Kinematic modeling for feedback control of an omnidirectional wheeled mobile robot. In *Proc. IEEE International Conference on Robotics and Automation*, pages 1772–1778, Raleigh, NC, March 1987.

[66] Igor E. Paromtchik and Ulrich Rembold. Practical approach to motion generation and control for an omnidirectional mobile robot. In *Proc. IEEE International Conference on Robotics and Automation*, volume 4, pages 2790–2795, San Diego, CA, May 1994.

[67] Micheal Peshkin and J. Edward Colgate. "Cobots" work with people. *IEEE Robotics and Automation Magazine*, 3(4), December 1996.

[68] François G. Pin and Stephen M. Killough. A new family of omnidirectional and holonomic wheeled platforms for mobile robots. *IEEE Transactions on Robotics and Automation*, 10(4):480–489, August 1994.

[69] M. H. Raibert, M. A. Chepponis, and H. B. Brown, Jr. Experiments in balance with a 3d one-legged hopping machine. *The International Journal of Robotics Research*, 3:75–92, 1984.

[70] R. Rajagopalan. A generic kinematic formulation for wheeled mobile robots. *Journal of Robotic Systems*, 14(2):77–91, 1997.

[71] R. Rajagopalan and N. Barakut. Velocity control of wheeled mobile robots using computed torque control and its performance for a differentially driven robot. *Journal of Robotic Systems*, 14(4):325–340, 1997.

[72] G. Rodriguez, K. Kreutz, and A. Jain. A spatial operator algebra for manipulator modeling and control. In *Proceedings of IEEE International Conference on Robotics and Automation*, pages 1374–1379, May 1989.

[73] Jeffrey S. Russakow. *Experiments in manipulation and assembly by two-arm, free-flying space robots*. PhD thesis, Stanford University, Stanford, CA, December 1995.

[74] Marvin Russell Jr. ODEX I: The first functionoid. *Robotics Age*, September-October 1983.

[75] Subir Kumar Saha, Jorge Angeles, and John Darcovich. The kinematic design of a 3-DOF isotropic mobile robot. In *Proc. IEEE International Conference on Robotics and Automation*, volume 1, pages 283–288, Atlanta, GA, May 1993.

[76] Nilanjan Sarkar, Xiaoping Yun, and Vijay Kumar. Control of mechanical systems with rolling constraints: Application to dynamic control of mobile robots. *The International Journal of Robotics Research*, 13(1):55–69, February 1994.

[77] Shashank Shekar. Wheel rolling constraints and slip in mobile robots. In *Proc. IEEE International Conference on Robotics and Automation*, pages 2601–2607, Albuquerque, NM, April 1997.

[78] James Slater, Robert Holmberg, John Slater, and Rich Legrand. Workshop participant. IEEE Robotics and Automation Conference, April 1997.

[79] James Slater, John Slater, and Rich Legrand. Vendor display. IEEE Robotics and Automation Conference, April 1996.

[80] Kuniharu Takayama, Eji Nakano, Yoshikazu Mori, and Takayuki Takahashi. Apparatus for controlling motion of normal wheeled omni-directional vehicle and method thereof. U.S. Patent #5739657, April 1996.

[81] Jun Tang, Keigo Watanabe, and Yamato Shiraishi. Desigh and traveling experiment of an omnidirectional holonomic mobile robot. In *Proceedings of the IEEE/RSJ International Conference on Intelligent Robots and Systems*, pages 66–72, Osaka, Japan, 1996.

[82] K. Thanjavur and R Rajagopalan. Ease of dynamic modelling of wheeled mobile robots (WMR's) using Kane's approach. In *Proc. IEEE International Conference on Robotics and Automation*, pages 2926–2931, Albuquerque, April 1997.

[83] Masayoshi Wada and Haruhiko Asada. Design and control of a variable footprint mechanism for holonomic omnidirectional vehicles and its application to wheelchairs. *IEEE Transactions on Robotics and Automation*, 15(6):978–989, December 1999.

[84] Masayoshi Wada and Shunji Mori. Holonomic and omnidirectional vehicle with conventional tires. In *Proc. IEEE International Conference on Robotics and Automation*, pages 3671–3676, Minneapolis, MN, April 1996.

[85] Masayoshi Wada and Shunji Mori. Modeling and control of a new type of omnidirectional holonomic vehicle. In *Fourth International Workshop on Advanced Motion Control*, volume 1, pages 265–270, Tsu, Japan, March 1996.

[86] Masayoshi Wada, Yasutaka Tominaga, and Shunji Mori. Omnidirectional holonomic mobile robot using nonholonomic wheels. In *Proceedings of the IEEE/RSJ International Conference on Intelligent Robots and Systems*, volume 3, pages 446–453, Pittsburgh, PA, August 1995.

[87] Kenneth J. Waldron. Mobility and controllability characteristics of mobile robotic platforms. In *Proc. IEEE International Conference on Robotics and Automation*, pages 237–243, St. Louis, MO, March 1985.

[88] K.J. Waldron, C.A. Klein, D. Pugh, V.J. Vohnout, E. Ribble, M. Patterson, , and R.B. McGhee. Operational experience with the adaptive suspension vehicle. In *Proceedings of the 7th World Congress on Theory of Machines and Mechanisms*, volume 3, pages 1495–1498, Sevilla, Spain, September 1987.

[89] H. H. Wang, S. M. Rock, and M. J. Lee. OTTER: The design and development of an intelligent underwater robot. *Autonomous Robots*, 3:297–320, 1996.

[90] Witaya Wannasuphoprasit, Prasad Akella, Micheal Peshkin, and J. Edward Colgate. Cobots: A novel material handling technology. In *Proc. ASME International Mechanical Engineering Congress and Exposition*, 1998.

[91] Mark West and Haruhiko Asada. Design of a holonomic omnidirectional vehicle. In *Proc. IEEE International Conference on Robotics and Automation*, pages 97–103, Nice, France, May 1992.

[92] Mark West and Haruhiko Asada. Design of ball wheel vehicles with full mobility, invariant kinematics and dynamics and anti-slip control. In *Proceedings of the ASME Design Technical Conferences, 23rd Biennial Mechanisms Conference ASME*, volume 72, pages 377–384, Minneapolis, MN, 1994.

[93] Mark West and Haruhiko Asada. Design and control of ball wheel omnidirectional vehicles. In *Proc. IEEE International Conference on Robotics and Automation*, volume 2, pages 1931–1938, Nagoya, Japan, 1995.

[94] Mark West and Haruhiko Asada. Method for designing ball wheels for omnidirectional vehicles. In *Proceedings of the 1995 ASME Design Engineering Technical Conferences, 21st Annual Design Automation Conference ASME*, volume 1, pages 803–809, Boston, MA, 1995.

[95] David Williams and Oussama Khatib. The virtual linkage: A model for internal forces in multi-grasp manipulation. In *Proc. IEEE International Conference on Robotics and Automation*, volume 3, pages 1025–1030, Atlanta, GA, May 1993.

[96] J. David Williams. *Characterization and control of multiple-grasp robotic systems*. PhD thesis, Stanford University, Stanford, CA, June 1995.

[97] B. Woodley, H. Jones, E. Frew, E. LeMaster, and S. Rock. A contestant in the 1997 international aerial robotics competition. In *AUVSI '97 Proceedings*, July 1997.

[98] Yoshio Yamamoto and Xiaoping Yun. A modular approach to dynamic modelling of a class of mobile manipulators. *The International Journal of Robotics Research*, 12(2):41–48, 1997.

[99] Mark Yim. New locomotion gaits. In *Proc. IEEE International Conference on Robotics and Automation*, pages 2508–2514, May 1994.

[100] Yilin Zhao and Spencer L. BeMent. Kinematics, dynamics and control of wheeled mobile robots. In *Proc. IEEE International Conference on Robotics and Automation*, volume 1, pages 91–96, Nice, France, May 1992.